Dissertation zur Erlangung des Doktorgrades
der Fakultät für Chemie und Pharmazie
der Ludwig-Maximilians-Universität München

Funktionelle Charakterisierung des Ionenkanals TPCN2

Michael Schieder
aus
Mühldorf am Inn

2011

Erklärung

Diese Dissertation wurde im Sinne von § 13 Abs. 3 bzw. 4 der Promotionsordnung vom 29. Januar 1998 (in der Fassung der sechsten Änderungssatzung vom 16. August 2010) von Herrn Prof. Dr. Christian Wahl-Schott betreut.

Ehrenwörtliche Versicherung

Diese Dissertation wurde selbständig, ohne unerlaubte Hilfe erarbeitet.
München, 10.10.2011

_____
(Michael Schieder)

Dissertation eingereicht am 11.10.2011

1. Gutachter Prof. Dr. C. Wahl-Schott
2. Gutachter Prof. Dr. M. Biel

Mündliche Prüfung am 28.10.2011

1. Inhaltsverzeichnis

1. Inhaltsverzeichnis..... I

2. Abkürzungen..... II

3. Publikationsliste..... III

4. Zusammenfassung..... IV

5. Einleitung..... 1

6. Zielsetzung..... 17

7. Kurzzusammenfassungen der Publikationen..... 18

7.1. The two-pore channel TPCN2 mediates NAADP-dependent Ca^{2+}-release from lysosomal stores.

7.2. Characterization of two-pore channel 2 (TPCN2)-mediated Ca^{2+}-currents in isolated lysosomes.

7.3. Planar patch clamp approach to characterize ionic currents from intact lysosomes.

8. Literaturverzeichnis…….. 23

9. Lebenslauf…….. 27

10. Danksagung…… 28

11. Anhang…… 29

2. Abkürzungen

ADP	Adenosindiphosphat
ATP	Adenosintriphosphat
BAPTA	1,2-Di-(o-Aminophenoxy) Ethyl-N,N,N',N'-tetraessigsäure
bp	Basenpaar
Ca^{2+}	Calcium
Ca^{2+}/H^{+}- Ex	Ca^{2+}/H^{+}-Austauscher
cADPR	cyklische ADP-Ribose
CatSper	*cation channel of sperm,* Kationenkanal der Spermien
CCK	Cholezystokinin
CICF	Ca^{2+}-induzierte Ca^{2+}-Freisetzung
CNG	*cyclic nucleotide gated,* Cyklonukleotid-aktiviert
COS7	*Cercopithecus aethiops, origin-defective SV-40,* CV-1-Affenzelllinie mit genetischem Material des SV40-Virus
DMEM	Dulbecco's modifiziertes Eagle Medium
DMSO	Dimethylsulfoxid
DNA	Desoxyribonucleinsäure
eGFP	enhanced green fluorescent protein, verstärkt grün fluoreszierendes Protein
EGTA	Ethylenglycol-bis(2-aminoethylether)-N,N,N',N'-tetraessigsäure
ER	sarko-/endoplasmatisches Retikulum
E_{rev}	Umkehrpotential
ET-1	Endothelin-1
GPN	Glycylphenylalanin-2-naphthylamid
H^{+}	Protonen
HEK293	*human embryonic kidney cells,* humane embryonale Nierenzelllinie Klon 293
HEPES	2-[4-(2-Hydroxyethyl)-1-piperazinyl]-Ethansulfonsäure

HRP	*horseradish peroxidase,* Meerretichperoxidase
I_{NAADP}	NAADP-aktivierbarer Ca^{2+}-Strom
IP_3	Inositol-1,4,5-trisphosphat
IP_3R	Inositol-1,4,5-trisphosphatrezeptor
kb	Kilobasen
K_d	Dissoziationskonstante
kDa	Kilodalton
KO	Knockout, defizient für das angegebene Gen
Ko-IP	Ko-Immunopräzipitation
LAK	Lymphokin-aktivierte Killerzellen
MSA	Methansulfonsäure
NA	*nicotinic acid,* Nikotinsäure
NAAD	*nicotinic acid adenine dinucleotide,* Nikotinsäureadenindinukleotid
NADP	*nicotinamid adenine dinucleotide phosphate,* Nikotinamidadenindinukleotid-phosphat
NAADP	*nicotinic acid adenine dinucleotide phosphate,* Nikotinsäureadenindinukleotid-phosphat
PAGE	Polyacrylamid-Gelelektrophorese
PCR	Polymerase-Kettenreaktion
RNA	Ribonucleinsäure
RyR	Ryanodinrezeptor
RNAse	Ribonuclease
SDS	*sodium dodecylsulfate,* Natriumdodecylsulfat
SERCA	sarko-/endoplasmatische retikuläre Ca^{2+} ATPase
SF	Selektivitätsfilter
SOCE	*store operated Ca^{2+} entry,* Ca^{2+}-Speicher abhängiger Ca^{2+}-Einstrom

SV	*slow vacuolar*, langsam vakuolär
TPCN	*two pore cation channel*, 2 Porenschleifenkationenkanal
TRP	*transient receptor potential*, transienter Rezeptorpotential-Kanal
WT	Wildtyp

3. Publikationsliste

Diese Doktorarbeit basiert auf den folgenden Publikationen:

I. X. Zong*, **M. Schieder***, H. Cuny, S. Fenske, C. Gruner, K. Rötzer, O. Griesbeck, H. Harz, M. Biel, C. Wahl-Schott

The two-pore channel TPCN2 mediates NAADP-dependent Ca^{2+}-release from lysosomal stores.

2009, *Pflugers Arch*, 458, 891

*X. Zong and M. Schieder contributed equally

II. **M. Schieder**, K. Rötzer, A. Brüggemann, M. Biel, C. A. Wahl-Schott

Characterization of two-pore channel 2 (TPCN2)-mediated Ca^{2+}-currents in isolated lysosomes.

2010, *J Biol Chem*, 285, 21219

III. **M. Schieder**, K. Rötzer, A. Brüggemann, M. Biel, C. Wahl-Schott

Planar patch clamp approach to characterize ionic currents from intact lysosomes.

2010, *Sci Signal*, 3, pl3

4. Zusammenfassung

Nikotinsäureadenindinukleotidphosphat (NAADP) ist ein sekundärer Botenstoff, der in nM Konzentrationen Ca^{2+} aus lysosomalen Speichern der Zelle freisetzt. In zahlreichen Säugerzellen (z.B. in Kardiomyozyten, Neuronen und ß-Zellen des Pankreas) wurden NAADP-abhängige Prozesse beschrieben.

In der vorliegenden Arbeit wurde der Nachweis erbracht, dass *two-pore*-Kanäle (TPCN), die lange gesuchten hochaffinen NAADP-Rezeptoren darstellen. TPCN-Kanäle gehören zur Superfamilie der spannungsabhängigen Kationenkanäle und sind strukturell insbesondere mit TRP-Kanälen verwandt. Der Grundbaustein von TRP-Kanälen ist eine Domäne mit sechs transmembranären α-Helices. Zwischen der fünften und sechsten Helix befindet sich eine schleifenförmige Struktur (*pore loop*), die den Selektivitätsfilter der ionenleitenden Pore darstellt. Ein funktioneller TRP-Kanal wird durch Tetramerisierung dieser Domänen gebildet. Bei TPCN-Kanälen sind zwei solcher Domänen, aus je sechs transmembranären α-Helices über einen intrazellulären Linker miteinander fusioniert. Da jede dieser Domänen einen *pore loop* enthält, werden sie als *two-pore*-Kanäle bezeichnet. Der native Kanal setzt sich wahrscheinlich aus einem TPCN-Dimer zusammen, sodass sich eine pseudotetramere Kanaltopologie ergibt.

Im Rahmen der Arbeit wurden die Kanäle TPCN1 und TPCN2 der Maus funktionell charakterisiert. Es zeigte sich auf Transkriptebene, dass beide Kanäle ubiquitär exprimiert werden, mit einer deutlich höheren Expression von TPCN1 gegenüber TPCN2. Proteinbiochemisch wurde der Nachweis erbracht, dass TPCN2-Kanäle Homomere bilden. Heteromere von TPCN2 und TPCN1 konnten dagegen nicht nachgewiesen werden. In weiteren proteinbiochemischen Experimenten zeigte sich, dass TPCN2 durch N-

Glykosylierung modifiziert wird. Die Glykosylierung erfolgt an zwei Asparaginen (N594/N601) in der Porenschleife der zweiten Kanaldomäne.

Zur funktionellen Charakterisierung von TPCN2 wurden Ca^{2+} Imaging Experimente an HEK293 Zellen durchgeführt, die transient TPCN2 exprimierten. Es zeigte sich, dass TPCN2-Kanäle NAADP-abhängig Ca^{2+} freisetzen. Charakteristisch ist die glockenförmige Dosis-Wirkungskurve mit einem Maximum bei etwa 30 nM NAADP. Der Rückgang der Ca^{2+}-Freisetzung bei Applikation µM NAADP-Konzentrationen spricht für eine Desensitisierung oder einen spezifischen Inaktivierungsmechanismus der Kanäle. Nach pharmakologischer Blockade der lysosomalen Ca^{2+}-Speicherung durch Bafilomycin A1, konnte keine NAADP-abhängige Ca^{2+}-Freisetzung beobachtet werden. Dieses Ergebnis spricht dafür, dass die NAADP-abhängige Ca^{2+}-Freisetzung aus den Lysosomen erfolgt. Nach Vorbehandlung der Zellen mit Thapsigargin, einer Substanz die die Ca^{2+}-Aufnahme in das ER blockiert, war die NAADP-abhängige Ca^{2+}-Freisetzung komplett erhalten. Das ER scheint daher, bei der primär durch NAADP-induzierten Ca^{2+}-Freisetzung keine Rolle zu spielen. Zusammengenommen zeigen die beschriebenen Analysen, dass TPCN2 die kennzeichnenden Eigenschaften des nativen NAADP-Rezeptors besitzt.

Im zweiten Teil der Arbeit wurde für die direkte funktionelle Charakterisierung der Kanäle ein neuer Ansatz etabliert, der Strommessungen an biochemisch aufgereinigten, isolierten Lysosomen ermöglicht. Die Hauptfaktoren, welche die elektrophysiologische Analyse erschweren sind die geringe Größe der Lysosomen (0.3 – 1 µm) und ihre geringe Membranstabilität. Beide Faktoren verhindern den Zugriff mittels der üblichen Patch Clamp Protokolle. Um diese Probleme zu umgehen, wurde die planare Patch Clamp Methode modifiziert und auf isolierte und mit Vacuolin-1 vergrößerte Lysosomen angewendet. Bei dieser Methode werden die Lysosomen während der Zellkultur durch Behandlung mit Vacuolin-1 vergrößert und anschließend auf einer Festphasenmatrix, dem planaren Glaschip

immobilisiert. Der Glaschip enthält eine Öffnung, die durch ihre Ausformung die Lysosomen bei elektrophysiologischen Experimenten mechanisch unterstützt, um ihre native Form zu erhalten.

Mit dem planaren Patch Clamp gelang es, direkt Ströme an intakten, einzelnen Lysosomen zu messen. Lysosomen, die TPCN2-Kanäle exprimierten, nicht aber Kontrolllysosomen ohne Überexpression, zeigten einen deutlichen NAADP-aktivierbaren Ca^{2+}-Strom (I_{NAADP}). Der I_{NAADP} hat eine glockenförmige NAADP-Dosis-Wirkungskurve, mit einem Aktivierungsgipfel im nM Bereich. Die Eigenschaften des I_{NAADP} stimmen sehr gut mit den Eigenschaften der Ca^{2+}-Antworten in Imaging Experimenten überein. Durch den direkten elektrophysiologischen Zugang zu den isolierten Lysosomen war es möglich weitere Eigenschaften zu untersuchen. Es zeigte sich, dass der I_{NAADP} durch den intralysosomalen pH reguliert wird und eine extrem hohe Ca^{2+}-Selektivität besitzt. Durch den Austausch einzelner Aminosäurereste im putativen Selektivitätsfilter der TPCN2-Kanäle, wurde die Ionenselektivität der Kanäle verändert. In ihrer Gesamtheit belegen die Untersuchungen, dass TPCN2 ein lysosomaler, NAADP-aktivierter, pH-regulierter Ca^{2+}-Kanal ist.

5. Einleitung

Die transiente Erhöhung der cytosolischen Ca^{2+}-Konzentration zählt zu den fundamentalen Prozessen der zellulären Signalverarbeitung und ist an der Regulation zahlreicher physiologischer Prozesse wie der Muskelkontraktion, der Hormon- und Neurotransmittersekretion, der Zellteilung, der Zellmotilität und der Immunantwort beteiligt (*1*). Intrazelluläre Ca^{2+}-Signale können auf zwei unterschiedliche Arten erzeugt werden (Abb. 1). Zum einen kann Ca^{2+} aus dem extrazellulären Raum über Ionenkanäle der Plasmamembran (z.B. spannungsaktivierte Ca^{2+}-Kanäle, TRP- und CNG-Kanäle (*2*)) in die Zelle einströmen. Zum anderen kann Ca^{2+} aus den intrazellulären Ca^{2+}-Speichern der Zelle, zu denen das sarko-/endoplasmatische Retikulum (ER), die Kernmembran und die Mitochondrien gehören, in das Cytosol freigesetzt werden. Die extra- und intrazelluläre Freisetzung von Ca^{2+} sind funktionell eng aneinander gekoppelt. Beispielsweise können ER Speicher aus denen Ca^{2+} freigesetzt wurde, durch extrazellulären Ca^{2+}-Einstrom wieder aufgefüllt werden (*3*). Dieser sogenannte s*tore-operated* Ca^{2+} *entry* (SOCE) wird durch einen spezifischen Proteinkomplex vermittelt, der einen Ca^{2+}-Sensor (STIM1/2), einen Ca^{2+}-Kanal der Plasmamembran (Orai1-3) und möglicherweise die Ca^{2+} ATPase des ER (SERCA) enthält (*4*). Die Ca^{2+}-Freisetzung aus intrazellulären Ca^{2+}-Speichern wird über sekundäre Botenstoffe wie z.B. IP_3 (Inositol-1,4,5-trisphosphat), cADP-Ribose (cyclische ADP-Ribose) oder Ca^{2+} selbst induziert. Die Produktion dieser Botenstoffe wird durch Hormone oder Neurotransmitter über Rezeptoren an der Zelloberfläche reguliert. Seit einiger Zeit gibt es Anhaltspunkte dafür, dass die Lysosomen neben den oben genannten „klassischen“ Ca^{2+}-Speichern, einen weiteren Ca^{2+}-Speicher in der Zelle darstellen.

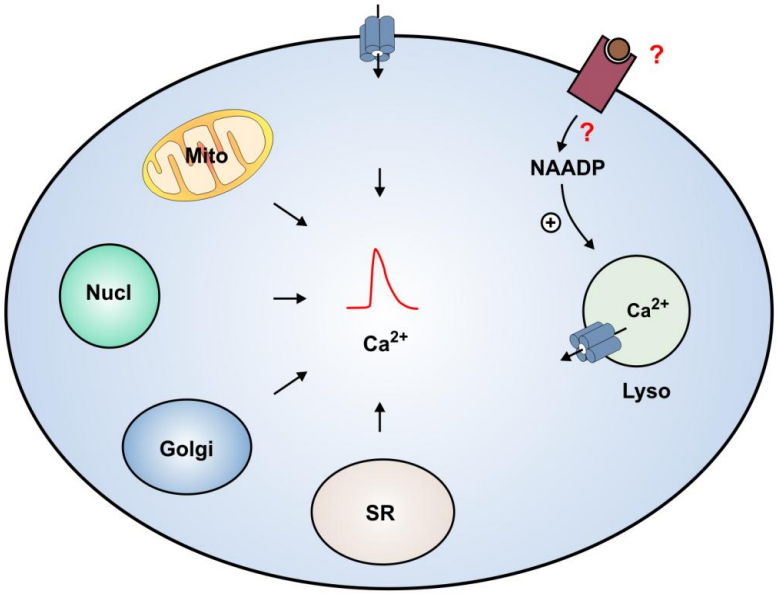

Abb. 1) Intrazelluläre Ca^{2+}-Signale können zum einen entstehen, indem Ca^{2+} aus dem extrazellulären Raum über Ionenkanäle der Plasmamembran (z.B. spannungsaktivierte Ca^{2+}-Kanäle, TRP- und CNG-Kanäle (*2*)) in die Zelle einströmt. Zum anderen kann Ca^{2+} aus den intrazellulären Ca^{2+}-Speichern der Zelle, zu denen das sarko-/endoplasmatische Retikulum (ER), die Kernmembran und die Mitochondrien gehören, in das Cytosol freigesetzt werden. Seit Kurzem ist bekannt, dass Lysosomen Ca^{2+} speichern und durch Nikotinsäureadenin-dinukleotidphosphat (NAADP) freisetzen können.

Bedeutung von Lysosomen für zelluläre Degradationsprozesse

Lysosomen sind ubiquitär vorkommende, sehr kleine Organellen (0,5 – 3 µm Durchmesser), die von der Zelle benötigt werden um Makromoleküle und fehlerhafte Organellen abzubauen (*5*). Das Lumen der Lysosomen ist durch die Tätigkeit einer vakuolären H^+ ATPase (V-H^+ ATPase) leicht sauer (pH 4 - 5). Hierdurch wird gewährleistet, dass lytische Enzyme wie Hydrolasen im Lumen des Lysosoms ihre größtmögliche Aktivität erreichen. Lysosomen können mit einer Reihe von anderen zellulären Organellen fusionieren (z.B. Phagosomen, Endosomen) und auf diesem Weg ihr lytisches Potential auf diese Organellen übertragen (*5-7*). Störungen im lysosomalen Export und Import von Metaboliten sind ursächlich für eine Reihe von Erkrankungen, insbesondere der lysosomalen Speicherkrankheiten (z.B. Mukolipidose IIIC und IV) oder der Osteopetrose (*8-12*).

Bedeutung von Lysosomen für intrazelluläre Ca^{2+} und pH Homöostase

Die Vielfalt von Ca^{2+}-leitenden lysosomalen Ionenkanälen (z.B. TRPV5/6, TRPML1, TRPM2 (*13*)) hat in den letzten Jahren zu der Hypothese geführt, dass Lysosomen nicht nur zur Degradation von Biomolekülen benötigt werden sondern auch Ca^{2+}-Speicher darstellen und Bestandteil Ca^{2+}-abhängiger zellulärer Signalwege sind (*14-15*). Im Einklang mit dieser Hypothese haben experimentelle Messungen ergeben, dass die lysosomale ($[Ca^{2+}]$ ~ 0.5 mM (*13, 16*)) und endosomale Ca^{2+}-Konzentration ($[Ca^{2+}]$ = 0.003 – 2 mM (*13, 17*)) um bis zu 10.000fach über der basalen cytosolischen Ca^{2+}-Konzentration liegt. Die lysosomale Ca^{2+}-Akkumulation ist über einen hypothetischen Ca^{2+}/H^{+}-Austausch funktionell mit dem lysosomalen pH gekoppelt (*13*). Es wird in diesem Zusammenhang postuliert, dass Lysosomen einen Ca^{2+}/H^{+}-Antiporter besitzen, der Ca^{2+} in die Lysosomen bzw. H^{+} aus den Lysosomen transportiert und der von einer hohen lysosomalen H^{+}-Konzentration abhängt. Demnach müsste eine lysosomale Ca^{2+}-Freisetzung zu einer lysosomalen Alkalisierung führen. Die hohe lysosomale H^{+}-Konzentration wird von der V-H^{+} ATPase energieabhängig generiert. Durch die Anreicherung von Protonen im Lumen der Endo-/Lysosomen, liegt der lysosomale pH-Wert normalerweise im sauren Bereich bei ca. 4 - 5 und der endosomale pH-Wert bei 5 - 6. Inhibiert man die V-H^{+} ATPase durch Bafilomycin A1, kann kein Ca^{2+} gespeichert werden (Abb. 2).

Es ist weitgehend unbekannt, inwieweit Ionenbewegungen über die beschriebenen Ionenkanäle, Transporter und Pumpen das lysosomale Membranpotential beeinflussen. Da Lysosomen sehr klein sind und eine sehr geringe elektrische Kapazität haben, kann man davon ausgehen, dass Ionenbewegungen starke Schwankungen im lysosomalen Membranpotential verursachen. Bisher gibt es jedoch keine verlässlichen, experimentellen Messungen des lysosomalen Membranpotentials, da Lysosomen bisher direkten elektrophysiologischen Messungen nicht zugänglich sind. Es gilt allerdings als gesichert, dass

das lysosomale Lumen positiv gegenüber dem Cytosol ist. In verwandten Organellen, den Phagosomen und synaptischen Vesikeln wurde ein Membranpotential von ca. +30 mV - +100 mV bestimmt (*13, 18-19*). Es besteht somit eine elektrochemische Triebkraft für einen Ca^{2+} Ausstrom aus den Organellen in das Cytosol.

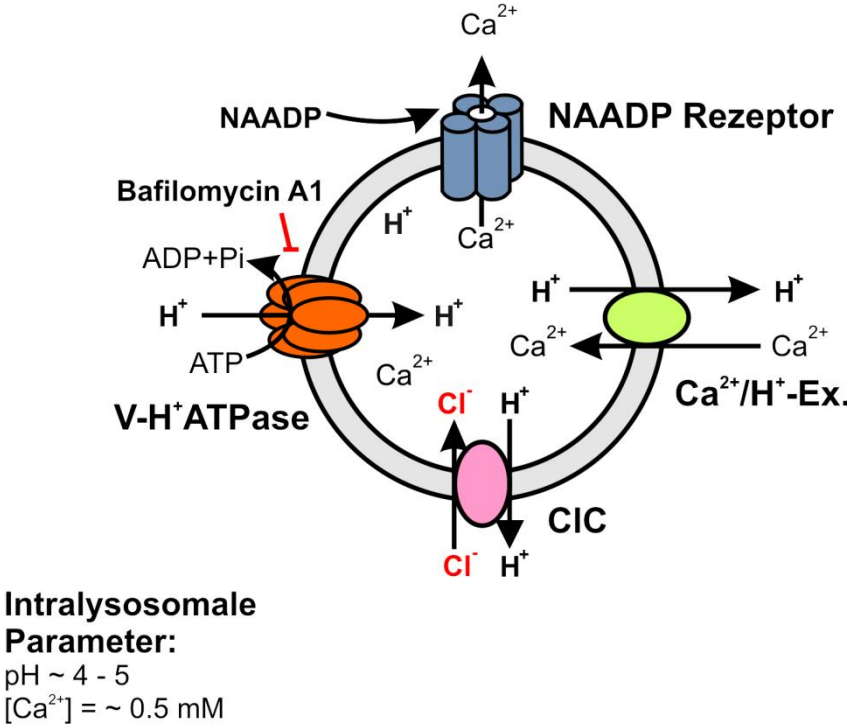

Abb. 2) Übersicht über wesentliche lysosomale Ionentransportvorgänge**.** Die V-H^+ ATPase pumpt unter ATP Verbrauch Protonen in das lysosomale Lumen. Durch die Tätigkeit dieser Pumpe sinkt der pH-Wert auf 4 - 5. Im Lumen des Lysosoms wird durch einen putativen Ca^{2+}/H^+-Antiporter eine Ca^{2+}-Konzentration von ca. 0.5 mM eingestellt. Nikotinsäureadenindinukleotidphosphat (NAADP) aktiviert seinen Rezeptor und setzt Ca^{2+} in das Cytosol frei. ClC: Chloridkanal, Ca^{2+}/H^+- Ex.: Ca^{2+}/H^+-Austauscher.

NAADP-Rezeptoren sind lysosomale Ca^{2+}-Freisetzungskanäle

Seit Längerem gibt es Hinweise darauf, dass der NAADP-Rezeptor ein lysosomaler Ca^{2+}-Freisetzungskanal ist. Die funktionellen Kennzeichen des Kanals sind im Folgenden zusammengefasst:

1) Aktivierung durch den sekundären Botenstoff NAADP (glockenförmige Dosis-Wirkungskurve mit einer hohen Affinität zu NAADP (Maximum im nM Bereich); Insensitivität gegenüber NADP)
2) Ubiquitäre Expression
3) Lokalisation in Lysosomen und Endosomen

1. Aktivierung durch den sekundären Botenstoff NAADP

Entdeckung und Struktur von NAADP

Die Ca^{2+}-freisetzende Wirkung von Nikotinsäureadenindinukleotidphosphat (NAADP) wurde ursprünglich in Seeigeleiern entdeckt. Diese Wirkung wurde zunächst fälschlicherweise dem Nikotinamidadenindinukleotid (NADP) zugeschrieben. Später gelang der eindeutige Nachweis, dass für die Ca^{2+}-freisetzende Wirkung NAADP verantwortlich war (*20*). NAADP ist strukturell sehr nahe verwandt mit NADP (Abb. 3). NADP verfügt über eine Amidgruppe in 3‘-Position des Pyridinringes, wohingegen das NAADP eine Carboxylgruppe in dieser Position besitzt (*20*). Strukturell sind für die Ca^{2+}-Freisetzung die Carboxylgruppe in 3‘-Position des Pyridinringes, die Phosphatgruppe in 2‘-Position der Ribose und die 6‘-Aminogruppe des Adenins verantwortlich (Abb. 3). Ist die Carboxylgruppe in 4‘-Position des Pyridinringes anstatt in 3‘-Position wie bei NAADP bzw. ein neutral geladener Substituent an der 3‘-Position (z.B. die Amidgruppe im NADP) wird die Ca^{2+}-Freisetzung ebenso verhindert wie bei Fehlen der 2‘-Phosphatgruppe. Ersetzt man die 6‘-Aminogruppe durch eine Hydroxylgruppe, wird die Aktivität von NAADP um den Faktor 1000 verringert (*21*).

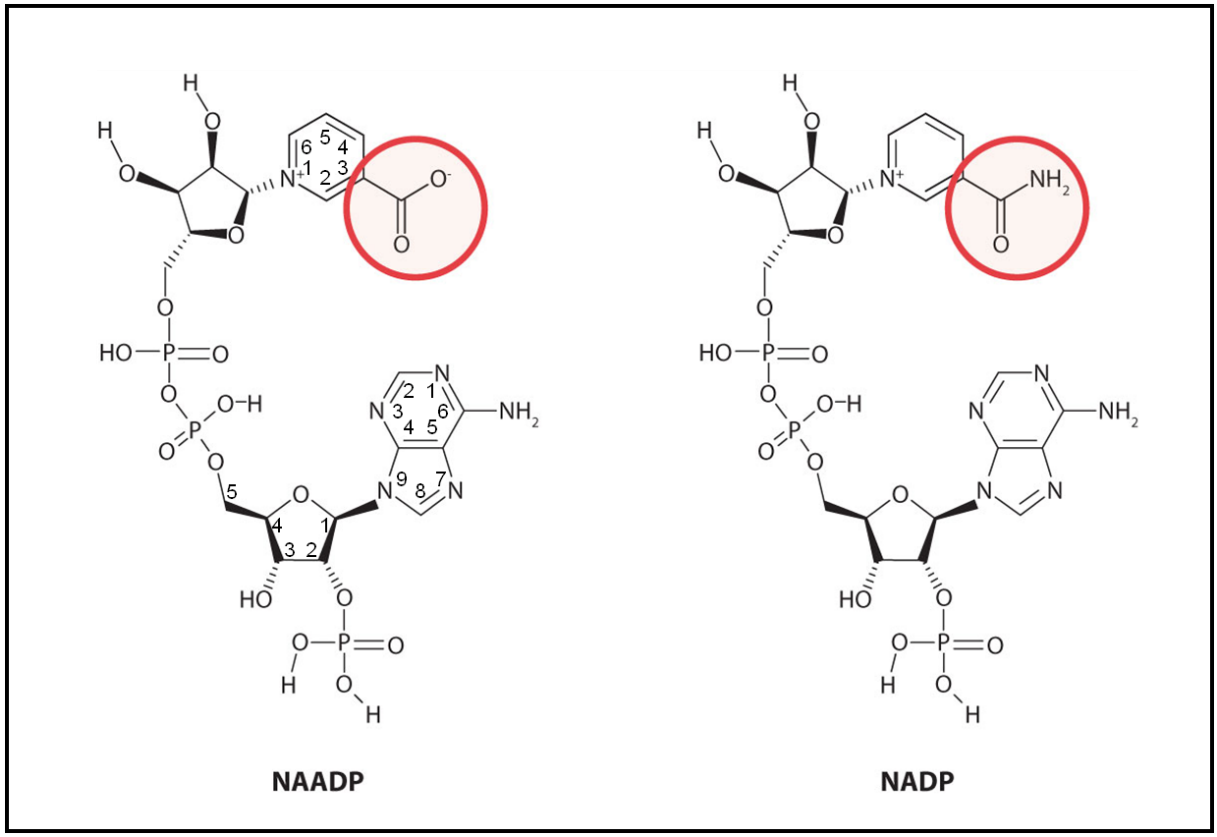

Abb. 3) Die chemischen Strukturen von NAADP und NADP. Der rote Kreis zeigt den einzigen strukturellen Unterschied zwischen NAADP und NADP (modifiziert nach A. Guse, *Sci.Signal.*, 2008)

Synthese und Abbau des NAADP

Es besteht momentan eine Kontroverse darüber, welche Enzyme in der Zelle NAADP synthetisieren. In Säugern wurden ADP-Ribosyl-Cyklasen beschrieben, die NAADP aus der Vorstufe NADP bilden. Zu dieser Gruppe von Enzymen gehört das Protein CD38, eine Cyklase die in vitro pH abhängig sowohl NAADP als auch cADPR synthetisiert (Abb. 4). Die Synthese von NAADP erfolgt über eine Basenaustauschreaktion, in der die Nikotinamidfunktion im NADP durch Nikotinsäure ersetzt wird (*22*). In Anwesenheit von hohen Ca^{2+} Konzentrationen wird die Basenaustauschreaktion unterdrückt und bereits synthetisiertes NAADP zu dem unwirksamen NAAD dephosphoryliert (*23*).

CD38 wurde ursprünglich als Ektoenzym beschrieben und vor Kurzem erstmals in Lysosomen nachgewiesen (*15*). Es ist allerdings unklar, auf welchem Weg NAADP aus dem Lysosom an seinen cytoplasmatischen Wirkort gelangt, da NAADP nicht membranpermeabel

ist. Man müsste daher postulieren, dass NAADP über einen hypothetischen Transporter aus den Lysosomen heraus transportiert werden kann.

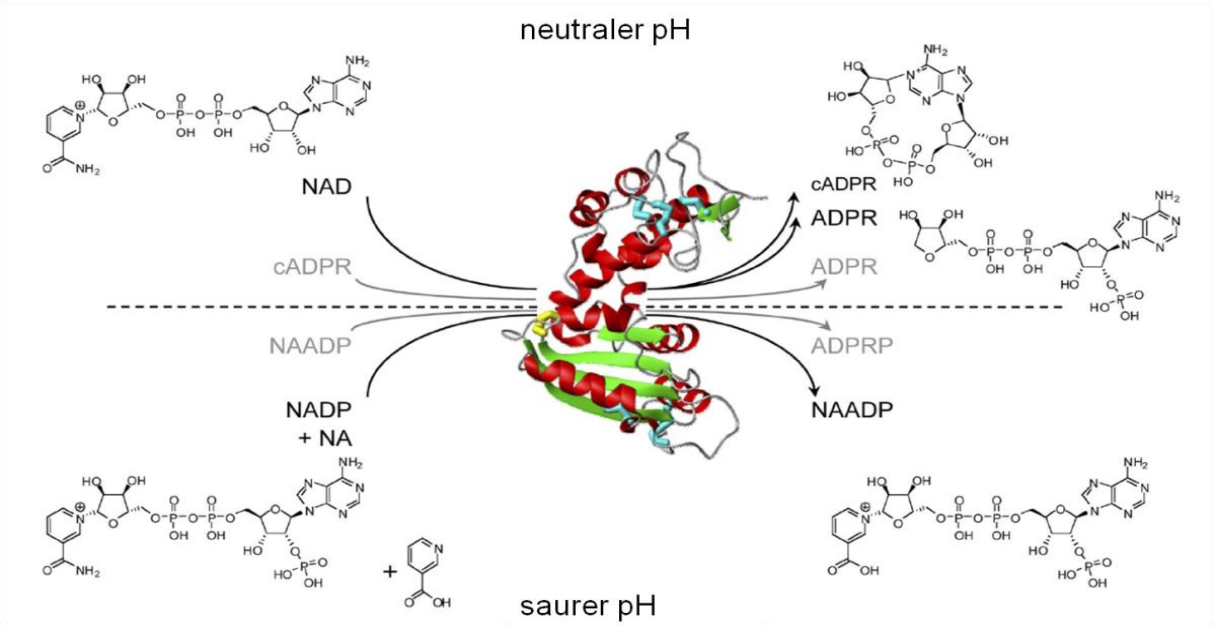

Abb. 4) CD38 produziert in Abhängigkeit vom pH-Wert NAADP oder cADPR, ADPR, ADPRP. Bei neutralem pH-Wert wird bevorzugt aus NAD cADPR bzw. ADPR gebildet bzw. cADPR zu ADPR umgewandelt. Bei einem sauren pH wird aus Nikotinamidadenindinukleotidphosphat (NADP) und Nikotinsäure (NA) durch eine Basenaustauschreaktion NAADP produziert. Zusätzlich kann NAADP zu ADPRP umgewandelt werden (modifiziert nach F. Malavasi et al., *Physio Rev*, 2008).

Eine weitere ungelöste Frage betrifft die Rezeptoren und Signalwege, welche die enzymatische Synthese von NAADP regulieren. Am besten untersucht sind die Signalwege von Cholezystokinin (CK) und Endothelin-1 (ET-1) (*24*). Bei Aktivierung dieser Signalwege kommt es neben der Bildung von NAADP zu einem parallelen Anstieg von IP_3. Es ist gegenwärtig nicht klar, ob ein Anstieg von NAADP regelmäßig von einem Anstieg weiterer sekundärer Botenstoffe begleitet ist oder auch isoliert auftreten kann. Weitere externe Stimuli für die NAADP Synthese sind Glukose in ß-Zellen des Pankreas (*25*) und die Stimulierung des T-Zellrezeptor/CD3 Komplexes in T-Zellen (*26*). Überdies hinaus fehlt der Anstieg der intrazellulären NAADP-Konzentration in CD 38 KO Mäusen nach Angiotensin II Stimulus von hepatischen Sternzellen bzw. nach Interleukin-8 Stimulus von Lymphokin-aktivierten Killerzellen (*27-28*).

Dosis-Wirkungskurve von NAADP

NAADP ist mit einem Wirkungsmaximum im nM Bereich der wirksamste aller bisher untersuchten Ca^{2+}-freisetzenden sekundären Botenstoffen. In Säugerzellen steigt die NAADP abhängige Ca^{2+}-Freisetzung konzentrationsabhängig mit einem sigmoidalen Kurvenverlauf an und erreicht ein Maximum bei 1 – 100 nM. Bei Verwendung von µM Konzentrationen wird die Ca^{2+}-Freisetzung inhibiert (*29*). Die NAADP-abhängige Ca^{2+}-Freisetzung hat also einen glockenförmigen Verlauf, der typisch ist für den NAADP-Rezeptor (Abb.5). Der Mechanismus für die Inaktivierung bzw. Desensitisierung ist bisher nicht aufgeklärt. Einer Hypothese zufolge existieren zwei verschiedene Bindungsstellen am NAADP-Rezeptor, die sich in den Affinitäten unterscheiden. Eine hochaffine Bindungsstelle soll für die Aktivierung, eine niederaffine Bindungsstelle soll für die Inaktivierung des Rezeptors verantwortlich sein. Die Existenz solcher Bindungsstellen wurde in Radioligandenbindungsstudien kürzlich bestätigt. An isolierten Membranen der ß-Zelllinie Min6 wurde eine hochaffine (K_d = 130 ± 31 nM) und eine niederaffine (K_d = 12 ± 0.6 µM) Bindungsstelle für NAADP nachgewiesen (*25*).

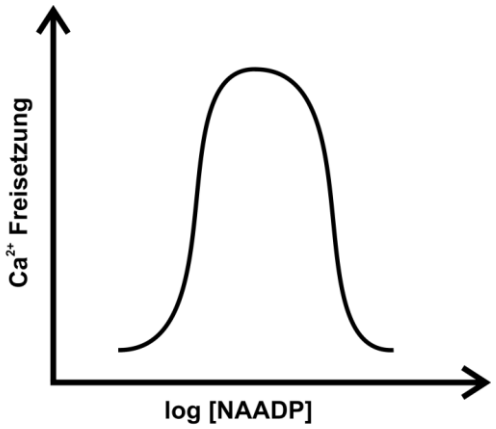

Abb. 5) Die Dosis-Wirkungskurve des nativen NAADP-Rezeptors ist glockenförmig mit einem Maximum zwischen 1 nM und 100 nM NAADP. Bei Verwendung µM Konzentrationen von NAADP sinkt die Ca^{2+}-Freisetzung als Folge der Inaktivierung des Rezeptors.

2. Ubiquitäre Expression des nativen NAADP-Rezeptors

Eine NAADP-abhängige Ca^{2+}-Freisetzung wurde in zahlreichen Zellen nachgewiesen (Tabelle 1) (*24*). Die physiologischen Prozesse, die von dieser Ca^{2+}-Freisetzung gesteuert werden sind bisher nur unvollständig untersucht. Es gibt erste Anhaltspunkte dafür, dass NAADP an der Regulation der Sekretion von Hormonen, der Kontraktion glatter Muskelzellen, der Aktivität von Neuronen, der Plättchenaktivierung und der T-Lymphozyten Regulierung beteiligt ist (*30*).

Tabelle 1: Gewebeverteilung des nativen NAADP-Rezeptors

Zelltyp bzw. Gewebe/Spezies	**NAADP-abhängige Ca^{2+}-Freisetzung**	**Bafilomycin A1 sensitiv**
Ei/Seeigel	√	√
Gehirn/Ratte	√	n.b.
Neuron/Meeresschnecke	√	n.b.
Neuromuskuläre Endplatte/Frosch	√	n.b.
Kortikales Neuron/Ratte	√	√
Herzmikrosomen/Hase	√	n.b.
Mesangialzellen/Ratte	√	n.b.
Oozyte/Seestern	√	n.b.
Oozyte/Aszidien	√	n.b.
glatte Muskelzelle/Ratte	√	√
Jurkat T-Zelle/Mensch	√	n.b.
Azinuszellen/Maus	√	√
ß-Zelle/Maus	√	n.b.
Pflanzenmikrosomen	√	n.b.

n.b.: nicht bestimmt

3. Lokalisation in Lysosomen und Endosomen

Die Lokalisation des nativen NAADP-Rezeptors im endolysosomalen System wurde mit pharmakologischen Tools in Ca^{2+} Imaging Experimenten in verschiedenen nativen Zellpräparationen nachgewiesen (*31-35*). Dazu wurden Zellen mit Fura-2 beladen und

entweder durch Gabe des membranpermeablen Acetoxymethylester des NAADPs oder durch intrazelluläre Applikation von NAADP eine Ca^{2+}-Freisetzung induziert. Für den funktionellen Nachweis des lysosomalen Ursprungs der NAADP-abhängigen Ca^{2+}-Freisetzung sprachen dabei folgende Kriterien:

1) Nach Vorbehandlung der Zellen mit Thapsigargin ist die NAADP-abhängige Ca^{2+}-Freisetzung induzierbar. Das bedeutet, die NAADP-abhängige Ca^{2+}-Freisetzung ist unabhängig vom ER.
2) Nach pharmakologischer Blockade der lysosomalen Ca^{2+}-Speicherung durch Bafilomycin A1 oder Glycylphenylalanin-2-naphthylamid (GPN) ist die NAADP-abhängige Ca^{2+}-Freisetzung nicht mehr induzierbar. Bafilomycin A1 ist ein Inhibitor der V-H^+ ATPase und zerstört den H^+-Gradienten, der für die Speicherung von Ca^{2+} benötigt wird (Abb. 2). GPN hemmt das lysosomale Enzym Cathepsin C und führt zur Schwellung bis hin zur Lyse des Lysosoms. Diese beiden Substanzen sind spezifisch für Lysosomen, d.h. sie haben keinen Einfluss auf die Funktion von anderen intrazellulären Speichern, wie dem ER oder den Mitochondrien.

Kopplungsmechanismus von nativen NAADP-Rezeptoren an sekundäre Ca^{2+}-abhängige Signalwege

Lysosomen sind mobile Organellen die mit einer Reihe zellulärer Membransysteme interagieren. Eine zunächst lokale Ca^{2+}-Freisetzung aus Lysosomen in der unmittelbaren Nähe von Ca^{2+}-abhängigen Effektoren könnte sekundäre Signaltransduktionswege anstoßen (Abb. 6). Zwei hypothetische Szenarien werden gegenwärtig in diesem Zusammenhang diskutiert (*24*). Erstens könnte lysosomal freigesetztes Ca^{2+} eine sekundäre Ca^{2+}-Freisetzung aus dem ER durch (Ko)Aktivierung von Ryanodinrezeptoren und/oder IP_3-Rezeptoren bewirken (Abb. 6A). Die anatomische Grundlage hierfür könnten die Lysosomen-ER

Junctions darstellen, die in glatten Muskelzellen der Pulmonalarterie beschrieben wurden. Es ist vorstellbar, dass ähnliche Mikrodomänen auch in anderen Zellen existieren. Zweitens könnte eine Ca^{2+}-Freisetzung in unmittelbarer Nähe der Plasmamembran dort lokalisierte Ca^{2+}-abhängige Ionenkanäle aktivieren (Abb. 6B) und damit Ionenströme sowie die globale zelluläre Erregbarkeit regulieren.

Neben den genannten Kopplungsmechanismen kann lysosomal freigesetztes Ca^{2+} möglicherweise auch auf die Funktion des jeweiligen Lysosoms selbst rückkoppeln (Abb. 6C). So wird vermutet, dass der luminale pH über einen solchen Feedbackmechanismus reguliert wird. Diese Hypothese beruht auf der Annahme, dass Lysosomen einen Ca^{2+}/H^{+}-Antiporter besitzen, der Ca^{2+} in die Lysosomen und H^{+} aus den Lysosomen heraus transportiert und von einer hohen lysosomalen H^{+}-Konzentration abhängt. Demnach müsste eine Zunahme der NAADP-vermittelten Ca^{2+}-Freisetzung zu einer lysosomalen Alkalisierung führen. Außerdem könnte der Rückkopplungsmechanismus die Fusion von Lysosomen mit Endosomen beeinflussen. (*docking*, Trigger, Fusion) (Abb. 6C).

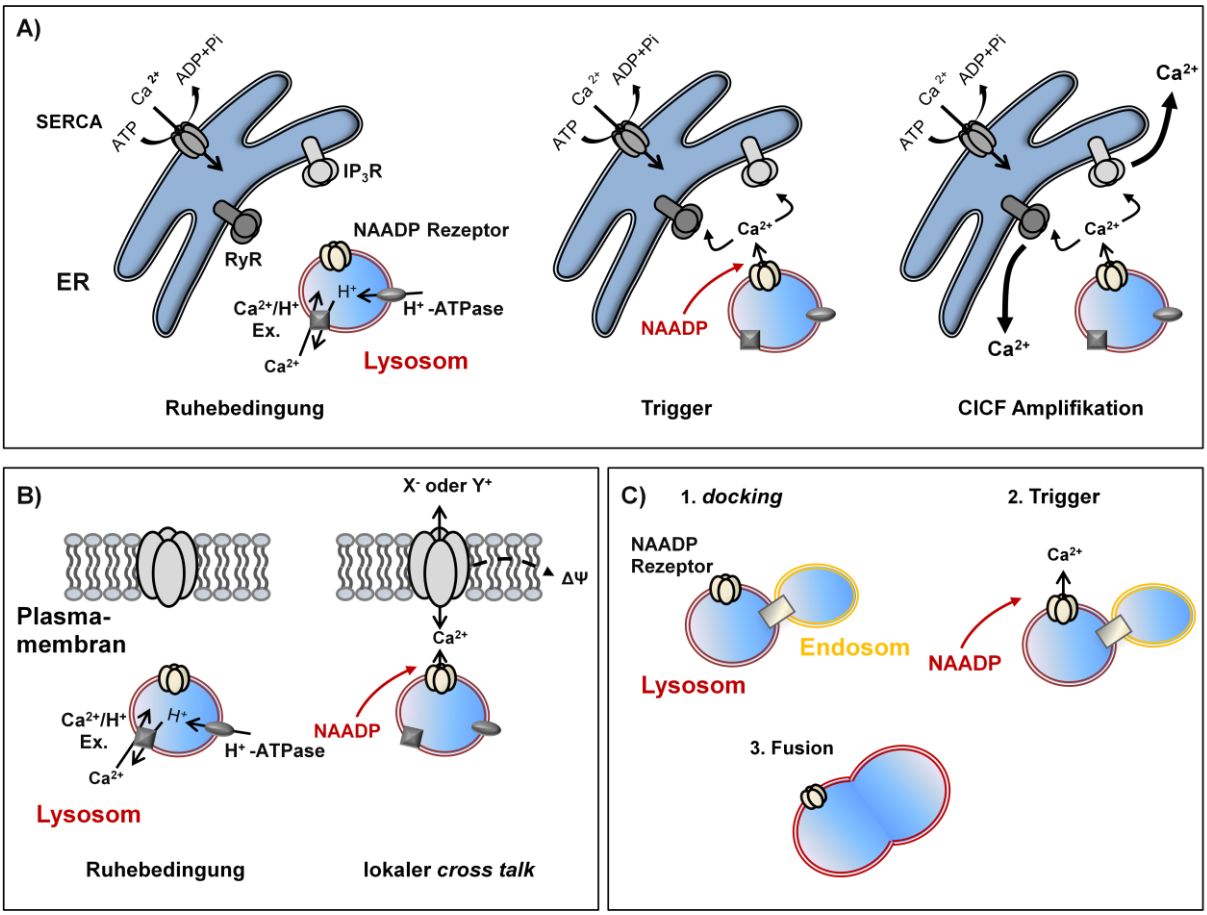

Abb. 6) Kopplungsmechanismus des nativen NAADP-Rezeptors an sekundäre Ca^{2+}-abhängige Signalwege. A) NAADP-abhängige Ca^{2+}-Freisetzung aus Lysosomen induziert eine Ca^{2+}-induzierte Ca^{2+}-Freisetzung aus dem ER (CICF). B) NAADP abhängige Ca^{2+}-Freisetzung aus Lysosomen aktiviert Ca^{2+}-abhängige Ionenkanäle in der Plasmamembran. C) NAADP reguliert die cytosolische und lysosomale Ca^{2+}-Konzentration und könnte die vesikuläre Fusion beeinflussen.

Identität des nativen NAADP-Rezeptors

In den letzten Jahren wurde intensiv nach dem molekularen Target gesucht, welches die NAADP-abhängige Ca^{2+}-Freisetzung vermittelt (NAADP-Rezeptor). Als Kandidaten wurden TRPML1-Kanäle (Mucolipin1), TRPM2-Kanäle und Ryanodinrezeptoren diskutiert (*24*). Allerdings ist die NAADP-Affinität dieser Kanäle zu niedrig, um als native Kandidaten für diesen Rezeptor in Frage zu kommen.

Entdeckung der *two-pore*-Kanäle

Vor Kurzem wurden die sogenannten *two-pore*-Kanäle (TPCN) entdeckt (*36*-*37*). TPCN-Kanäle gehören zur Superfamilie der spannungsabhängigen Kationenkanäle und sind strukturell insbesondere mit TRP-Kanälen verwandt. Der Grundbaustein von TRP-Kanälen ist eine Domäne mit sechs transmembranären α-Helices. Zwischen der fünften und sechsten Helix befindet sich eine schleifenförmige Struktur (*pore loop*), die den Selektivitätsfilter der ionenleitenden Pore darstellt. Ein funktioneller TRP-Kanal wird durch Tetramerisierung dieser Domänen gebildet. Bei TPCN-Kanälen sind zwei solcher Domänen, aus je sechs transmembranären α-Helices über einen intrazellulären Linker miteinander fusioniert. Da jede dieser Domänen einen *pore loop* enthält werden sie als *two-pore*-Kanäle bezeichnet. Der native Kanal setzt sich wahrscheinlich aus einem TPCN-Dimer zusammen, sodass sich eine pseudotetramere Kanaltopologie ergibt. Abbildung 7 zeigt die postulierte Struktur dieser Kanäle.

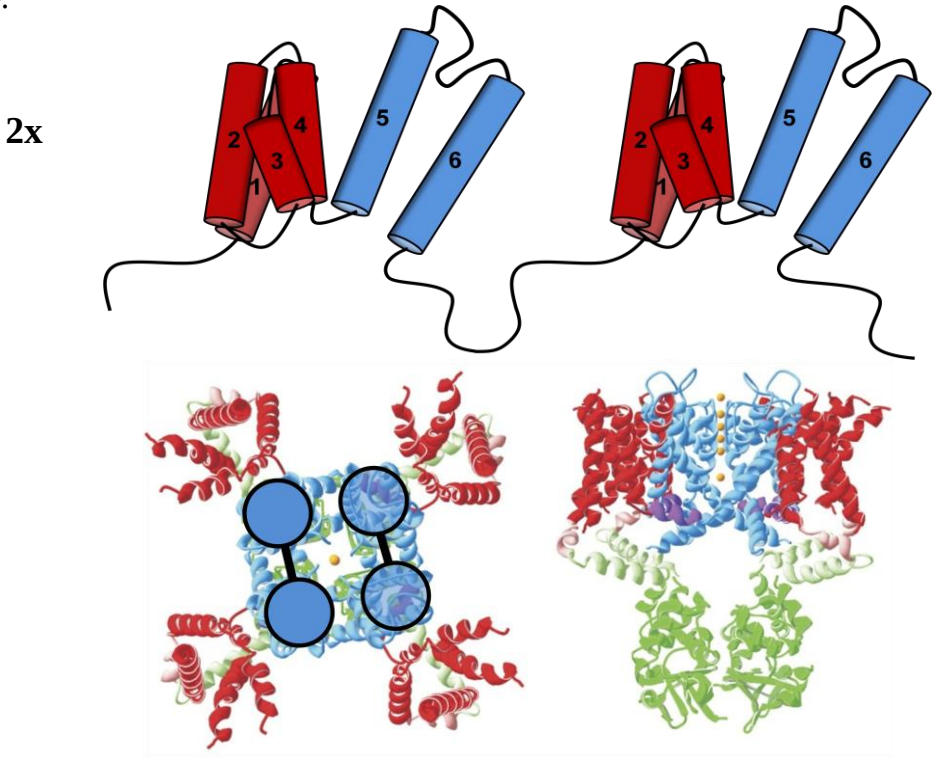

Abb. 7) Membrantopologie von TPCN-Kanälen. Oben: Struktur des TPCN-Kanal-Monomers. Unten: TPCN-Kanäle als Dimere. Die beiden Domänen des Monomers sind als Kreise dargestellt, die über einen Interdomänenlinker (schwarz) miteinander verbunden sind. Die beiden TPCN Monomere sind über die Kristallstruktur des *shaker* Kaliumkanals gelagert. (modifiziert nach F. Tombola, *Annu. Rev. Cell Dev. Biol.*, 2006)

Im Genom aller bisher untersuchten Säugetiere wurden die Gene für TPCN1 und TPCN2 identifiziert. Einige Säuger (u.a. Rind, Pferd und Kaninchen) besitzen zusätzlich ein Gen für TPCN3. Beim Menschen und Schimpansen ist das TPCN3-Gen trunkiert. Im Ratten- und Mäusegenom fehlt es vollständig. Daneben kommen TPCN-Gene in einigen Invertebraten und sogar in Pflanzen vor, nicht jedoch in *C. elegans* und in *Drosophila melanogaster* (*38*).

Erste Hinweise auf die Funktion der TPCN-Kanäle konnten durch Untersuchungen der Pflanze *Arabidopsis thaliana* gewonnen werden. In dieser Pflanze kommt lediglich ein *two-pore*-Kanal vor, der als AtTPC1 bezeichnet wird. Dieser Kanal wird in der Pflanzenvakuole exprimiert, einer Organelle die homolog zu den Lysosomen der Säugetiere ist. AtTPC1 leitet einen stark spannungsabhängigen, auswärtsgleichrichtenden Strom aus der Vakuole (Abb. 8) (*39*). Der Strom wird durch Ca^{2+} reguliert, d.h. nur in Gegenwart von hohen cytosolischen Ca^{2+}-Konzentrationen (> 5 µM) ist eine Ionenkanalaktivität messbar (*39*). Für die Regulation durch Ca^{2+} sind vermutlich die beiden vorhandenen EF-Hand-Motive im Interdomänenlinker des Kanalproteins verantwortlich (*40*). Dieser Strom ist in der Pflanzenphysiologie schon lange als SV Strom (*slow vacuolar current*) bekannt. Eine physiologische Rolle des SV Stroms wurde in mehreren Arbeiten beim hyperosmotischen Stress, der pathogenen Stressantwort, dem Wachstum, dem oxidativen Stress, dem Kälteschock, der Blätterwundheilung, der Auskeimung sowie der Stomatabewegung gezeigt (*38*). Zwischen dem TPCN-Kanal in Pflanzen und den TPCN-Kanälen in Säugetieren besteht eine Sequenzhomologie von etwa 20%. Daher sind direkte Schlussfolgerungen aus den Ergebnissen der Pflanze, über die Funktion der Kanäle in Säugetieren nicht möglich.

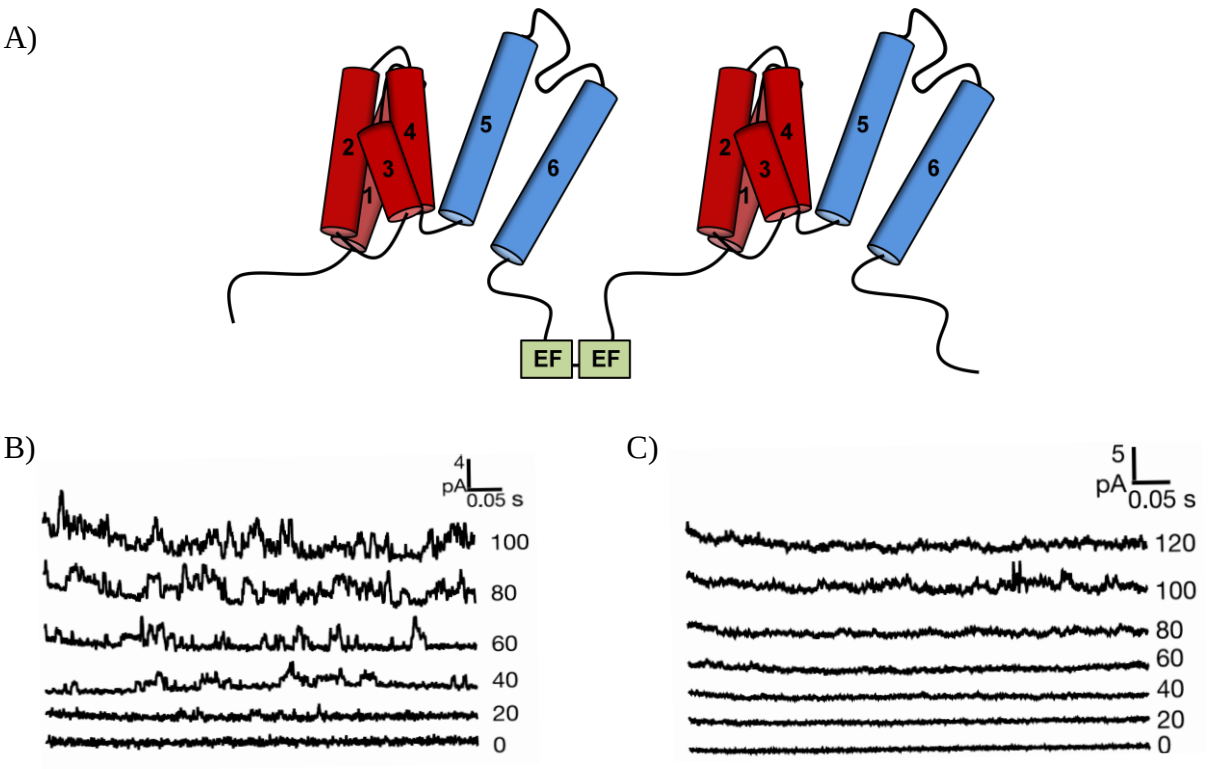

Abb. 8) Membrantopologie und Funktion des AtTPC1-Kanals A) Der AtTPC1-Kanal besitzt zwei EF-Hand-Motive im Interdomänenlinker. Diese EF-Hand-Motive sind in den TPCN-Kanälen der Säuger nicht vorhanden. Insgesamt besteht zwischen AtTPC1 und den TPCN-Kanälen der Säuger eine Sequenzhomologie von ~20%. B) Der auswärtsgleichrichtende stark Ca^{2+}-abhängige Ca^{2+}-Strom aus der Vakuole von *Arabidopsis thaliana*. C) Nach Knockdown des AtTPC1-Gens kann kein Ca^{2+}-Strom mehr beobachtet werden. (modifiziert nach Peiter et al., *Nature*, 2005)

Im Jahr 2000 wurde von Ishibashi et al. die erste Arbeit über einen TPCN-Kanal, eines Säugetiers publiziert. Die Autoren haben TPCN1 aus der Niere der Ratte kloniert und die Gewebeverteilung analysiert. Sie fanden heraus, dass TPCN1 besonders hoch im inneren medullären Sammelrohr der Niere exprimiert wird. Daneben wiesen sie den Kanal in der Leber, der Lunge, der Milz sowie im Herz, dem Gehirn und dem Skelettmuskel nach. Eine Expression in heterologen Zellsystemen und eine funktionelle Charakterisierung des TPCN1-Kanals gelang den Autoren nicht (*36*).

Die erste Arbeit über TPCN2 wurde 2008 publiziert. In dieser Arbeit zeigten Sulem et al. eine Beteiligung von TPCN2 bei der Haut- und Haarpigmentierung, in einer genetischen Studie an

Europäern (*41*). Die Funktion des TPCN2-Kanals war zu diesem Zeitpunkt vollkommen unbekannt.

6. Zielsetzung

Das Ziel der vorliegenden Arbeit war es die Hypothese zu bestätigen, dass der TPCN2-Ionenkanal der NAADP-Rezeptor ist. Dafür wurden folgende Fragen adressiert:

1) Welche grundlegenden Eigenschaften besitzt der TPCN2-Kanal (z.B. Gewebeverteilung, subzelluläre Lokalisation)?
2) Besitzt der TPCN2-Kanal die funktionellen Eigenschaften des nativen NAADP-Rezeptors (lysosomale, NAADP-abhängige Ca^{2+}-Freisetzung mit glockenförmiger Dosis-Wirkungskurve)?
3) Welches sind die elektrophysiologischen Eigenschaften des TPCN2-Kanals?

7. Kurzzusammenfassungen der Publikationen

7.1. The two-pore channel TPCN2 mediates NAADP-dependent Ca^{2+}-release from lysosomal stores

X. Zong*, **M. Schieder***, H. Cuny, S. Fenske, C. Gruner, K. Rötzer, O. Griesbeck, H. Harz, M. Biel, C. Wahl-Schott

2009; *Pflugers Arch*; 458, 891

*X. Zong and M. Schieder contributed equally

In der vorliegenden Arbeit wurde erstmals die *full length* cDNA von TPCN1 und TPCN2 aus dem Gehirn der Maus kloniert sowie biochemisch und funktionell charakterisiert. Mit Hilfe von Northern Blot Analysen und *in situ* Hybridisierungsexperimenten wurde die Gewebeverteilung beider Transkripte untersucht. Für beide Kanäle konnte ein Haupttranskript mit der berechneten Länge nachgewiesen werden. Es zeigte sich, dass die mRNA für TPCN1 und TPCN2 nahezu ubiquitär in unterschiedlichsten murinen Organen und Geweben vorkommt. Insgesamt war die Expression von TPCN1 höher, als die von TPCN2. In der weiteren Analyse haben wir uns auf den TPCN2-Kanal konzentriert. Um die Möglichkeit zu testen, ob TPCN2-Kanäle Homomere bilden wurden Ko-Immunopräzipitationsversuche (Ko-IP) durchgeführt. Dazu wurde TPCN2 mit einem myc-*tag* oder einem eGFP-*tag* fusioniert und in HEK293 Zellen koexprimiert. Bei den Ko-IP Experimenten kam heraus, dass TPCN2-Kanäle Homomere bilden. In analogen Experimenten konnten keine heteromeren Kanalkomplexe zwischen TPCN2 und TPCN1 nachgewiesen werden. In weiteren proteinbiochemischen Experimenten konnten wir zeigen, dass TPCN2 durch N-Glykosylierung modifiziert wird. Die Glykosylierung erfolgt an zwei Asparaginen (N594/N601) in der Porenschleife der zweiten Kanaldomäne. Zur Analyse der subzellulären Verteilung von TPCN2 wurden konfokalmikroskopische Untersuchungen durchgeführt. Diese Versuchsreihe ergab eine strikte intrazelluläre Lokalisation des Kanals, welche den Lysosomen zugeordnet werden konnte. Die funktionelle Charakterisierung von TPCN2 wurde

mit Ca^{2+} Imaging Experimenten durchgeführt. Dazu wurden HEK293 Zellen mit TPCN2 transfiziert und mit Fura-2 beladen. Die intrazelluläre Lokalisation des TPCN2 legt die Vermutung nahe, dass der Kanal durch sekundäre Botenstoffe aktiviert wird. Bisher ist der einzige bekannte sekundäre Botenstoff, der Ca^{2+} aus Lysosomen freisetzt Nikotinsäureadenindinukleotidphosphat (NAADP). Wir haben uns daher in den Ca^{2+} Imaging Experimenten auf NAADP konzentriert. Es zeigte sich, dass TPCN2-Kanäle NAADP-abhängig Ca^{2+} freisetzen. Charakteristisch ist die glockenförmige Dosis-Wirkungskurve mit einem Maximum bei etwa 30 nM NAADP. Der Rückgang der Ca^{2+}-Freisetzung bei Applikation von µM NAADP-Konzentrationen spricht für eine Desensitisierung oder einen spezifischen Inaktivierungsmechanismus der Kanäle. Der molekulare Mechanismus hierfür ist bisher nicht untersucht. Nach pharmakologischer Blockade der lysosomalen Ca^{2+}-Speicherung durch Bafilomycin A1, konnte keine NAADP-abhängige Ca^{2+}-Freisetzung beobachtet werden. Dieses Ergebnis spricht dafür, dass die NAADP-abhängige Ca^{2+}-Freisetzung aus den Lysosomen erfolgt. Nach Vorbehandlung der Zellen mit Thapsigargin, einer Substanz die die Ca^{2+}-Aufnahme in das ER blockiert, war die NAADP-abhängige Ca^{2+}-Freisetzung komplett erhalten. Das ER scheint daher bei der primär durch NAADP-induzierten Ca^{2+}-Freisetzung keine Rolle zu spielen.

Zusammengenommen zeigen die beschriebenen Analysen, dass der TPCN2-Kanal die kennzeichnenden Eigenschaften des nativen NAADP-Rezeptors besitzt.

7.2. Characterization of two-pore channel 2 (TPCN2)-mediated Ca^{2+}-currents in isolated lysosomes

M. Schieder, K. Rötzer, A. Brüggemann, M. Biel, C. A. Wahl-Schott

2010; *J Biol Chem*; 285, 21219

In bisherigen Studien wurden TPCN2-Kanäle ausschließlich mit Hilfe von Ca^{2+} Imaging Experimenten funktionell charakterisiert. Ca^{2+} Imaging Experimente an intakten Zellen lassen zwar Rückschlüsse über die Aktivierung der TPCN2-Kanäle zu, eignen sich aber nicht zur direkten funktionellen Analyse der Kanäle. Wir haben daher einen neuen Ansatz etabliert, der Strommessungen an biochemisch aufgereinigten und isolierten Lysosomen ermöglicht. Die Hauptfaktoren, welche die elektrophysiologische Analyse erschweren sind die geringe Größe der Lysosomen (0.3 – 1 µm) und ihre geringe Membranstabilität. Beide Faktoren verhindern den Zugriff mittels der üblichen Patch Clamp Protokolle. Um diese Probleme zu umgehen, wurde die planare Patch Clamp Methode modifiziert und auf isolierte und mit Vacuolin-1 vergrößerte Lysosomen angewendet. Bei dieser Methode werden die Lysosomen während der Zellkultur durch Behandlung mit Vacuolin-1 vergrößert und anschließend auf einer Festphasenmatrix, dem planaren Glaschip immobilisiert. Der Glaschip enthält eine Öffnung, die durch ihre Ausformung die Lysosomen bei elektrophysiologischen Experimenten mechanisch unterstützt, um ihre native Form zu erhalten.

Nach umfangreichen Verbesserungen an der Methode gelang es uns, direkt Ströme an intakten, einzelnen Lysosomen zu messen. Lysosomen, die TPCN2-Kanäle exprimierten, nicht aber Kontrolllysosomen ohne Überexpression zeigten einen deutlichen NAADP-aktivierbaren Ca^{2+}-Strom (I_{NAADP}). Der I_{NAADP} hat eine glockenförmige NAADP-Dosis-Wirkungskurve, mit einem Aktivierungsgipfel im nM Bereich. Die Eigenschaften des I_{NAADP} stimmen sehr gut mit den Eigenschaften der Ca^{2+}-Antworten in Imaging Experimenten überein. Durch den direkten elektrophysiologischen Zugang zu den isolierten Lysosomen war es möglich weitere Eigenschaften zu untersuchen. Es zeigte sich, dass I_{NAADP} durch den

intralysosomalen pH reguliert wird und eine extrem hohe Ca^{2+}-Selektivität besitzt. Die beiden *pore loops* der putativen Porenregion von TPCN2 zeigen eine deutliche Homologie zu den *pore loops* von hoch Ca^{2+}-selektiven Vertretern der TRP-Kanal Familie (TRPV5 und TRPV6). Insbesondere ist ein saurer Aminosäurerest im *pore loop* II der TPCN2-Kanäle konserviert (E643), der bei TRPV5 und TRPV6 für die hohe Ca^{2+}-/Mg^{2+}-Selektivität essentiell ist. Wir haben herausgefunden, dass der Austausch dieses Aminosäurerestes gegen eine ungeladene Aminosäure zum Verlust der hohen Ca^{2+}-Selektivität von TPCN2 führt. Dieses Ergebnis spricht für eine direkte Rolle von E643 bei der Ausbildung des Selektivitätsfilters und bildet die strukturelle Grundlage der hohen Ca^{2+}-Selektivität. In ihrer Gesamtheit belegen unsere Untersuchungen, dass TPCN2 ein NAADP-aktivierter und pH-regulierter Ca^{2+}-Kanal ist.

7.3. Planar patch clamp approach to characterize ionic currents from intact lysosomes

M. Schieder, K. Rötzer, A. Brüggemann, M. Biel, C. Wahl-Schott

2010; *Sci Signal*; 3, pl3

Diese Arbeit enthält in Protokollform eine detaillierte Beschreibung des von uns entwickelten planaren Patch Clamp Verfahrens, zur Charakterisierung von Ionenkanälen in isolierten Lysosomen. Mit dieser Methode können neben Lysosomen auch Mitochondrien und sehr wahrscheinlich auch das Endoplasmatische Retikulum (ER) untersucht werden. Das planare Patch Clamp Verfahren stellt somit einen großen Fortschritt in der Untersuchung von intrazellulären Ionenkanälen dar.

8. Literaturverzeichnis

1. M. J. Berridge, P. Lipp, M. D. Bootman, The versatility and universality of calcium signalling. *Nat Rev Mol Cell Biol* **1**, 11 (Oct, 2000).
2. F. H. Yu, W. A. Catterall, The VGL-chanome: a protein superfamily specialized for electrical signaling and ionic homeostasis. *Sci STKE* **2004**, re15 (Oct 5, 2004).
3. P. G. Hogan, R. S. Lewis, A. Rao, Molecular basis of calcium signaling in lymphocytes: STIM and ORAI. *Annu Rev Immunol* **28**, 491 (Mar, 2010).
4. L. Vaca, SOCIC: the store-operated calcium influx complex. *Cell Calcium* **47**, 199 (Mar, 2010).
5. J. P. Luzio, P. R. Pryor, N. A. Bright, Lysosomes: fusion and function. *Nat Rev Mol Cell Biol* **8**, 622 (Aug, 2007).
6. X. P. Dong, X. Wang, H. Xu, TRP channels of intracellular membranes. *J Neurochem* **113**, 313 (Apr 1).
7. R. Ruivo, C. Anne, C. Sagne, B. Gasnier, Molecular and cellular basis of lysosomal transmembrane protein dysfunction. *Biochim Biophys Acta* **1793**, 636 (Apr, 2009).
8. T. J. Jentsch, T. Maritzen, A. A. Zdebik, Chloride channel diseases resulting from impaired transepithelial transport or vesicular function. *J Clin Invest* **115**, 2039 (Aug, 2005).
9. B. Nilius, G. Owsianik, T. Voets, J. A. Peters, Transient receptor potential cation channels in disease. *Physiol Rev* **87**, 165 (Jan, 2007).
10. B. Nilius, T. Voets, J. Peters, TRP channels in disease. *Sci STKE* **2005**, re8 (Aug 2, 2005).
11. R. Puertollano, K. Kiselyov, TRPMLs: in sickness and in health. *Am J Physiol Renal Physiol* **296**, F1245 (Jun, 2009).
12. E. J. Parkinson-Lawrence *et al.*, Lysosomal storage disease: revealing lysosomal function and physiology. *Physiology (Bethesda)* **25**, 102 (Apr).

13. X. P. Dong, X. Wang, H. Xu, TRP channels of intracellular membranes. *J Neurochem* **113**, 313 (Apr, 2010).

14. A. Galione, NAADP, a new intracellular messenger that mobilizes Ca2+ from acidic stores. *Biochem Soc Trans* **34**, 922 (Nov, 2006).

15. A. H. Guse, H. C. Lee, NAADP: a universal Ca2+ trigger. *Sci Signal* **1**, re10 (2008).

16. K. A. Christensen, J. T. Myers, J. A. Swanson, pH-dependent regulation of lysosomal calcium in macrophages. *J Cell Sci* **115**, 599 (Feb 1, 2002).

17. J. V. Gerasimenko, A. V. Tepikin, O. H. Petersen, O. V. Gerasimenko, Calcium uptake via endocytosis with rapid release from acidifying endosomes. *Curr Biol* **8**, 1335 (Dec 3, 1998).

18. W. Van der Kloot, Loading and recycling of synaptic vesicles in the Torpedo electric organ and the vertebrate neuromuscular junction. *Prog Neurobiol* **71**, 269 (Nov, 2003).

19. B. E. Steinberg, N. Touret, M. Vargas-Caballero, S. Grinstein, In situ measurement of the electrical potential across the phagosomal membrane using FRET and its contribution to the proton-motive force. *Proc Natl Acad Sci U S A* **104**, 9523 (May 29, 2007).

20. H. C. Lee, R. Aarhus, A derivative of NADP mobilizes calcium stores insensitive to inositol trisphosphate and cyclic ADP-ribose. *J Biol Chem* **270**, 2152 (Feb 3, 1995).

21. H. C. Lee, R. Aarhus, Structural determinants of nicotinic acid adenine dinucleotide phosphate important for its calcium-mobilizing activity. *The Journal of biological chemistry* **272**, 20378 (Aug 15, 1997).

22. F. Malavasi *et al.*, Evolution and function of the ADP ribosyl cyclase/CD38 gene family in physiology and pathology. *Physiological reviews* **88**, 841 (Jul, 2008).

23. G. Berridge, R. Cramer, A. Galione, S. Patel, Metabolism of the novel Ca2+-mobilizing messenger nicotinic acid-adenine dinucleotide phosphate via a 2'-specific Ca2+-dependent phosphatase. *Biochem J* **365**, 295 (Jul 1, 2002).

24. A. Galione, NAADP receptors. *Cold Spring Harb Perspect Biol* **3**, a004036 (Jan, 2011).

25. R. Masgrau, G. C. Churchill, A. J. Morgan, S. J. Ashcroft, A. Galione, NAADP: a new second messenger for glucose-induced Ca2+ responses in clonal pancreatic beta cells. *Curr Biol* **13**, 247 (Feb 4, 2003).

26. A. Gasser, S. Bruhn, A. H. Guse, Second messenger function of nicotinic acid adenine dinucleotide phosphate revealed by an improved enzymatic cycling assay. *J Biol Chem* **281**, 16906 (Jun 23, 2006).

27. S. Y. Kim, B. H. Cho, U. H. Kim, CD38-mediated Ca2+ signaling contributes to angiotensin II-induced activation of hepatic stellate cells: attenuation of hepatic fibrosis by CD38 ablation. *J Biol Chem* **285**, 576 (Jan 1, 2010).

28. S. Y. Rah, M. Mushtaq, T. S. Nam, S. H. Kim, U. H. Kim, Generation of cyclic ADP-ribose and nicotinic acid adenine dinucleotide phosphate by CD38 for Ca2+ signaling in interleukin-8-treated lymphokine-activated killer cells. *J Biol Chem* **285**, 21877 (Jul 9, 2010).

29. J. M. Cancela, G. C. Churchill, A. Galione, Coordination of agonist-induced Ca2+-signalling patterns by NAADP in pancreatic acinar cells. *Nature* **398**, 74 (Mar 4, 1999).

30. M. X. Zhu, J. Ma, J. Parrington, A. Galione, A. M. Evans, TPCs: Endolysosomal channels for Ca2+ mobilization from acidic organelles triggered by NAADP. *FEBS Lett* **584**, 1966 (May 17, 2010).

31. A. Macgregor *et al.*, NAADP controls cross-talk between distinct Ca2+ stores in the heart. *J Biol Chem* **282**, 15302 (May 18, 2007).

32. E. Brailoiu *et al.*, Messenger-specific role for nicotinic acid adenine dinucleotide phosphate in neuronal differentiation. *J Biol Chem* **281**, 15923 (Jun 9, 2006).

33. A. Menteyne, A. Burdakov, G. Charpentier, O. H. Petersen, J. M. Cancela, Generation of specific Ca(2+) signals from Ca(2+) stores and endocytosis by differential coupling to messengers. *Curr Biol* **16**, 1931 (Oct 10, 2006).

34. M. Yamasaki *et al.*, Organelle selection determines agonist-specific Ca2+ signals in pancreatic acinar and beta cells. *J Biol Chem* **279**, 7234 (Feb 20, 2004).

35. N. P. Kinnear, F. X. Boittin, J. M. Thomas, A. Galione, A. M. Evans, Lysosome-sarcoplasmic reticulum junctions. A trigger zone for calcium signaling by nicotinic acid adenine dinucleotide phosphate and endothelin-1. *J Biol Chem* **279**, 54319 (Dec 24, 2004).

36. K. Ishibashi, M. Suzuki, M. Imai, Molecular cloning of a novel form (two-repeat) protein related to voltage-gated sodium and calcium channels. *Biochem Biophys Res Commun* **270**, 370 (Apr 13, 2000).

37. T. Furuichi, K. W. Cunningham, S. Muto, A putative two pore channel AtTPC1 mediates Ca(2+) flux in Arabidopsis leaf cells. *Plant & cell physiology* **42**, 900 (Sep, 2001).

38. S. Patel, J. S. Marchant, E. Brailoiu, Two-pore channels: Regulation by NAADP and customized roles in triggering calcium signals. *Cell Calcium* **47**, 480 (Jun, 2010).

39. E. Peiter *et al.*, The vacuolar Ca2+-activated channel TPC1 regulates germination and stomatal movement. *Nature* **434**, 404 (Mar 17, 2005).

40. R. D. Burgoyne, J. L. Weiss, The neuronal calcium sensor family of Ca2+-binding proteins. *Biochem J* **353**, 1 (Jan 1, 2001).

41. P. Sulem *et al.*, Two newly identified genetic determinants of pigmentation in Europeans. *Nat Genet* **40**, 835 (Jul, 2008).

11. Anhang

Publikation I

Pflugers Arch - Eur J Physiol (2009) 458:891–899
DOI 10.1007/s00424-009-0690-y

ION CHANNELS, RECEPTORS AND TRANSPORTERS

The two-pore channel TPCN2 mediates NAADP-dependent Ca^{2+}-release from lysosomal stores

Xiangang Zong · Michael Schieder · Hartmut Cuny · Stefanie Fenske · Christian Gruner · Katrin Rötzer · Oliver Griesbeck · Hartmann Harz · Martin Biel · Christian Wahl-Schott

Received: 30 May 2009 / Accepted: 2 June 2009 / Published online: 26 June 2009

Abstract Second messenger-induced Ca^{2+}-release from intracellular stores plays a key role in a multitude of physiological processes. In addition to 1,4,5-inositol trisphosphate (IP_3), Ca^{2+}, and cyclic ADP ribose (cADPR) that trigger Ca^{2+}-release from the endoplasmatic reticulum (ER), nicotinic acid adenine dinucleotide phosphate (NAADP) has been identified as a cellular metabolite that mediates Ca^{2+}-release from lysosomal stores. While NAADP-induced Ca^{2+}-release has been found in many tissues and cell types, the molecular identity of the channel (s) conferring this release remained elusive so far. Here, we show that TPCN2, a novel member of the two-pore cation channel family, displays the basic properties of native NAADP-dependent Ca^{2+}-release channels. TPCN2 transcripts are widely expressed in the body and encode a lysosomal protein forming homomers. TPCN2 mediates intracellular Ca^{2+}-release after activation with low-nanomolar concentrations of NAADP while it is desensitized by micromolar concentrations of this second messenger and is insensitive to the NAADP analog nicotinamide adenine dinucleotide phosphate (NADP). Furthermore, TPCN2-mediated Ca^{2+}-release is almost completely abolished when the capacity of lysosomes for storing Ca^{2+} is pharmacologically blocked. By contrast, TPCN2-specific Ca^{2+}-release is unaffected by emptying ER-based Ca^{2+} stores. In conclusion, these findings indicate that TPCN2 is a major component of the long-sought lysosomal NAADP-dependent Ca^{2+}-release channel.

Keywords TPCN2 · Two-pore channels · NAADP · Ca^{2+}-release · Lysosome · Acidic stores

Xiangang Zong and Michael Schieder contributed equally to this work.

Electronic supplementary material The online version of this article (doi:10.1007/s00424-009-0690-y) contains supplementary material, which is available to authorized users.

X. Zong · M. Schieder · H. Cuny · S. Fenske · C. Gruner · K. Rötzer · M. Biel · C. Wahl-Schott
Center for Integrated Protein Science CIPS-M and Zentrum für Pharmaforschung, Department Pharmazie, Ludwig-Maximilians-Universität München, Butenandtstr. 5-13, 81377 Munich, Germany

O. Griesbeck
Max Planck Institute of Neurobiology, Martinsried, Germany

H. Harz
BioImaging Zentrum der Ludwig-Maximilians-Universität München, Munich, Germany

M. Biel (✉) · C. Wahl-Schott (✉)
Department Pharmazie, Pharmakologie für Naturwissenschaften, Ludwig-Maximilians-Universität München, Butenandtstr. 5-13, 81377 München, Germany
e-mail: martin.biel@cup.uni-muenchen.de
e-mail: christian.wahl@cup.uni-muenchen.de

Introduction

Ca^{2+}-release from intracellular stores is a fundamental cellular process that is involved in the control of numerous physiological functions including muscle contraction, secretion, cell motility, and control of immune response [3, 11]. Given the diversity and complexity of these processes, it does not come as a surprise that Ca^{2+}-release is controlled by a complex array of signaling pathways and second messengers [19, 23, 29, 32]. NAADP is the latest entry in the list of Ca^{2+}-releasing molecules [19, 20]. This molecule is synthesized in the cell by ADP cyclases by exchanging the nicotinamide moiety of NADP with

nicotinic acid [21]. Notably, among all known Ca^{2+}-releasing agents, NAADP is the most potent one acting in the low-nanomolar concentration range [14]. The Ca^{2+}-releasing activity of NAADP was first discovered in the mid-1990s in acidic lysosome-related organelles of sea urchin eggs [20] and has since been demonstrated in many mammalian tissues and cell types [13, 17]. NAADP-mediated Ca^{2+}-release is characterized by a number of characteristic features. First of all, NAADP-dependent Ca^{2+}-release displays a characteristic bell-shaped dose-response curve with a peak in the low nanomolar concentration range and total loss of activity at high micromolar concentrations [8, 22]. Moreover, the native NAADP-dependent Ca^{2+}-release channel is insensitive to NADP which differs from NAADP only by the replacement of a carboxyl by an amid group [15]. Finally, in contrast to IP_3- and Ca^{2+}/cADPR-sensitive stores, NAADP mainly seems to induce Ca^{2+}-release from acidic lysosomal stores [10, 13], although in some cell types, NAADP-mediated Ca^{2+}-release was also found in ER-derived stores, including the nuclear envelope [15]

The molecular identity of the cellular NAADP receptor has been a matter of controversy [13, 17]. It was suggested that there may be no unique receptor for NAADP but that NAADP, like Ca^{2+} and cADPR, is an agonist of the ryanodine receptor (RyR) complex present in ER-derived calcium stores [15]. Other studies suggested that members of the transient receptor potential (TRP) channel family including TRPM2 [1] and TRPML1 [34] may be the cellular target protein of NAADP. However, the micromolar concentrations of NAADP required to fully activate these channel are one to two orders higher than those found for NAADP-mediated Ca^{2+}-release in a variety of cells. Since none of the so-far analyzed proteins matches the hallmarks of native NAADP-sensitive release channels in a satisfying fashion, we hypothesized that the major receptor of NAADP may be formed by another not yet characterized protein.

Materials and methods

Cloning of TPCN1 and TPCN2

For cloning of TPCN1, two cDNA fragments were amplified from mouse brain RNA by RT-PCR using the SuperScript III-One-Step Kit (Invitrogen; primers for fragment 1: TTA GAA ATG CCT CTG ATG GAA and ATG CTT TGA GGT GAA ATT CCC A; primers for fragment 2: CAG ACA GCA TTG GTT TGA TGA G and GTG GGG TTT CTT CCT AGT GGT CTC GAG CCT CAT ACC AGA CAC AGA CAC). Following restriction digests, the two fragments were assembled in pcDNA3 using the Hind III site in the 5′ untranslated region, the central EcoR I site, and the Xho I site generated by PCR in the 3′ untranslated region (fragment 1=1,413 bp, fragment 2=1,548 bp). For cloning of TPCN2, the complete open-reading frame was amplified from mouse brain RNA. The forward primer (GGC TGT GGT ACC GCC ACC ATG GCG GCA GAA GAG CAG C) binds to the 5′ end and contains a Kozak consensus sequence and a Kpn I restriction site for cloning; the reverse Primer (GCC GCT CGA GAG GCC AGC ATC TCT GTC CTG) binds to the 3′ untranslated region and contains a Xho I restriction site for cloning. After restriction digest with KpnI and XhoI, the 2,255-bp fragment was cloned into pcDNA3 vector (Invitrogen). All cloned sequences were verified by sequencing.

Northern blot

A mouse multiple tissue Northern blot (Applied Biosystems/Ambion, Austin, TX) containing 2 μg poly(A) RNA from heart, brain, liver, spleen, kidney, lung, thymus, testis, ovary, and embryo was hybridized with probes against TPCN1 and TPCN2. Probes covered the entire coding regions and were generated by random-primed labeling with a α^{32}P-dCTP (Roche, Basel, Switzerland). The membrane was hybridized overnight in stringent conditions. After two washing steps, the hybridized probe was visualized with a phosphorimager after an exposure time of 24 h or using a film (Hyperfilm MP, GE Healthcare, Piscataway, NJ) after a radiographic exposure time of 14 days at –80°C. The same blot was probed subsequently with TPCN1 and TPCN2 probes. The blot was stripped between each hybridization with SDS-containing buffer.

Production of TPCN2-specific antibodies

Polyclonal rabbit antisera were raised against a peptide (CDILE EPKEE ELMEK LHKHP) corresponding to aa 707 to 725 of TPCN2 plus a N-terminal cystein. For affinity purification of antibodies, the peptide was coupled to SulfoLink Coupling Gel (Thermo Fisher Scientific, Walthan, USA) in a column. Serum was loaded onto column and washed. Bound antibodies were eluted with 100 mM Glycin-HCl pH 2.8 in 800 μl aliquots and immediately neutralized with Tris-base.

Deglycosylation assay

The glycosylation deficient TPCN2 mutant (N594Q/N601Q) was cloned using the QuickChange Kit (Stratagene, La Jolla, CA). The deglycosylation assay was performed as described previously [25]. Briefly, HEK293 cells were transfected with TPCN2, TPCN2N594Q/N601Q, or EGFP-TPCN1 using the calcium phosphate method and lysed; 10 μg of

whole-cell lysates were incubated in the presence or absence of PNGase F or endoglycosidase H (both New England Biolabs, Ipswich, MA), according to the manufacturer's instruction. The protein denaturation was performed for 10 min at 45°C, the enzyme incubation for 1 h at 37°C. Cell lysates were then analyzed. Subsequently, proteins were subjected to Western blot analysis.

Coimmunoprecipitation in HEK293 cells

For coimmunoprecipitation experiments, TPCN2 and TPCN1 fusion proteins were generated with either myc tag fused at the N-terminus or with EGFP sequence fused at the N-terminus. For expression of recombinant proteins, HEK293 cells were transfected using the calcium phosphate method. Three days after transfection, HEK293 cells were lysed as described previously [30]. Equal amounts of protein (measured by Bradford assay) were incubated overnight at 4°C with 40 µl of protein A-Sepharose (GE Healthcare, Chalfont St. Giles, UK) and a specific antibody (Cell Signaling Technology, Beverly, MA) directed against the myc tag of examined proteins and 500 µl of buffer containing 50 mM Tris HCl (pH 7.4), 150 mM NaCl, 1 mM EDTA, and 50 mM Triton X-100, supplemented with PI. Beads were pelleted by centrifugation and washed three times with cold buffer containing 20 mM Tris HCl (pH 7.4), 5 mM $MgCl_2$, 0.5 mM DTT, 20% (*v*/*v*) Glycerol supplemented with PI. Interacting proteins were visualized after boiling for 5 min in Laemmli sample buffer by SDS/PAGE, Western blot analysis, and ECL (GE Healthcare). The antibodies used were as follows: anti-GFP for detection of EGFP-TPCN2 fusion protein. An antibody against GST (GE Healthcare) was used as control.

Immunocytochemistry

For immunodetection, COS-7 cells grown on glass coverslips in a 24-well plate were transiently transfected with TPCN2 cDNA using Fugene 6 (Roche Diagnostics). Cells were cultured in DMEM supplemented with 10% fetal calf serum and kept at 37°C, 10% CO_2 and fixed 1 or 2 days after transfection with 4% paraformaldehyde in PBS. Cells were permeabilized and blocked with 0.5% Triton X-100 and 5% Chemiblock (Millipore, Billerica, USA) in PBS. Cells were incubated with anti-TPCN2 (1:1000), anti-Myc (Cell Signaling, Danvers, MA; 1:1,000), anti-GFP (Clontech, Mountain View, USA; 1:500), anti-HA (Cell Signaling; 1:1000), anti-lamp1 (Abcam, Cambridge, USA; 1:250), and anti-Calnexin (Santa Cruz Biotechnology, Santa Cruz, USA; 1:100) primary antibodies in 2% Chemiblock (Millipore) and 0.3% Triton X-100 for 1 h. Then, cells were washed four times with PBS for 5 min each and incubated with AMCA (1:100), Cy2 (1:200), Cy3 (1:400), and Cy5 (1:400) secondary antibodies (all Jackson ImmunoResearch, West Grove, PA) in 2% Chemiblock (Millipore) for 1 h. Unbound antibodies were removed by three washing steps with PBS. For the staining of membranes and organelles, TRITC-WGA (membranes; 1:100; Sigma), Mitotracker Red CMX Ros (Mitochondria; 1:1,500; Invitrogen), and Hoechst 33342 (Nuclei; 0.4 µg/ml; Invitrogen) were used according to manufacturers' instructions. For visualization of lysosomes, in some experiments, a lamp1-EGFP fusion protein was co-expressed with TPCN2 (kind gift of Esteban C. Dell'Angelica, Dept Human Genetics, UCLA, USA). The glass coverslips were then mounted onto glass slides with Permafluor (Sigma, St. Louis, MO). Cells were visualized under a Zeiss LSM 510 laser confocal microscope as previously described [25].

Cell surface expression

To determine surface expression of TPCN2 in COS-7 cells, the HA epitope was inserted into the loop between the putative first and second transmembrane domains of TPCN2. Two mutagenic primers (GTC GGG AAC ATC GTA TGG GTA AGT CTT TGT GAA GGA AGA TGG G and TAC GAT GTT CCC GAC TAC GCA GAT GTG CGC TAC CGT TC) have been used to insert the hemagglutinin sequence (YPYDVPDYA) in frame between amino acid residues 92 and 93 of TPCN2 using the QuikChange Kit (Stratagene) according to the manufacturer's instruction. The sequence has been verified by sequencing. After transfection, cells were analyzed by immunocytochemistry as described above except for omitting the permeabilization step with Triton X-100 (nonpermeabilized cells). Control cells were treated equally but permeabilized.

Ca^{2+} imaging

Two days after transfection with TPCN2-EGFP or with the empty EGFP vector using Fugene 6 (Roche, Basel, Switzerland), HEK293 cells were loaded with Fura-2AM (5 µM) before measuring $[Ca^{2+}]_i$ and subsequently placed in extracellular recording solution containing (in mM) 140 NaCl, 5 KCl, 3 $MgCl_2$, 10 glucose, and 10 HEPES, pH 7.4. The fluorescence intensity of individual patch-clamped cells was monitored with a dual excitation fluorometric system using a Carl Zeiss Axiovert 135 fluorescence microscope equipped with a ×40 Plan-Apochromat 1.3 oil objective. The monochromatic light source (Polychrom II, TILL-Photonics) was tuned to excite Fura-2 fluorescence at 340 nm (F340) and 380 nm (F380) with a sampling frequency of 0.5 Hz for 3 ms each. Emission was detected at 450–550 nm using a PCO SensiCam VGA camera (Kelheim, Germany) and recorded and analyzed using

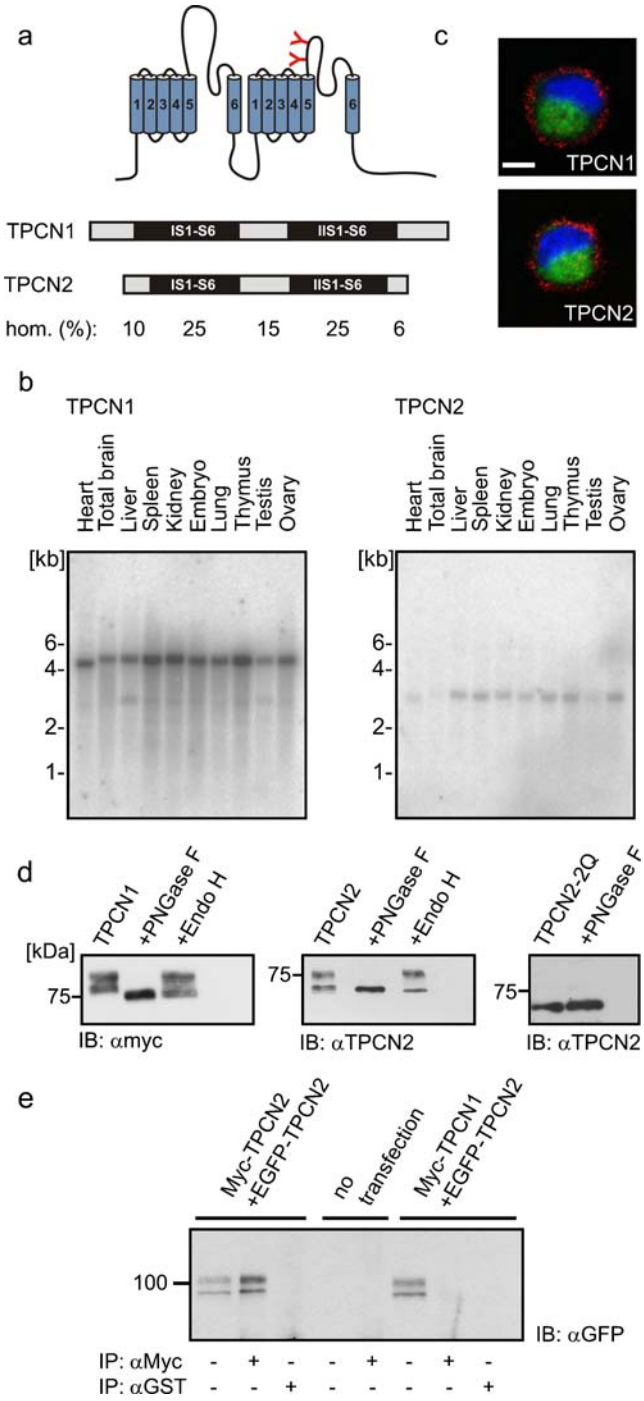

Fig. 1 Properties of two-pore channels. **a** *Upper panel* Transmembrane topology of TPCN1 and TPCN2. The predicted N-glycosylation sites are marked by *red forks*. *Lower panel* Schematic representation of the primary sequence of TPCN1 and TPCN2. The degree of sequence identity within the N- and C-termini, the two transmembrane building blocks and the interdomain linker is indicated. **b** Mouse multiple tissue northern blots of TPCN1 (*left panel*) and TPCN2 (*right panel*) demonstrate expression in all tissues investigated. **c** EGFP-TPCN1 (*upper panel*) and EGFP-TPCN2 (*lower panel*) channels expressed in HEK293 cells are localized intracellularly (*green* TPCN channels; *red* membrane marker, *blue* nuclei; *scale bar* 5 µm). **d** Western blots with lysates from HEK293 cells containing myc-tagged TPCN1 (*left panel*), wild-type TPCN2 (*middle*) panel, and a glycosylation-deficient TPCN2 double-mutant (TPCN-2Q; *right panel*). Ten micrograms of protein were applied per lane. **e** Lysates of HEK293 cells cotransfected with myc-tagged TPCN2 and EGFP-tagged TPCN2 (*lanes 1–3*) or myc-tagged TPCN1 and EGFP-tagged TPCN2 (*lanes 6–8*) were immunoprecipitated with anti-myc antibody (*lanes 2*, *5*, *7*) or anti-GST (control, *lanes 3 and 8*), blotted and probed with anti-GFP. *Lanes 1*, *6* input, *lane 4* negative control

Tillvision (Till Photonics, Martinsried, Germany). For internal perfusion with NAADP, NADP, or IP_3, Fura-2AM-loaded HEK293 cells were patched in standard whole-cell configuration. After establishing base line $[Ca^{2+}]_i$, the membrane was perforated, and the recording was continued in current clamp mode (I=0) [4]. Patch pipette solution contained in mM—140 KCl, 10 HEPES, 1 $MgCl_2$, and 0.05 BAPTA (pH 7.4) [6]. Fura-2 (pentapotassium salt, Invitrogen, Carlsbad, USA) was added to the standard internal solution at 7 µM in addition to preloading. Changes in Fura-2 fluorescence are reported as the fluorescence ratios (F_{340}/F_{380}) and are translated into apparent intracellular calcium concentration according to [16].

Statistics

All values are given as mean±SEM; n is the number of experiments. An unpaired t test was performed for the comparison between two groups. Significance was tested by ANOVA followed by Dunett test if multiple comparisons were made. Values of $P<0.05$ were considered significant.

Results

In our search for novel intracellular Ca^{2+}-release channels, we analyzed mammalian homologs of the two-pore cation channel TPC1, a Ca^{2+}-activated release channel identified in the vacuolar membrane of Arabidopsis thaliana and other plants [26]. A rat homolog of TPC1, designated TPCN1 was originally cloned from rat kidney but was not functionally characterized [18]. Based on sequence data from the gene bank, we cloned full-length murine TPCN1 and a novel homolog of this channel, TPCN2. Murine TPCN1 and TPCN2 show an overall sequence identity of about 20% to each other and to plant TPC1 [26] (Fig. 1a, Supplementary Fig. S1). TPCN channels represent a distinct branch within the superfamily of pore-loop channels [12, 31]. They are composed of two homologous building blocks each containing six transmembrane helices (S1–S6) and an ion-conducting pore loop between S5 and S6. The two putative pore loops of TPCN1 and TPCN2 show substantial homology to the pore of TPC1. In contrast to TPC1 both murine channels do not contain EF hand

motifs that may act as Ca^{2+} sensors in TPC1. Transcripts of TPCN1 and TPCN2 are widely expressed in the body (Fig. 1b, Supplementary Figs. S2, S3) with expression levels of TPCN1 usually being higher than those of TPCN2 (Fig. 1b, Supplementary Fig. S3). The size of the detected mRNA transcripts corresponds well to the size of the predicted sequence (4,705 bp for TPCN1 and 2,909 bp for TPCN2). Upon heterologous expression in HEK293 or COS-7 cells, both TPCN1 and TPCN2 are strictly localized in intracellular compartments (Figs. 1c, 2). Removal of the cytosolic N- and C-termini, as well as deletion of cryptic ER retention signals [33], present in the primary sequences of TPCN1 or TPCN2 (dileucine motifs starting at position 8 and 692 and a RxR motive starting at position 313 in TPCN2) did not result in increased expression in the plasma membrane (not shown). Two protein bands were detected in immunoblots for either TPCN1 or TPCN2 (Fig. 1d, left lanes in left and middle panels, see also Supplementary Fig. S4 for generation and validation of the TPCN2 antibody). The respective lower bands represent the core-glycosylated proteins since they are shifted to slightly lower molecular weights after incubation with endo-glycosidase H (EndoH). The upper band corresponds to the fully glycosylated mature channel which is resistant to Endo H and is sensitive to treatment with N-glycosidase F (PNGase F). Mutation of the two putative N-glycosylation sites in TPCN2 (N594 and N601) resulted in the production of a non-glycosylated protein (Fig. 1d, right panel). The size of the non-glycosylated TPCN1 and TPCN2 proteins was smaller than predicted from the primary sequence (78.5

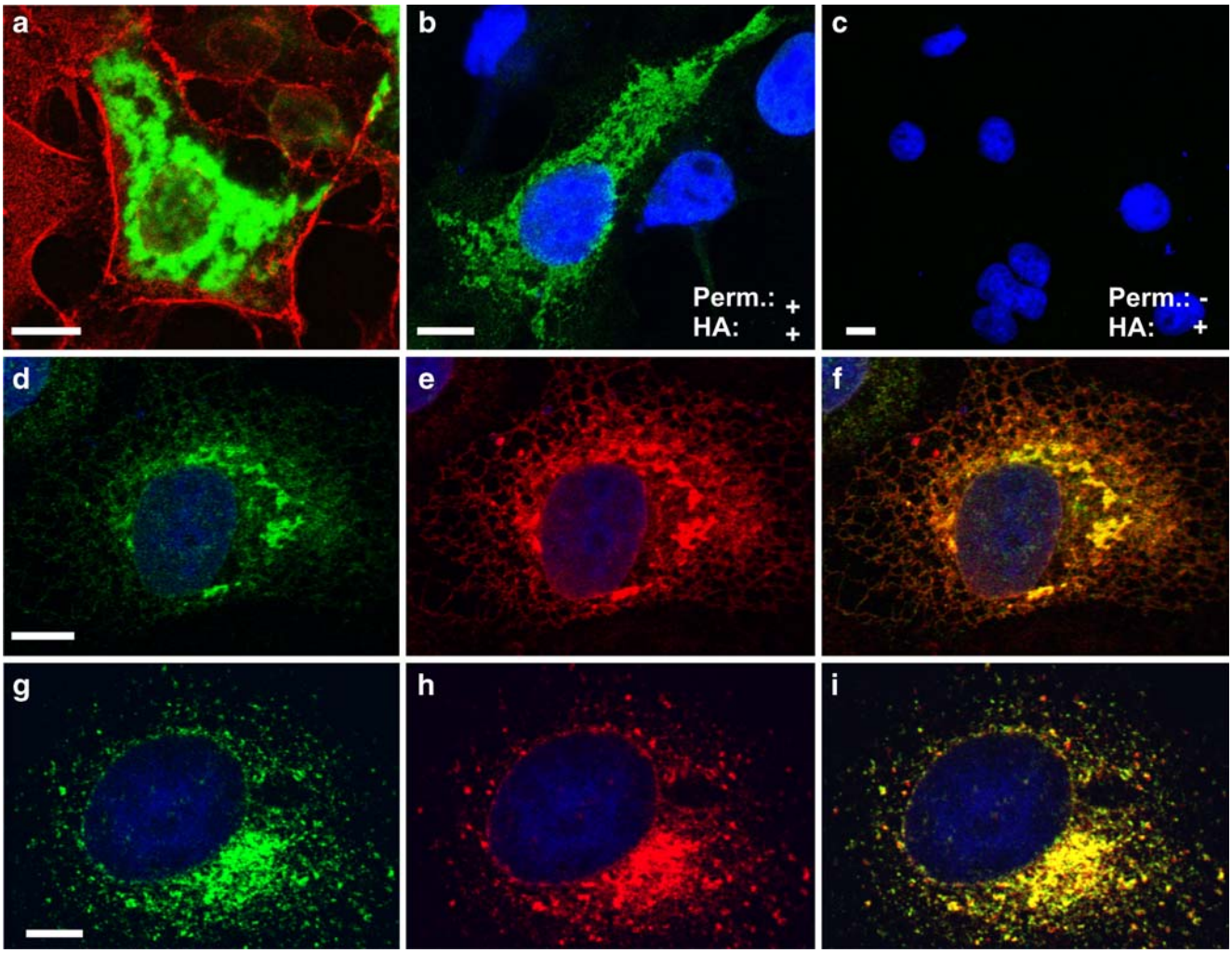

Fig. 2 TPCN2 is localized in the lysosomes. Immunocytochemistry of TPCN2 in COS-7 cells. **a** Strong TPCN2 staining (*green*) is observed in intracellular compartments. By contrast, TPCN2 is absent from the plasma membrane (visualized in *red* by a specific maker). **b** After permeabilization, HA-tagged TPCN2 is detected intracellularily. **c** HA-tagged TPCN2 is not detected in the membrane of non permeabilized cells. **d–f** Colocalization of TPCN2 (*green*) and the ER marker protein calnexin (*red*). Most TPCN2-positive structures (**d**) costaine for endoplasmic reticulum (**e**), yielding yellow in the overlay (**f**). **g–i** Colocalization of TPCN2 (*green*) and lamp1 (*red*). Most TPCN2-positive structures (**g**) costained for lysosomes (**h**), yielding yellow in the overlay (**i**). (*bars* 10 μm)

vs. 94.3 kDa for TPCN1 and 63 vs. 83.5 kDa for TPCN2). The apparent smaller molecular weight very likely arises from an aberrant gel mobility of the two proteins because it was also observed with EGFP-tagged TPCN channel proteins and with antibodies that were targeted to either N- or C-termini. Given the principal topology of pore-loop cation channels, it is very likely that two TPCN channel subunits assemble to form a complex with pseudo-tetrameric symmetry. Indeed, co-immunoprecipitation experiments showed that TPCN2 assembles with each other to form homomers (Fig. 1e). By contrast, TPCN2 did not form immunocomplexes with TPCN1 indicating that TPCN2–TPCN1 heteromers are not formed in the cell (Fig. 1e).

We next analyzed the subcellular expression of heterologously expressed TPCN2 in COS-7 cells. Using wild-type TPCN2 (Fig. 2a) and TPCN2 channels carrying a HA tag in the linker region between S1 and S2 (Fig. 2b, c), we confirmed that the channel is expressed purely in intracellular compartments. Within the cell, TPCN2 was present in the ER (Fig. 2d–f) and colocalized with the lysosomal-associated membrane protein 1 (lamp1) that is a specific marker for acidic lysosomes (Fig. 2g–i, Supplementary Fig. S5). By contrast, there was no significant overlap of the TPCN2 signal with a mitochondrial marker (MitoTracker, Supplementary Fig. S6).

The presence of TPCN2 in the ER and in lysomomes suggested that the protein may be a candidate for the NAADP-sensitive release channel [10, 13, 15]. In order to test this hypothesis, we measured calcium transients by using Fura-2 fluoresence in HEK293 cells (Fig. 3). Fluorescence was measured in the whole-cell patch-clamp configuration with a Ca^{2+}-free extracellular solution to ensure that changes in fluorescence were due to intracellular release. Cells transfected with TPCN2 that was N-terminally fused with EGFP to monitor expression (Supplementary Fig. S4) showed a similar basal Ca^{2+} concentration (62.9±21.4 nM; n=15) as control cells transfected with EGFP alone (50.6± 19.5 nM; n=8). Intracellular application of 30 nM NAADP produced a robust Ca^{2+} transient in TPCN2-transfected cells (Fig. 3a, c). The peak Ca^{2+} concentration was 292±54.9 nM (n=28) which is in excellent agreement with Ca^{2+} concentrations obtained in native cells after stimulation by NAADP [24, 28]. By contrast, control cells transfected with EGFP did not respond to NAADP (P<0.001; Fig. 3b, upper trace). Moreover, a close structural homolog of NAADP, NADP [15] did not yield a Ca^{2+} transient in TPCN2-transfected cells (P<0.001; Fig. 3b, middle trace). Remarkably, cells transfected with a TPCN1-EGFP fusion protein displayed no NAADP-sensitive Ca^{2+}-release (P<0.001). The dose–response curve of TPCN2 for NAADP has the typical bell-shape described for the native mammalian release channel [8, 22] (Fig. 3d). The channel starts to get activated in the low nanomolar range of NAADP, reaches a peak at about 30 nM and inactivated at higher concentrations of NAADP. At micromolar NAADP concentrations, the channel is totally inactive.

In HEK293 and COS-7 cells, TPCN2 was localized in the ER and the lyosomes. We tested from which of these compartments the observed Ca^{2+}-release was originating. Preincubation of the cells with bafilomycin, a specific

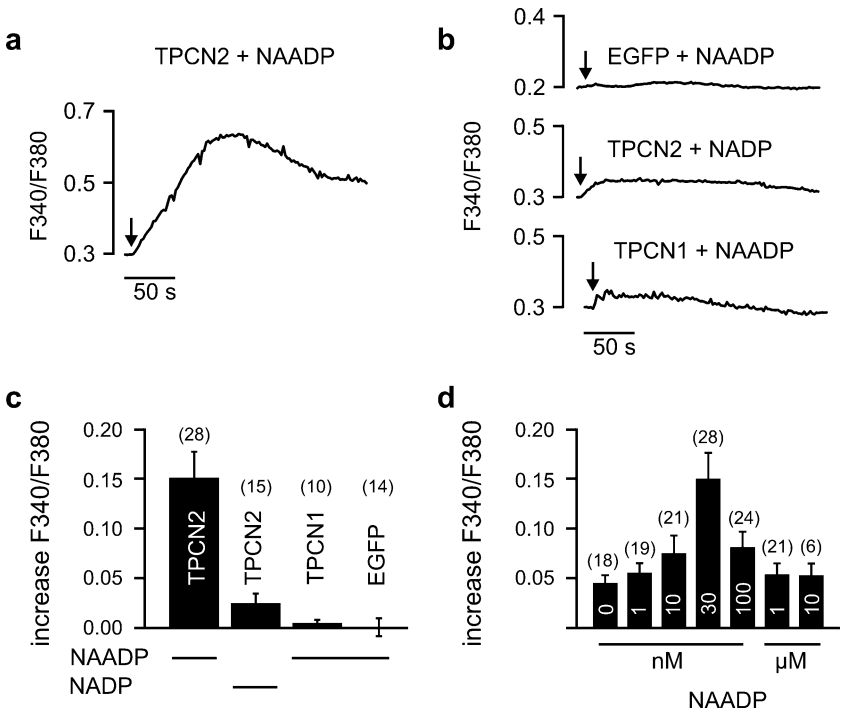

Fig. 3 NAADP triggers Ca^{2+}-release in HEK293 cells transfected with TPCN2. Application of 30 nM NAADP via the patch pipette induces Ca^{2+}-release from internal stores in cells transfected with TPCN2-EGFP (**a**) but not in cells transfected with EGFP alone (**b**, *upper panel*) or cells transfected with TPCN1-EGFP (**b**, *lower panel*). In cells transfected with TPCN2-EGFP, NADP (30 nM; negative control) did not induce Ca^{2+}-release (**b**, *middle panel*). The *arrows* in **a**, **b** indicate the start of cell perfusion. **c** Population data for experiments performed in (**a**, **b**). **d** Dose–response relationship of NAADP. All values are given as mean ± SEM. Number of cells measured is indicated in *brackets* in (**c**) and (**d**)

blocker of the vacuolar type-H^+ ATPase [5], almost completely abolished NAADP-mediated Ca^{2+}-release (Fig. 4a, d). By contrast, when ER stores were depleted by preincubation with the Ca^{2+}-ATPase inhibitor thapsigargin, NAADP-sensitive Ca^{2+}-release was not significantly reduced (Fig. 4b, d). IP_3 which opens IP_3Rs in the ER induced Ca^{2+}-release in control cells but did not evoke Ca^{2+} transients in thapsigargin-pretreated cells ($P<0.001$), demonstrating that the ER is functionally intact in TPCN2 expressing cells (Fig. 4c, d). These findings indicate that the observed Ca^{2+}-release in TPCN2 expressing cells arises from lysosomal stores while the channel in the ER is functionally silent. The reason for the lack of activity of the channel in the ER has to be determined. However, one may speculate that TPCN2 requires an acidic pH as present in the lysomes and/or the assembly with proteins specifically expressed in lysosomes to acquire biological activity.

Discussion

Here, we show that TPCN2, a novel member of the two-pore cation channel family, displays the basic functional properties of the native NAADP-dependent Ca^{2+}-release channel. TPCN2 transcripts are widely expressed in the body and have been found in all tissues and organs investigated. TPCN2 encodes a glycosylated 75 kD protein forming homomers. Given the principal transmembrane topology of pore-loop cation channels, it is very likely that two TPCN channel subunits assemble with each other to form a complex with pseudo-tetrameric symmetry. This finding is in principal agreement with the reported molecular mass of the NAADP receptor of approximately 120 kDa [2, 9] that roughly corresponds to a TPCN2 dimer. The TPCN2 protein is specifically localized in intracellular compartments and is totally absent from the plasma membrane. Within the cells, the protein was present in acidic lysosomes and in the ER. Since our functional studies strongly indicate that only the lysosomal fraction of TPCN2 is sensitive to NAADP, the presence of TPCN2 in the ER probably reflects an overexpression phenomenon, as reported for other proteins, including ion channels [27].

Several lines of evidence support the notion that TPCN2 is a key component of long-sought lysosomal NAADP receptor. First of all, TPCN2 is the first channel identified that responds to NAADP in the correct physiological

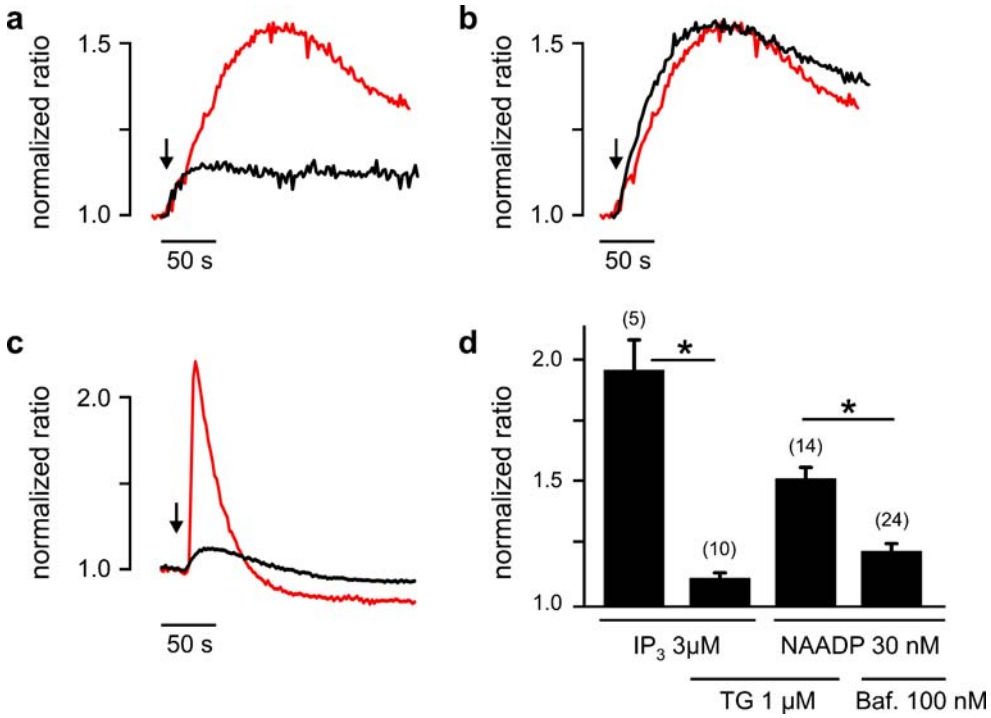

Fig. 4 TPCN2 mediates NAADP-dependent Ca^{2+}-release from lysosomes. **a** In HEK293 cells transfected with TPCN2-EGFP, preincubation (45 min) with 100 nM bafilomycin almost completely abolished NAADP (30 nM)-induced Ca^{2+}-release (*black line*). *Red line* control without pretreatment. **b** In HEK293 cells transfected with TPCN2-EGFP, preincubation (15 min) with 1 μM thapsigargin did not reduce NAADP-sensitive Ca^{2+}-release (*black line*). *Red line* same control as in (**a**). **c** Effect of thapsigargin (1 μM) on the IP3 (3 μM)-induced Ca^{2+}-release. Experiments were performed either with (*black line*) or without (*red line*) thapsigargin preincubation (1 μM; 15 min). *Arrows* in (**a–c**) indicate the start of cell perfusion. **d** Population data for experiments shown in (**a–c**). Number of cells measured is indicated in *brackets*. *Tg* thapsigargin; *Baf* bafilomycin; *IP3* Inositol-1,4,5-trisphosphate. Fluorescent ratio were normalized for better comparison

concentration range (low nM) [14]. Secondly, as described for native channels, TPCN2 is inactivated by micromolar NAADP concentrations [8, 22]. Thirdly, the channel is insensitive to the NAADP homolog NADP [15]. Also, the homologous TPCN1 channel is totally insensitive to NAADP. Fourthly, the increase in the intracellular Ca^{2+} concentration in cells expressing TPCN2 was in the same range as described for native NAADP-release channels [24, 28]. Fifthly, TPCN2 is localized in the acidic lysosomes, the subcelluar organelles where NAADP-dependent Ca^{2+}-release was originally described [10]. Importantly, TPCN2 activity is abolished by maneuvers that deplete the lysosomes [10, 13] indicating that the protein is fully operative in these organelles. By contrast, TPCN2 present in the ER was functionally silent. While we cannot exclude that TPCN2 requires assembly with another cellular protein to form a functional Ca^{2+}-release channel, the simplest interpretation of our work is that TPCN2 itself forms the lysosomal NAADP-sensitive Ca^{2+}-release channel. Further in vivo studies will be required to dissect the signaling cascades that control activation and modulation of TPCN2.

Acknowledgements Lamp1-EGFP was a kind gift of Esteban C. Dell'Angelica (Dept Human Genetics, UCLA; USA). This work was supported by the Deutsche Forschungsgemeinschaft (DFG).

Note added in proof: during the submission process, a paper was published presenting similar findings that TPCN2 mediates NAADP-dependent Ca^{2+}-release from acidic organelles [7].

References

1. Beck A, Kolisek M, Bagley LA, Fleig A, Penner R (2006) Nicotinic acid adenine dinucleotide phosphate and cyclic ADP-ribose regulate TRPM2 channels in T lymphocytes. Faseb J 20:962–964
2. Berridge G, Dickinson G, Parrington J, Galione A, Patel S (2002) Solubilization of receptors for the novel Ca^{2+}-mobilizing messenger, nicotinic acid adenine dinucleotide phosphate. J Biol Chem 277:43717–43723
3. Berridge MJ, Lipp P, Bootman MD (2000) The versatility and universality of calcium signalling. Nat Rev Mol Cell Biol 1:11–21
4. Boittin FX, Galione A, Evans AM (2002) Nicotinic acid adenine dinucleotide phosphate mediates Ca^{2+} signals and contraction in arterial smooth muscle via a two-pool mechanism. Circ Res 91:1168–1175
5. Bowman EJ, Siebers A, Altendorf K (1988) Bafilomycins: a class of inhibitors of membrane ATPases from microorganisms, animal cells, and plant cells. Proc Natl Acad Sci U S A 85:7972–7976
6. Broad LM, Armstrong DL, Putney JW Jr (1999) Role of the inositol 1,4,5-trisphosphate receptor in Ca(2+) feedback inhibition of calcium release-activated calcium current (I(crac)). J Biol Chem 274:32881–32888
7. Calcraft PJ, Ruas M, Pan Z, Cheng X, Arredouani A, Hao X, Tang J, Rietdorf K, Teboul L, Chuang KT, Lin P, Xiao R, Wang C, Zhu Y, Lin Y, Wyatt CN, Parrington J, Ma J, Evans AM, Galione A, Zhu MX (2009) NAADP mobilizes calcium from acidic organelles through two-pore channels. Nature 459:596–600
8. Cancela JM, Churchill GC, Galione A (1999) Coordination of agonist-induced Ca^{2+}-signalling patterns by NAADP in pancreatic acinar cells. Nature 398:74–76
9. Churamani D, Dickinson GD, Patel S (2005) NAADP binding to its target protein in sea urchin eggs requires phospholipids. Biochem J 386:497–504
10. Churchill GC, Okada Y, Thomas JM, Genazzani AA, Patel S, Galione A (2002) NAADP mobilizes Ca(2+) from reserve granules, lysosome-related organelles, in sea urchin eggs. Cell 111:703–708
11. Clapham DE (2007) Calcium signaling. Cell 131:1047–1058
12. Clapham DE, Garbers DL (2005) International Union of Pharmacology. L. Nomenclature and structure-function relationships of CatSper and two-pore channels. Pharmacol Rev 57:451–454
13. Galione A, Petersen OH (2005) The NAADP receptor: new receptors or new regulation? Mol Interv 5:73–79
14. Galione A, Ruas M (2005) NAADP receptors. Cell Calcium 38:273–280
15. Gerasimenko JV, Maruyama Y, Yano K, Dolman NJ, Tepikin AV, Petersen OH, Gerasimenko OV (2003) NAADP mobilizes Ca2+ from a thapsigargin-sensitive store in the nuclear envelope by activating ryanodine receptors. J Cell Biol 163:271–282
16. Grynkiewicz G, Poenie M, Tsien RY (1985) A new generation of Ca^{2+} indicators with greatly improved fluorescence properties. J Biol Chem 260:3440–3450
17. Guse AH, Lee HC (2008) NAADP: a universal Ca^{2+} trigger. Sci Signal 1:re10
18. Ishibashi K, Suzuki M, Imai M (2000) Molecular cloning of a novel form (two-repeat) protein related to voltage-gated sodium and calcium channels. Biochem Biophys Res Commun 270:370–376
19. Lee HC (2001) Physiological functions of cyclic ADP-ribose and NAADP as calcium messengers. Annu Rev Pharmacol Toxicol 41:317–345
20. Lee HC, Aarhus R (1995) A derivative of NADP mobilizes calcium stores insensitive to inositol trisphosphate and cyclic ADP-ribose. J Biol Chem 270:2152–2157
21. Malavasi F, Deaglio S, Funaro A, Ferrero E, Horenstein AL, Ortolan E, Vaisitti T, Aydin S (2008) Evolution and function of the ADP ribosyl cyclase/CD38 gene family in physiology and pathology. Physiol Rev 88:841–886
22. Masgrau R, Churchill GC, Morgan AJ, Ashcroft SJ, Galione A (2003) NAADP: a new second messenger for glucose-induced Ca2+ responses in clonal pancreatic beta cells. Curr Biol 13:247–251
23. Mikoshiba K (2007) IP3 receptor/Ca^{2+} channel: from discovery to new signaling concepts. J Neurochem 102:1426–1446
24. Morgan AJ, Galione A (2007) NAADP induces pH changes in the lumen of acidic Ca^{2+} stores. Biochem J 402:301–310
25. Much B, Wahl-Schott C, Zong X, Schneider A, Baumann L, Moosmang S, Ludwig A, Biel M (2003) Role of subunit heteromerization and N-linked glycosylation in the formation of functional hyperpolarization-activated cyclic nucleotide-gated channels. J Biol Chem 278:43781–43786
26. Peiter E, Maathuis FJ, Mills LN, Knight H, Pelloux J, Hetherington AM, Sanders D (2005) The vacuolar Ca2+-activated channel TPC1 regulates germination and stomatal movement. Nature 434:404–408

27. Schroeder BC, Waldegger S, Fehr S, Bleich M, Warth R, Greger R, Jentsch TJ (2000) A constitutively open potassium channel formed by KCNQ1 and KCNE3. Nature 403:196–199
28. Steen M, Kirchberger T, Guse AH (2007) NAADP mobilizes calcium from the endoplasmic reticular Ca(2+) store in T-lymphocytes. J Biol Chem 282:18864–18871
29. Streb H, Irvine RF, Berridge MJ, Schulz I (1983) Release of Ca^{2+} from a nonmitochondrial intracellular store in pancreatic acinar cells by inositol-1,4,5-trisphosphate. Nature 306:67–69
30. Wahl-Schott C, Baumann L, Cuny H, Eckert C, Griessmeier K, Biel M (2006) Switching off calcium-dependent inactivation in L-type calcium channels by an autoinhibitory domain. Proc Natl Acad Sci U S A 103:15657–15662
31. Yu FH, Catterall WA (2004) The VGL-chanome: a protein superfamily specialized for electrical signaling and ionic homeostasis. Sci STKE 2004:15
32. Zalk R, Lehnart SE, Marks AR (2007) Modulation of the ryanodine receptor and intracellular calcium. Annu Rev Biochem 76:367–385
33. Zerangue N, Schwappach B, Jan YN, Jan LY (1999) A new ER trafficking signal regulates the subunit stoichiometry of plasma membrane K(ATP) channels. Neuron 22:537–548
34. Zhang F, Jin S, Yi F, Li PL (2008) TRP-ML1 functions as a lysosomal NAADP-sensitive Ca(2+) release channel in coronary arterial myocytes. J Cell Mol Med. doi:10.1111/j.1582-4934.2008.00486.x

Supplemental Materials

Supplemental Experimental Procedures

RT-PCR

Murine poly(A) RNA from several tissues was isolated using the RNeasy mini kit (Qiagen, Hilden, Germany) following manufacturer's instruction and subjected to RT-PCR using the SuperScript III-One-Step Kit (Invitrogen) and gene specific primers. Exon spanning primer pairs were used for amplification of two pore channels and GAPDH to preclude amplification of genomic DNA. Primers for TPCN1 were CAC AAC TGG GAG ATG AAT TAT CA (sense) and TTG AAG GTG TCG AAC ACC ACG (antisense); primers for TPCN2 were GAC AAC AAC TCA GCT GTA TGT G (sense) and TGC CGA CTA ATG GTC TGC CAA (antisense). First strand cDNA was generated for 30 min at 55°C. For the PCR amplification the following conditions were used: 40 cycles (94°C for 30 s, 56°C for 30 s, and 68°C for 45 s) for TPCN1; 40 cycles (94°C for 30 s, 57°C for 30 s, and 68°C for 40 s) for TPCN2 and 20 cycles (94°C for 30 s, 55°C for 30 s, and 68°C for 40 s). Experimental conditions were optimized for each primer pair. Amplified cDNA was visualized on PAGE gels.

In situ hybridization

For *in situ* hybridization of TPCN1, a 471 bp covering the inter-domain-linker and part of the second domain was cloned into the same vector; opposing T3 and T7 RNA polymerase promoters were flanked by XbaI and EcoRI sites. For *in situ* hybridization of TPCN2, a 424 bp fragment of TPCN2 covering the c-terminal 131 amino acids and part of the 3'-UTR (bp1837-2261) was cloned into pBluescript II SK vector (Stratagene, La Jolla, CA) containing opposing T3 and T7 RNA polymerase promoters flanked by HindIII and XhoI restriction sites. All inserts were sequenced on both strands. Antisense and sense (control) radioactive probes labeled with

[α-^{35}S]UTP (1250Ci/mmol; Perkin Elmer) were *in vitro* transcribed from linearized vectors with [^{35}S]UTP and T7 or T3 RNA polymerase (Roche), respectively. Buffers were used according to manufacturer's protocol. Unincorporated nucleotides were removed by gel chromatography with a column (Nick-column, GE Healthcare). Probes were diluted to $10x10^6$ cpm/µl in hybridization buffer plus 0,5 µg/µl tRNA and stored at –20°C.

Serial 16 µm sections were cut in a mikrotom kryostat HM 500 (Microm GmbH, Walldof, Germany), fixed in 4% paraformaldehyde in phosphate-buffered saline (PBS), acetylated, dehydrated and hybridized as described in [1]. Sections were dehydrated and exposed to high-resolution X-ray films (Kodak Biomax, Sigma) for four days. Specificity of the signals was verified by comparing two independent probes and by using sense probes.

Supplementary References

1. Ludwig A, Flockerzi V, Hofmann F (1997) Regional expression and cellular localization of the alpha1 and beta subunit of high voltage-activated calcium channels in rat brain. J Neurosci 17:1339-49

Supplemental Figures

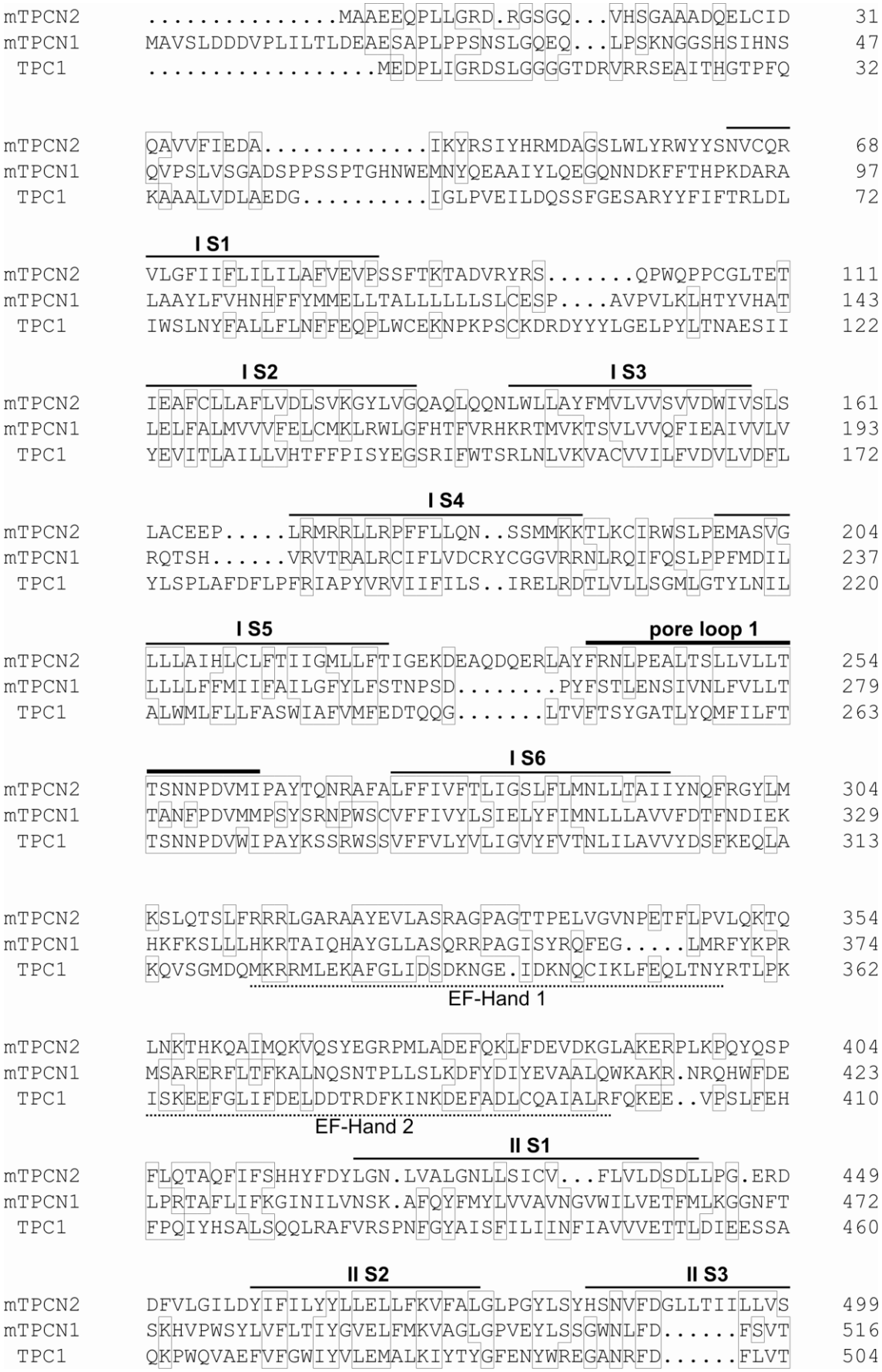
mTPCN2 ..............MAAEEQPLLGRD.RGSGQ...VHSGAAADQELCID 31
mTPCN1 MAVSLDDDVPLILTLDEAESAPLPPSNSLGQEQ...LPSKNGGSHSIHNS 47
TPC1 ..................MEDPLIGRDSLGGGGTDRVRRSEAITHGTPFQ 32
mTPCN2 QAVVFIEDA.............IKYRSIYHRMDAGSLWLYRWYYSNVCQR 68
mTPCN1 QVPSLVSGADSPPSSPTGHNWEMNYQEAAIYLQEGQNNDKFFTHPKDARA 97
TPC1 KAAALVDLAEDG..........IGLPVEILDQSSFGESARYYFIFTRLDL 72
I S1
mTPCN2 VLGFIIFLILILAFVEVPSSFTKTADVRYRS.......QPWQPPCGLTET 111
mTPCN1 LAAYLFVHNHFFYMMELLTALLLLLLSLCESP....AVPVLKLHTYVHAT 143
TPC1 IWSLNYFALLFLNFFEQPLWCEKNPKPSCKDRDYYYLGELPYLTNAESII 122
I S2
I S3
mTPCN2 IEAFCLLAFLVDLSVKGYLVGQAQLQQNLWLLAYFMVLVVSVVDWIVSLS 161
mTPCN1 LELFALMVVVFELCMKLRWLGFHTFVRHKRTMVKTSVLVVQFIEAIVVLV 193
TPC1 YEVITLAILLVHTFFPISYEGSRIFWTSRLNLVKVACVVILFVDVLVDFL 172
I S4
mTPCN2 LACEEP.....LRMRRLLRPFFLLQN..SSMMKKTLKCIRWSLPEMASVG 204
mTPCN1 RQTSH......VRVTRALRCIFLVDCRYCGGVRRNLRQIFQSLPPFMDIL 237
TPC1 YLSPLAFDFLPFRIAPYVRVIIFILS..IRELRDTLVLLSGMLGTYLNIL 220
I S5
pore loop 1
mTPCN2 LLLAIHLCLFTIIGMLLFTIGEKDEAQDQERLAYFRNLPEALTSLLVLLT 254
mTPCN1 LLLLFFMIIFAILGFYLFSTNPSD.........PYFSTLENSIVNLFVLLT 279
TPC1 ALWMLFLLFASWIAFVMFEDTQQG.......LTVFTSYGATLYQMFILFT 263
I S6
mTPCN2 TSNNPDVMIPAYTQNRAFALFFIVFTLIGSLFLMNLLTAIIYNQFRGYLM 304
mTPCN1 TANFPDVMMPSYSRNPWSCVFFIVYLSIELYFIMNLLLAVVFDTFNDIEK 329
TPC1 TSNNPDVWIPAYKSSRWSSVFFVLYVLIGVYFVTNLILAVVYDSFKEQLA 313
mTPCN2 KSLQTSLFRRRLGARAAYEVLASRAGPAGTTPELVGVNPETFLPVLQKTQ 354
mTPCN1 HKFKSLLLHKRTAIQHAYGLLASQRRPAGISYRQFEG.....LMRFYKPR 374
TPC1 KQVSGMDQMKRRMLEKAFGLIDSDKNGE.IDKNQCIKLFEQLTNYRTLPK 362
EF-Hand 1
mTPCN2 LNKTHKQAIMQKVQSYEGRPMLADEFQKLFDEVDKGLAKERPLKPQYQSP 404
mTPCN1 MSARERFLTFKALNQSNTPLLSLKDFYDIYEVAALQWKAKR.NRQHWFDE 423
TPC1 ISKEEFGLIFDELDDTRDFKINKDEFADLCQAIALRFQKEE..VPSLFEH 410
EF-Hand 2
II S1
mTPCN2 FLQTAQFIFSHHYFDYLGN.LVALGNLLSICV...FLVLDSDLLPG.ERD 449
mTPCN1 LPRTAFLIFKGINILVNSK.AFQYFMYLVVAVNGVWILVETFMLKGGNFT 472
TPC1 FPQIYHSALSQQLRAFVRSPNFGYAISFILIINFIAVVVETTLDIEESSA 460
II S2
II S3
mTPCN2 DFVLGILDYIFILYYLLELLFKVFALGLPGYLSYHSNVFDGLLTIILLVS 499
mTPCN1 SKHVPWSYLVFLTIYGVELFMKVAGLGPVEYLSSGWNLFD......FSVT 516
TPC1 QKPWQVAEFVFGWIYVLEMALKIYTYGFENYWREGANRFD......FLVT 504

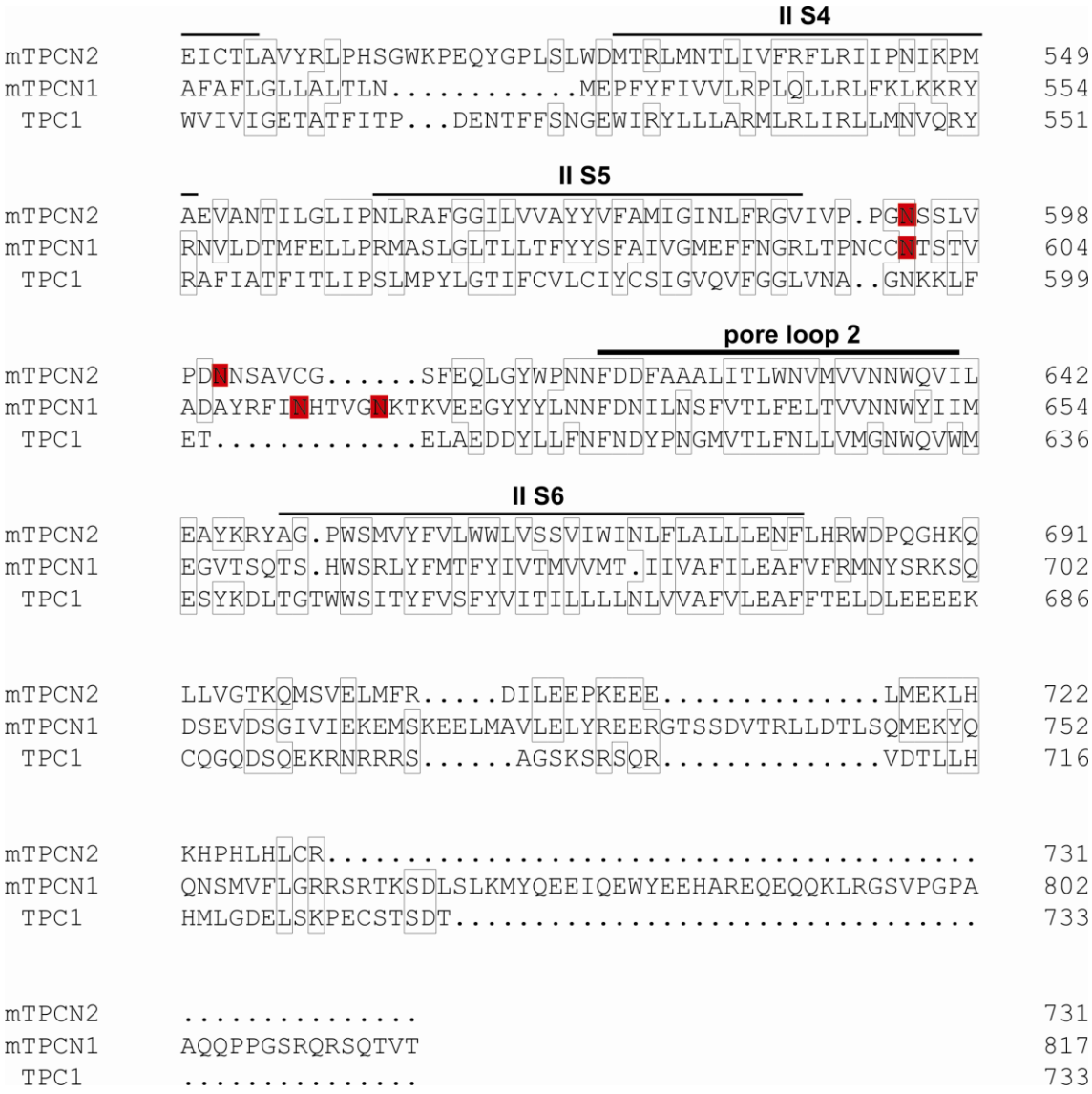

Fig. S1 Sequence alignment of mouse TPCN1, TPCN2 and TPC1 from Arabidopsis thaliana. Bars on top of the alignment indicate the putative transmembrane segments of domain 1 (IS1-IS6) and domain 2 (IIS1-IIS6) including the two pore loops. The two EF hand motifs present in the sequence of TPC1 are marked by dotted lines. Putative N-linked glycosylation sites are marked in red.

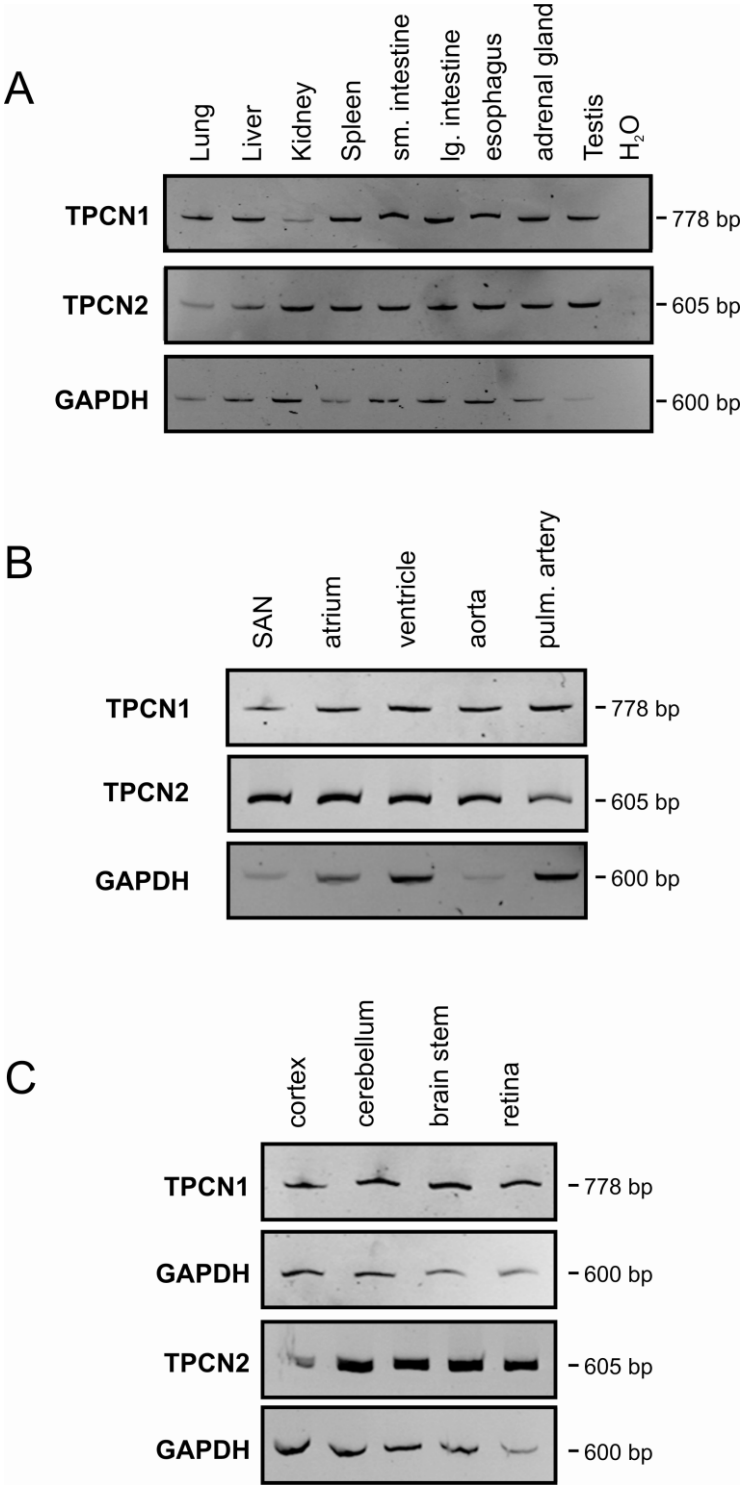

Fig. S2 Tissue Expression of TPCN1 and TPCN2. Poly(A) RNA was used for RT-PCR analyses targeting TPCN1 and TPCN2 and GAPDH transcripts in multiple murine tissues (A) in the cardiovascular system (B) and brain (C). SAN, sinoatrial node. pulm., pulmonary.

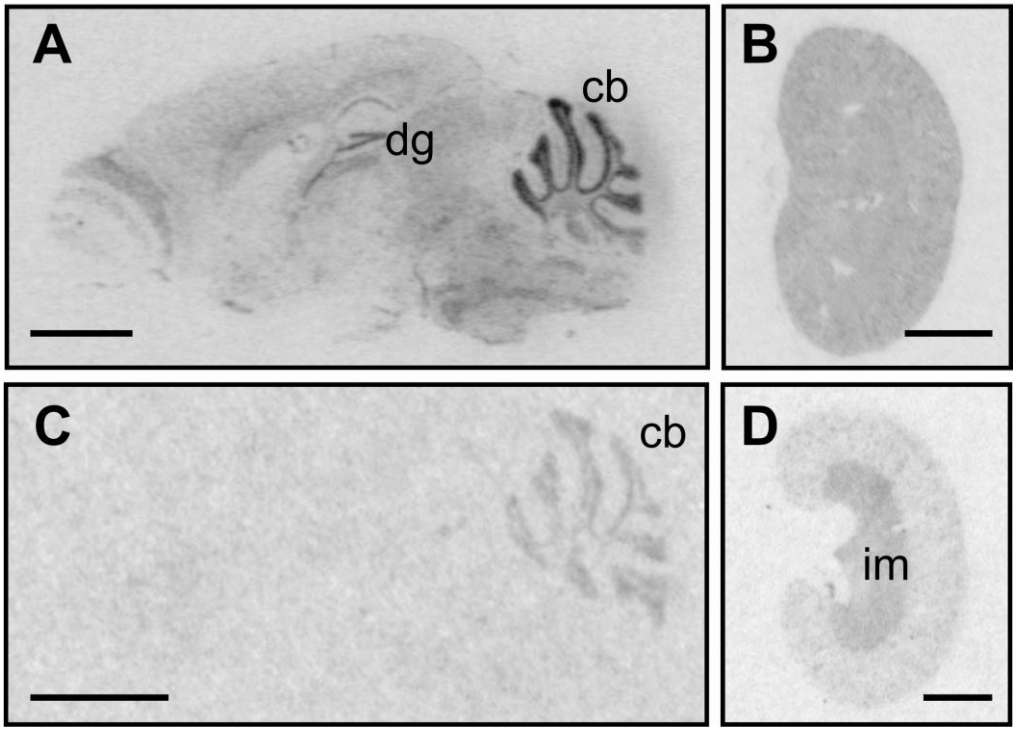

Fig. S3 Expression of TPCN1 and TPCN2 channel transcripts mouse brain and kidney. Autoradiograms of whole brain sections hybridized with riboprobes against TPCN1 (A) and TPCN2 (C) reveal high TPCN1 expression in the cerebellum, dendate gyrus of the hippocampus and moderate expression in the remaining brain. TPCN2 is mainly restricted to the cerebellum (C). TPCN1 and TPCN2 expression overlaps in the cerebellum. (B) and (D), Expression of two pore channels in the kidney. TPCN1 is evenly expressed throughout the renal cortex and medulla (B), while TPCN2 is mainly expressed in the inner renal medulla (D). TPCN1 and TPCN2 expression overlaps in the inner renal medulla. dg: dentate gyrus; cb: cerebellum; im: inner medulla of the kidney;. Scale bar in (A-D): 2.5 mm, in (E-J): 200µm.

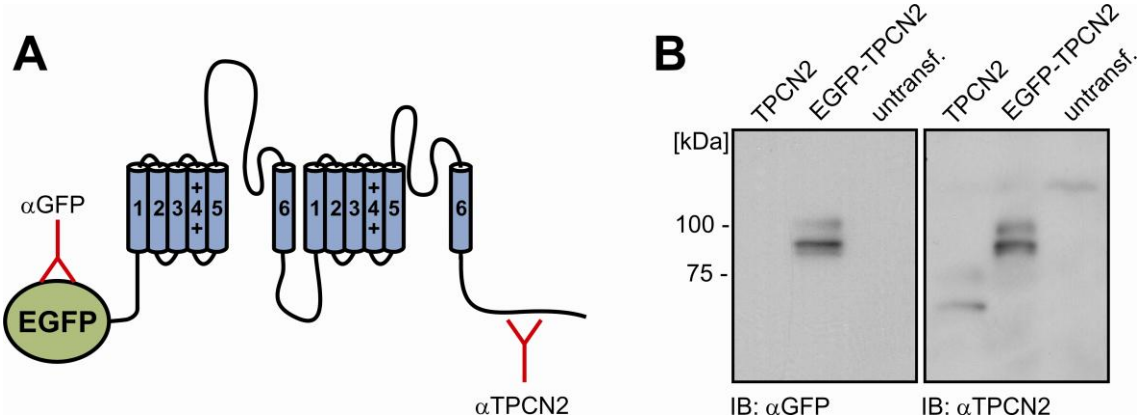

Fig. S4 Evaluation of the anti-TPCN2 antibody using a EGFP-tagged TPCN2 fusion protein. (A), Antibodies directed against EGFP and TPCN2 are indicated. (B), Lysates from HEK-293 cells transfected with TPCN2 (lane1) or EGFP-TPCN2 fusion protein (lane 2). lane 3: lysates from unfransfected HEK-293 cells (negative control) 20 µg total protein from HEK cell lysates was used for each lane. Anti-TPCN2 and anti-GFP antibody both specifically recognize gylcosylated and unglycosylated EGFP-TPCN2 fusion protein.

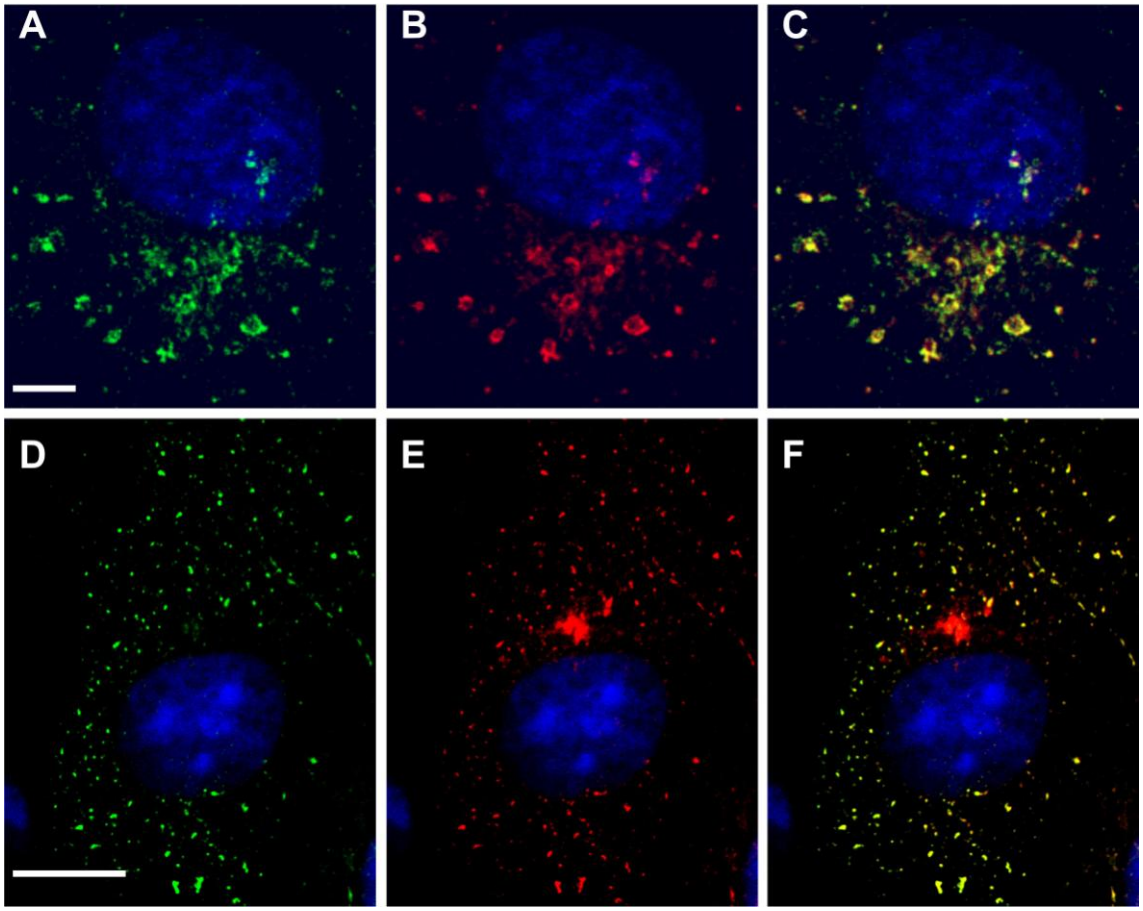

Fig. S5 TPCN2 is localized in lysosomes in COS-7 cells. Confocal image demonstrating colocalization of TPCN2 (green) and lysosomes (red) in high resolution in two different cells (cell 1: A-C, cell 2: D-F). scale bars: 5 µm

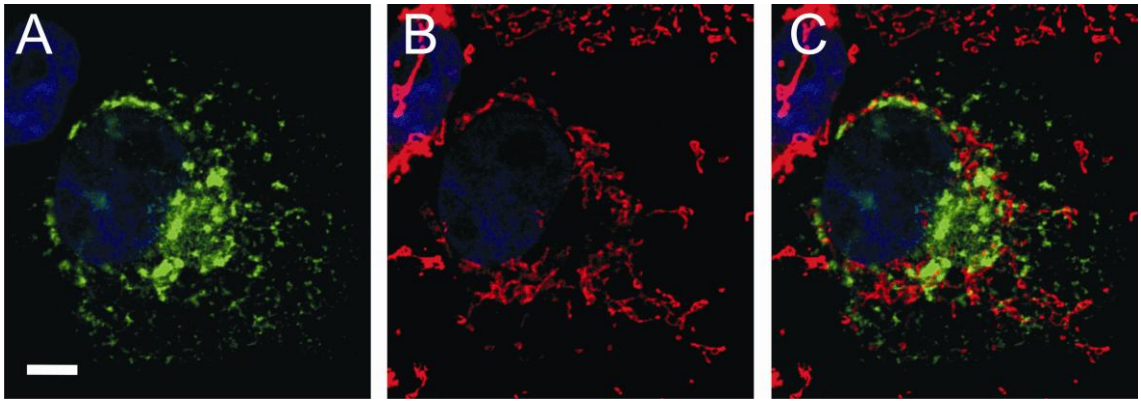

Fig. S6 TPCN2 is not localized in mitochondria of COS-7 cells. Immunocytochemistry of TPCN2 in COS-7 cells. (A), Intracellular staining of TPCN2 (green) and mitoctracker (B, red). Merged image in c shows no costaining with mitochondria. scale bars: 5 μm.

Publikation II

This paper is available online at www.jbc.org

THE JOURNAL OF BIOLOGICAL CHEMISTRY VOL. 285, NO. 28, pp. 21219–21222, July 9, 2010

Characterization of Two-pore Channel 2 (TPCN2)-mediated Ca^{2+} Currents in Isolated Lysosomes*[S]

Received for publication, May 10, 2010, and in revised form, May 18, 2010
Published, JBC Papers in Press, May 21, 2010, DOI 10.1074/jbc.C110.143123

Michael Schieder[‡], Katrin Rötzer[‡], Andrea Brüggemann[§], Martin Biel[‡1], and Christian A. Wahl-Schott[‡2]

From the [‡]Center for Integrated Protein Science CIPS-M and Zentrum für Pharmaforschung, Department Pharmazie, Ludwig-Maximilians-Universität München, Butenandtstrasse 5-13, D-81377 München and [§]Nanion Technologies GmbH, Erzgiessereistrasse 4, D-80335 Munich, Germany

Two-pore channels (TPCNs) have been proposed to form lysosomal Ca^{2+} release channels that are activated by nicotinic acid adenine dinucleotide phosphate. Here, we employ a glass chip-based method to record for the first time nicotinic acid adenine dinucleotide phosphate -dependent currents through a two-pore channel (TPCN2) from intact lysosomes. We show that TPCN2 is a highly selective Ca^{2+} channel that is regulated by intralysosomal pH. Using site-directed mutagenesis, we identify an amino acid residue in the putative pore region that is crucial for conferring high Ca^{2+} selectivity. Our glass chip-based method will provide electrophysiological access not only to lysosomal TPCN channels but also to a broad range of other intracellular ion channels.

Nicotinic acid adenine dinucleotide phosphate (NAADP)[3] is a second messenger that releases Ca^{2+} from intracellular stores at low nanomolar concentrations. NAADP-evoked Ca^{2+} release has been demonstrated in invertebrates and numerous mammalian cell types including pancreatic acinar and β-cells, cardiac and smooth muscle cells, T-lymphocytes, platelets, and neurons (1). Recent studies using NAADP binding assays and Ca^{2+} imaging experiments indicated that members of the two-pore channel family (TPCN1–3) constitute the native NAADP receptor (2, 3). TPCNs share sequence homology with members of the transient receptor potential (TRP) cation channel family, suggesting that they may directly form the NAADP-gated Ca^{2+} conductance. However, direct proof of ion channel activity of TPCNs is still missing, leaving open the possibility that another ion channel protein assembled with TPCNs could underlie the Ca^{2+} current. A major obstacle to address this key issue is that TPCNs are strictly localized in endolysosomal organelles, in particular acidic lysosomes that are not readily accessible to standard patch clamp measurements. Here we present a new method to record ionic currents in isolated lysosomes. Specifically, we provide direct evidence that TPCN2 is a highly selective Ca^{2+} channel and identify an amino acid residue in the putative pore region that is crucial for conferring Ca^{2+} selectivity.

EXPERIMENTAL PROCEDURES

Generation and Culture of Stable Cell Lines—Stable cell lines for enhanced GFP-tagged murine wild type TPCN2 (3) and mutant TPCN2 were generated using the Flp-In™ system (Invitrogen) according to manufacturer's protocol. Mutations in the putative selectivity filter of murine TPCN2 (N257A and E643A) were introduced using the QuikChange site-directed mutagenesis kit (Stratagene, LA Jolla, CA). Cells were cultured in Dulbecco's modified Eagle's medium supplemented with 10% fetal calf serum, 100 units/ml penicillin, 100 μg/ml streptomycin, 100 μg/ml hygromycin and kept at 37 °C, 10% CO_2.

Preparation of Lysosomes—To increase the size of the lysosomes (usually <0.5 μM), cells were treated with 1 μM vacuolin for 2 h. This small compound is known to selectively increase the size of endosomes and lysosomes (4, 5). Lysosomes were prepared according to Schenkman and Cinti (6). Briefly, control HEK293 cells or HEK293 cells stably overexpressing wild type or recombinant mTPCN2 channels were homogenized in 0.25 M sucrose, 10 mM Tris-Cl, pH 7.4, on ice using a potter homogenizer to obtain the whole cell lysates. The lysates were centrifuged at 14,000 × *g* for 15 min at 4 °C, and the supernatant was treated with 8 mM $CaCl_2$ (final concentration) on ice for 5 min with gentle stirring. Ca^{2+} causes aggregation of lysosomes. To precipitate aggregated lysosomes, a second centrifugation step at 25,000 × *g* for 15 min at 4 °C was used. The supernatant was collected, and the pellet was washed in 150 mM KCl, 10 mM Tris-Cl, pH 7.4, followed by a final centrifugation step at 25,000 × *g* for 15 min at 4 °C. The pellet containing purified lysosomes was collected and subjected to Western blotting.

Western Blots—Whole cell lysates were prepared by homogenizing HEK293 cells stably expressing wild type and mutated TPCN2 channels using a potter homogenizer. The lysates were centrifuged at 14.000 × *g* for 15 min at 4 °C, and the supernatant was collected. Proteins were boiled in Laemmli sample buffer for 5 min and subsequently visualized by SDS-PAGE, Western blot analysis, and ECL (GE Healthcare). The antibodies used were as follows: anti-GFP (Clontech) for detection of EGFP-TPCN2 fusion protein.

* This work was supported by grants from the Deutsche Forschungsgemeinschaft and the Bayerische Forschungsstiftung.

[S] The on-line version of this article (available at http://www.jbc.org) contains supplemental Fig. 1S and Table 1S.

[1] To whom correspondence may be addressed: Dept. Pharmazie, Pharmakologie für Naturwissenschaften, Ludwig-Maximilians-Universität München, Butenandtstr. 5-13, D-81377 München, Germany. Tel.: 49-89-2180-77328; Fax: 49-89-2180-77326; E-mail: martin.biel@cup.uni-muenchen.de.

[2] To whom correspondence may be addressed: Dept. Pharmazie, Pharmakologie für Naturwissenschaften, Ludwig-Maximilians-Universität München, Butenandtstr. 5-13, D-81377 München, Germany. Tel.: 49-89-2180-77654; Fax: 49-89-2180-77326; E-mail: christian.wahl@cup.uni-muenchen.de.

[3] The abbreviations used are: NAADP, nicotinic acid adenine dinucleotide phosphate; NADP, nicotinamide adenine dinucleotide phosphate; TPCN, two-pore channel; TRP, transient receptor potential; GFP, green fluorescent protein; WLR, whole lysosome recordings; F, farad; m, murine; h, human.

β-Hexosaminidase Assay—β-Hexosaminidase assay was performed as described in Ref. 7. Briefly, whole cell lysates or lysosomal preparations of HEK293 cells stably expressing GFP-TPCN2 were added to substrate buffer composed of 0.1 M sodium citrate, pH 4.6, containing 0.04% (w/v) NaN_3, 0.2% (w/v) bovine serum albumin, 0.5% (w/v) Triton X-100, and 10 mM substrate (*p*-nitrophenyl-2-acetamido-2-deoxy-β-D-glucopyranoside; Sigma). The reaction was stopped with 5 volumes of 0.4 M glycine, pH 10.4, and A_{405} was measured in a spectrophotometer. Parallel experiments were performed using substrate buffer not containing Triton X-100 to measure the amount of disrupted lysosomes. Enzyme activity of intact lysosomes was calculated as ((activity in the presence of Triton X-100) − (activity in the absence of Triton X-100)).

Live Cell Imaging—HEK293 cells stably expressing wild type and mutated TPCN2 channels were grown on μ-Dishes (ibidi) in Dulbecco's modified Eagle's medium supplemented with 10% fetal calf serum containing 100 units/ml penicillin, 100 μg/ml streptomycin, and 100 μg/ml hygromycin and kept at 37 °C, 10% CO_2. After 2, days the cells were incubated with 100 nM LysoTracker Red DND-99 (Invitrogen) for 30 min, 37 °C. To avoid background staining, the medium was changed, and the cells were immediately visualized under a Zeiss LSM 510 laser confocal microscope.

Whole Lysosome Recordings (WLR)—For whole lysosome recordings, a planar patch clamp system (Port-a-Patch, Nanion, Munich, Germany) was used. Purified lysosomes were resuspended in a washing solution containing (in mM) 150 KCl, 10 Tris-Cl, pH 7.4. Mean lysosomal capacitance was 165 ± 28 fF ($n = 15$). During seal formation, the bath solution contained (in mM) 120 potassium methanesulfonate, 10 EGTA, 10 HEPES, and KOH was used to adjust pH to 7.2. After seal formation, the lysosomal membrane was ruptured by applying a brief suction pulse to achieve whole lysosome configuration. Currents were recorded using an EPC-10 patch clamp amplifier (HEKA, Lambrecht, Germany) and PatchMaster acquisition software (HEKA). Data were digitized at 25 μs and filtered at 2.8 kHz. Fast and slow capacitive transients were cancelled by the compensation circuit of the EPC-10. Membrane potentials were corrected for liquid junction potential, which was calculated by pCLAMP 10 (Molecular Devices, Sunnyvale, CA). Liquid junction potentials were +4.4 mV for standard solutions, +2 mV for recording conditions of chloride currents, and 8.4 mV for bi-ionic recording conditions. For all experiments, salt-agar bridges were used to connect the reference Ag-AgCl wire to the bath solution to minimize voltage offsets. All recordings were obtained at room temperature. The membrane potential was held at −80 mV, and 500-ms voltage ramps from −100 to +100 mV were applied every 5 s. For the application of NAADP or NADP, standard external solution was completely exchanged by standard solution containing NAADP or NADP, respectively. To dissect I_{NAADP}, the current in the absence of NAADP was subtracted from the current obtained in the presence of NAADP. The current amplitude at −100 mV was extracted from individual ramp current records and used to calculate the current amplitude. To calculate P_{Ca}/P_K when Ca^{2+} was the only permeating cation in the lysosomal solution, we used $P_{Ca}/P_K = \gamma_{Ca}[K]_e/(4\gamma_K \times [Ca^{2+}]_i) \times \exp(E_{rev} \times F/RT) \times (\exp(E_{rev} \times F/RT) + 1)$, where F is the Faraday constant, R is the gas constant, T is temperature, and E_{rev} is the reversal potential. $[K]_e$ is the concentration of K^+ in the external solution, and $[Ca^{2+}]_i$ is the concentration of Ca^{2+} in the internal solution. The activity coefficients γ_{Ca} and γ_K were 0.5 and 0.75, respectively.

Solutions for Electrophysiology—Supplemental Table 1S summarizes the external and internal solutions used for electrophysiological recordings of single lysosomes. Unless stated otherwise, the standard external and standard internal solutions were used for whole lysosome recordings. To investigate the pH dependence of lysosomal currents, in some experiments, the pH of the standard internal solution was adjusted to 7.2. In a subset of experiments, standard external solution containing 100 nM Ca^{2+} was used instead of 2 mM Ca^{2+}. Methanesulfonate was used to replace most of the Cl^- to reduce the background from an endogenous chloride conductance (supplemental Fig. 1S). For bi-ionic experiments, extralysosomal solution containing only K^+ ($external_{K+}$) and internal solution containing only Ca^{2+} ($internal_{Ca2+}$) as permeant cations were used. Chloride currents were recorded using external solution containing high Cl^- ($external_{highCL-}$) and standard internal solution.

Statistics—All values are given as mean ± S.E. n is the number of experiments. An unpaired *t* test was performed for the comparison between two groups. Values of $p < 0.05$ were considered significant.

RESULTS AND DISCUSSION

To characterize currents through TPCNs in single lysosomes, we employed a direct patch clamp approach that was used in a recent study to characterize lysosomal TRP channels (8). However, all of our attempts to employ the protocol described in the latter study to characterize lysosomes of a stable cell line overexpressing TPCN2 failed.

Because maintenance of lysosomal integrity was the major problem preventing current measurements with glass pipettes, we tested an alternative approach where lysosomes are attached to a small hole (<1 μm) in a microstructured planar glass chip. Fig. 1*A* gives an outline of our protocol. We isolated lysosomes of a stable HEK293 cell line overexpressing GFP-tagged-TPCN2. Before harvesting, the cells were treated with vacuolin to enlarge the lysosomes (8). Lysosomes obtained using this protocol contained high amounts of TPCN2 (Fig. 1*B*) and revealed diameters of up to 8 μm (range: 3–8 μm; Fig. 1*C*). The integrity of the lysosomal preparation was verified using the β-hexosaminidase assay (7, 9). Using this highly purified lysosomal preparation, we performed WLR by a planar patch clamp device.

In TPCN2-expressing lysosomes, NAADP-dependent currents (I_{NAADP}) could be recorded using voltage ramps from −100 mV to +100 mV (Fig. 1*D*). I_{NAADP} was activated by low nanomolar concentrations of NAADP (60 nM), whereas it was not present at low micromolar NAADP (5 μM) and was insensitive to NADP (Fig. 1, *D* and *E*). These findings were consistent with the activation profile of TPCN2 as determined in Ca^{2+} imaging experiments (2, 3). The current-voltage relationship of I_{NAADP} was non-rectifying and exhibited a reversal potential of

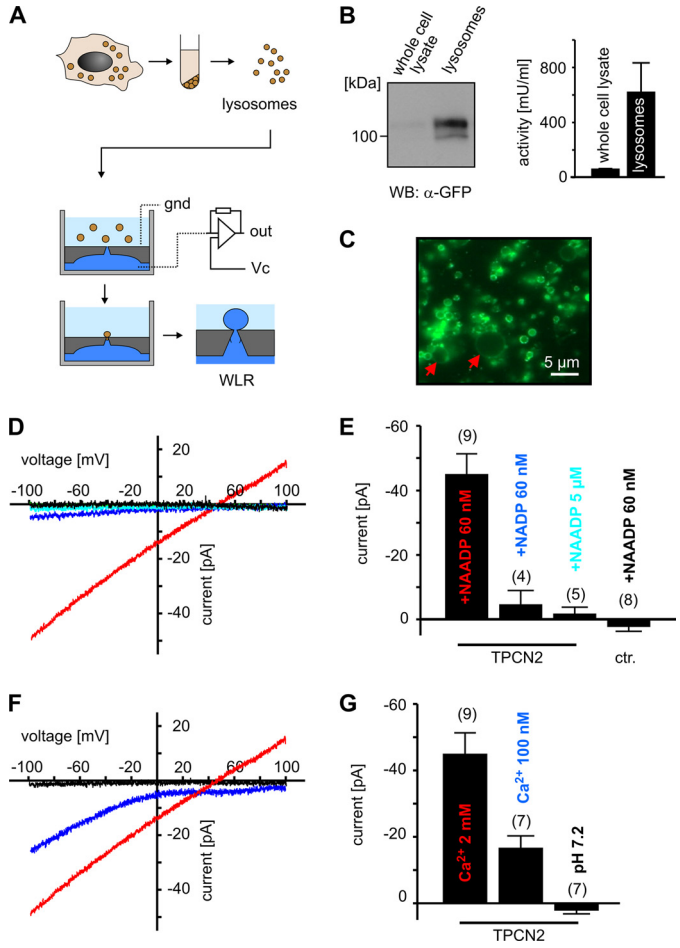

FIGURE 1. **TPCN2-mediated currents in single lysosomes.** *A*, workflow of lysosomal preparation and of the planar patch clamp method used for WLR. *gnd*, ground; V_c, command voltage; *out*, output of the amplifier circuitry. *B*, *left panel*, Western blot (*WB*) analysis of whole cell lysates (*left lane*) and purified lysosomes (*right lane*) of HEK293 cells expressing GFP-TPCN2 (12 μg of protein/lane). *Right panel*, activity of the lysosomal enzyme β-hexosaminidase of whole cell lysates ($n = 3$) and lysosomal preparations ($n = 3$) obtained from HEK293 cells expressing GFP-TPCN2. *C*, epifluorescence image of vacuolin-treated lysosomes expressing GFP-TPCN2. The *red arrows* mark two enlarged lysosomes. *D*, current-voltage relations of TPCN2 currents from single lysosomes in the presence of 60 nM NAADP (*red*), 60 nM NADP (dark blue), and 5 μM NAADP (*light blue*). *Black trace*, NAADP-dependent current of a wild type lysosome (control). Currents were recorded using standard external and internal solutions. Note that inward currents are currents that flow out of the lysosomes into the cytosol. *E*, population data for current amplitudes at −100 mV obtained from experiments shown in *D*. *ctr.*, control. *F*, current-voltage relations of TPCN2 currents from single lysosomes in the presence of 60 nM NAADP measured with standard external solution containing 2 mM Ca^{2+} (*red*, same as in *D*), 100 nM Ca^{2+} (*dark blue*), and standard internal solution. *Black trace*, current recorded in standard external solution and standard internal solution adjusted to pH 7.2. *G*, population data for current amplitudes at −100 mV obtained from experiments shown in *F*.

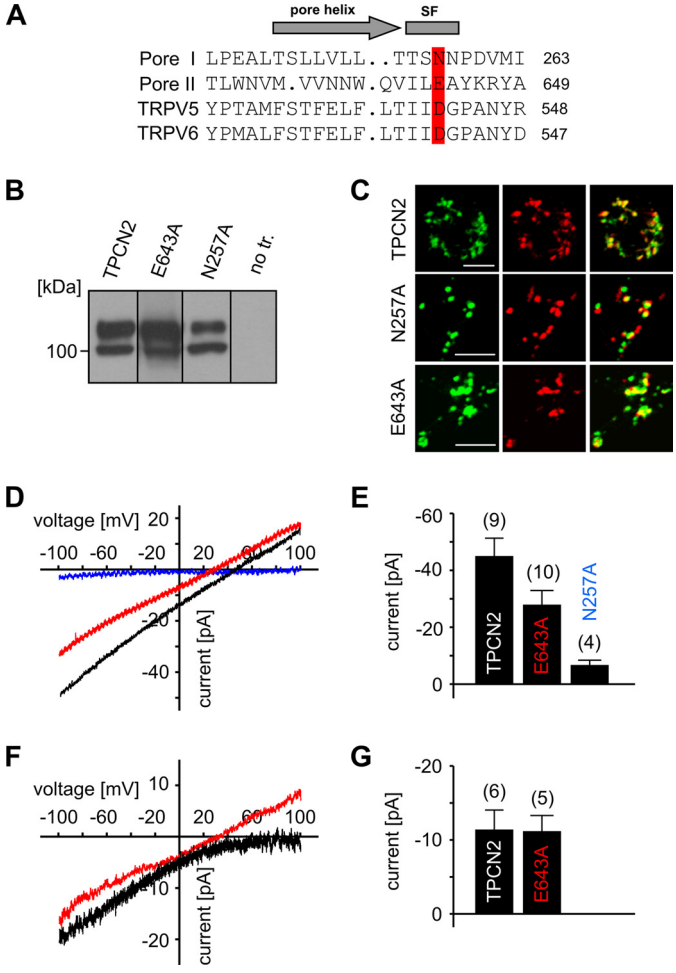

FIGURE 2. **Mutation E643A alters ion selectivity of TPCN2.** *A*, alignment of the putative pore region of TPCN2 with that of TRPV5 and TRPV6 channels. *Highlighted* residues in TPCN2 were mutated to generate N257A and E643A constructs, respectively. *SF*, putative selectivity filter. *B*, Western blots of HEK293 cells stably expressing wild type and mutated TPCN2 channels (30 μg of protein/lane obtained from whole cell lysates). *no tr.*, no transfection. *C*, confocal microscopy of HEK293 cells expressing wild type and mutated TPCN2 channels indicates that wild type and mutant TPCN2 are targeted to the lysosomes (*green*, TPCN2; *red*, LysoTracker; *yellow*, overlay; *scale bar*, 5 μm). *D*, effect of pore mutations on Ca^{2+} permeability of TPCN2. Current-voltage relations of TPCN2 (*black*), N257A (*dark blue*), and E643A (*red*)-mediated currents in the presence of 60 nM NAADP. *E*, population data for current amplitudes obtained in similar experiments as shown in *D*. Currents were recorded in standard internal and external solution. *F*, current-voltage relation obtained for TPCN2 (*black*) and E643A (*red*) using bi-ionic conditions (external$_{K+}$ and internal$_{Ca2+}$ solution). *G*, population data for similar experiments as shown in *F*.

44.4 ± 5 mV ($n = 5$) that closely matches the calculated reversal potential for Ca^{2+} (42.5 mV). This indicated that TPCN2-mediated currents are highly selective for Ca^{2+} and strongly argued against a relevant permeability for K^+ (E_{rev}: −14 mV) in the presence of Ca^{2+}. In agreement with this hypothesis, lowering the $[Ca^{2+}]_{cytosol}$ to 100 mM shifted the reversal potential to >100 mV (Fig. 1*F*). Current recordings using bi-ionic conditions revealed that the average permeability ratio for P_{Ca}/P_K was >1000 (E_{rev} >100 mV; Fig. 2*F*). Increasing intralysosomal pH to 7.2 completely abolished TPCN2-mediated currents, indicating that intralysosomal protons are required for NAADP-dependent channel opening (Fig. 1*F*).

If TPCN2 itself forms the ion-conducting pore, it should be possible to change the ion selectivity of I_{NAADP} by introducing mutations into the pores of TPCN2. The two putative pore loops of TPCN2 share substantial homology with members of the TRP channel family (Fig. 2*A*). In particular, an acidic residue, which confers Ca^{2+}/Mg^{2+} selectivity in TRPV5 and TRPV6 (10, 11), is conserved in pore loop II (Glu-643 in mTPCN2 and Asp-660 in hTPCN2). This residue aligns in pore loop I with an asparagine that is also conserved in TPCNs (Asn-257 in mTPCN2). We mutated both residues individually to alanine and analyzed the mutants functionally. Although

N257A protein was produced and expressed in lysosomes (Fig. 2, *B* and *C*), no I_{NAADP} was detected for this mutant (Fig. 2, *D* and *E*). By contrast, the E643A mutant gave rise to substantial I_{NAADP} (Fig. 2*D*). Importantly, the reversal potentials of E643A-mediated current was significantly less positive (22.1 ± 4.0 mV ($n = 9$); $p < 0.01$) than that of wild type TPCN2 (44.4 ± 5 mV ($n = 5$); Fig. 2, *D* and *E*). This change implied that mutant TPCN2 had lost some of its very high selectivity for Ca^{2+} over monovalent cations. In support of this interpretation, current recordings using bi-ionic conditions revealed that the average permeability ratio for P_{Ca}/P_K changed from >1000 in wild type TPCN2 to a permeability ratio of 8 in mutant TPCN2 (Fig. 2*F*; E_{rev}: 36 ± 6.5 mV ($n = 4$)).

In summary, we report for the first time NAADP-mediated ionic currents in single lysosomes expressing TPCN2. We show that TPCN2 forms a highly selective Ca^{2+} conductance and identify an acidic residue in pore loop II of the protein that is a key determinant of ion selectivity. In conjunction with previous biochemical and imaging studies (2, 3), our results establish TPCN2 as an NAADP-gated Ca^{2+} channel. The planar patch clamp method used in this study was by far superior to conventional patch clamp methods, allowing us to reliably characterize currents from a large number of isolated lysosomes. There is initial evidence that this technique will also allow the characterization of other lysosomal ion channels (*e.g.* chloride current; see supplemental Fig. 1S) that could not be directly studied so far. Finally, we expect that our method will be very useful to characterize ionic channels in other types of organelles and intracellular compartments (*e.g.* the endoplasmic reticulum or the nuclear envelope).

REFERENCES

1. Zhu, M. X., Ma, J., Parrington, J., Galione, A., and Evans, A. M. (2010) *FEBS Lett.* **584,** 1966–1974
2. Calcraft, P. J., Ruas, M., Pan, Z., Cheng, X., Arredouani, A., Hao, X., Tang, J., Rietdorf, K., Teboul, L., Chuang, K. T., Lin, P., Xiao, R., Wang, C., Zhu, Y., Lin, Y., Wyatt, C. N., Parrington, J., Ma, J., Evans, A. M., Galione, A., and Zhu, M. X. (2009) *Nature* **459,** 596–600
3. Zong, X., Schieder, M., Cuny, H., Fenske, S., Gruner, C., Rötzer, K., Griesbeck, O., Harz, H., Biel, M., and Wahl-Schott, C. (2009) *Pflugers. Arch.* **458,** 891–899
4. Cerny, J., Feng, Y., Yu, A., Miyake, K., Borgonovo, B., Klumperman, J., Meldolesi, J., McNeil, P. L., and Kirchhausen, T. (2004) *EMBO Rep.* **5,** 883–888
5. Huynh, C., and Andrews, N. W. (2005) *EMBO Rep.* **6,** 843–847
6. Schenkman, J. B., and Cinti, D. L. (1978) *Methods Enzymol.* **52,** 83–89
7. Kasper, D., Planells-Cases, R., Fuhrmann, J. C., Scheel, O., Zeitz, O., Ruether, K., Schmitt, A., Poët, M., Steinfeld, R., Schweizer, M., Kornak, U., and Jentsch, T. J. (2005) *EMBO J.* **24,** 1079–1091
8. Dong, X. P., Cheng, X., Mills, E., Delling, M., Wang, F., Kurz, T., and Xu, H. (2008) *Nature* **455,** 992–996
9. Kornak, U., Kasper, D., Bösl, M. R., Kaiser, E., Schweizer, M., Schulz, A., Friedrich, W., Delling, G., and Jentsch, T. J. (2001) *Cell* **104,** 205–215
10. Voets, T., Janssens, A., Droogmans, G., and Nilius, B. (2004) *J. Biol. Chem.* **279,** 15223–15230
11. Voets, T., Prenen, J., Vriens, J., Watanabe, H., Janssens, A., Wissenbach, U., Bödding, M., Droogmans, G., and Nilius, B. (2002) *J. Biol. Chem.* **277,** 33704–33710

Supplemental information

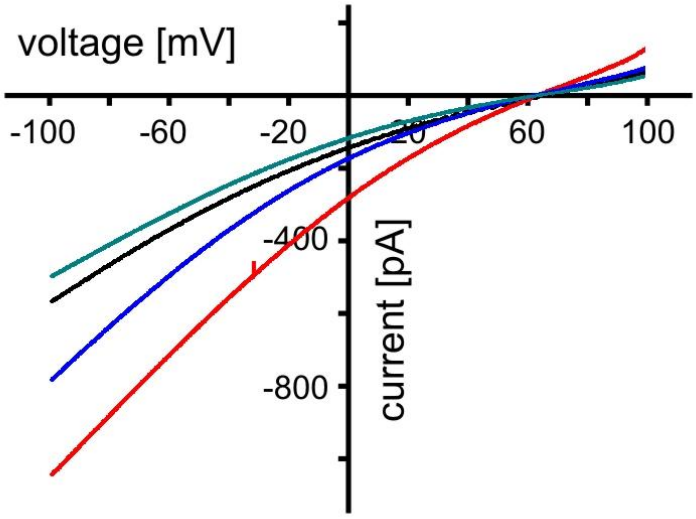

Supplemental Figure 1S**. Chloride currents in four isolated lysosomes.** The membrane potential was held at -80 mV and 500 ms voltage ramps from -100 to +100 mV were applied every 5s. Chloride currents were determined as difference currents between IV curves recorded in the absence (standard external solution) and presence of external Cl^- ($external_{highCl}$ solution). The internal solution was standard internal. The reversal potential of chloride currents was 65 ± 0.6 mV (n=4) which is close to the calculate reversal potential for chloride (67.5) mV.

Supplemental Table 1S. Solutions for electrophysiology

	KMSA	KCl	KF	Ca MSA	$CaCl_2$	$MgCl_2$	mannitol	pH
external solutions								
standard	60		60	2				7.2
$external_{K+}$			60				160	7.2
$external_{high\ Cl-}$		60	60		2			7.2
internal solutions								
standard	70			60		2		4.6
$internal_{Ca2+}$				60			120	4.6

Concentrations are given in mM. All solutions contain 10 mM HEPES. External solutions were titrated with KOH, internal standard was titrated with MSA, $internal_{Ca2+}$ was titrated by HCl. Mannitol was used to adjust osmolarity.

Publikation III

Science Signaling
AAAS

` Planar Patch Clamp Approach to Characterize Ionic Currents from Intact Lysosomes

Michael Schieder, Katrin Rötzer, Andrea Brüggemann, Martin Biel and Christian Wahl-Schott (7 December 2010)
Science Signaling **3** (151), pl3. [DOI: 10.1126/scisignal.3151pl3]

Science Signaling (ISSN 1937-9145) is published weekly, except the last week in December, by the American Association for the Advancement of Science, 1200 New York Avenue, NW, Washington, DC 20005.

ELECTROPHYSIOLOGY

Planar Patch Clamp Approach to Characterize Ionic Currents from Intact Lysosomes

Michael Schieder,[1] Katrin Rötzer,[1] Andrea Brüggemann,[2] Martin Biel,[1]* Christian Wahl-Schott[1]*

Published 7 December 2010; Volume 3 Issue 151 pl3

INTRODUCTION

MATERIALS

EQUIPMENT

- Cell Culture
- Lysosomal Preparation
- Electrophysiology

RECIPES

INSTRUCTIONS

- Chloridating Electrodes
- Cell Culture
- Preparation of Lysosomes
- PatchControl and Patchmaster Software Setup
- Electrophysiological Recordings
- Manual Exchange of the Internal Solution
- Improving Seal Formation
- Preparation and Placement of Agar Bridges

TROUBLESHOOTING

- Poor or No Lysosome Recovery
- Inadequate Seal Formation or Unstable Seal

NOTES AND REMARKS

REFERENCES AND NOTES

[1]Center for Integrated Protein Science CIPS-M and Zentrum für Pharmaforschung–Department Pharmazie, Ludwig-Maximilians-Universität München, Butenandtstrasse 5 -13, D-81377 München, Germany. [2]Nanion Technologies GmbH, Erzgiessereistrasse 4, D-80335 Munich, Germany.

*Corresponding authors: Department Pharmazie, Pharmakologie für Naturwissenschaften, Ludwig-Maximilians-Universität München, Butenandtstr. 5 -13, D-81377 München, Germany. E-mail: christian.wahl@cup.uni-muenchen.de (C.W.-S.); martin.biel@cup.uni-muenchen.de (M.B.)

Since its launch in the early 1980s, the patch clamp method has been extensively used to study ion channels in the plasma membrane, but its application to the study of intracellular ion channels has been limited. Unlike the plasma membrane, intracellular membranes are usually not stable enough to withstand mechanical manipulation by glass electrodes during seal formation and rupturing of the membrane. To circumvent these problems, we developed a method involving the immobilization of isolated organelles on a solid matrix planar glass chip. This glass chip contains a microstructured hole that supports the formation of gigaseals and subsequent electrophysiological recordings despite the high fragility of intracellular membranes. Here, we report the experimental details of this method using lysosomes, which are the smallest cellular organelles, as a model system. We demonstrate that we can record endogenous ionic currents from wild-type lysosomes, as well as from lysosomes overexpressing ion channels, and expect that this method will provide electrophysiological access to a broad range of intracellular ion channels.

Introduction

The development of the patch clamp method by Neher and Sakmann revolutionized the electrophysiological characterization of ion channels in cells (*1*). This technology made possible the resolution of ionic currents even through single channels in the plasma membrane and has become the standard method for the functional characterization of ion channels. However, the patch clamp technology has been mostly limited to the characterization of ion channels in the plasma membrane. In contrast, ion channels localized in intracellular compartments, such as lysosomes, endosomes, mitochondria, and cisternae of the endoplasmic reticulum (ER), are not readily accessible by glass pipettes that are used to perform patch clamp analysis.

The membrane of intracellular organelles makes up more than 95% of the total cell membrane system. Thus, it is not surprising that the group of intracellular ion channels is at least as large as that of ion channels in the plasma membrane. Intracellular ion channels are present in various cellular organelles (Table 1). Among these, intracellular Ca^{2+}-release channels have raised particular interest, because these channels are fundamental for the control of numerous physiologic functions, including muscle contraction, secretion, cell motility, and immune response (*2*). Traditionally, intracellular Ca^{2+} release has been attributed to ryanodine and inositol trisphosphate (IP_3) receptors in the sarcoplasmic and endoplasmic reticulum (SR/ER) and the nuclear envelope (*2*–*6*). Ca^{2+} flux through these channels has been functionally investigated with bilayer studies and Ca^{2+}-imaging experiments. There is growing evidence that lysosomes are also critically involved in Ca^{2+} signaling (*7*–*10*). Furthermore, specific Ca^{2+}-release channels and numerous other ion channels have been identified in the lysosomal-endosomal compartment (Table 1). Loss of function or dysfunction of lysosomal ion channels is involved in human lysosomal storage diseases (Table 1) (*11*–*14*), which suggests that lysosomal ion channels are pathophysiologically relevant proteins that have potential to become drug targets.

So far, a limited number of methods are available for the characterization of intracellular ion channels. The standard method is the reconstitution of purified ion channel proteins or membranes of isolated cell organelles into synthetic phospholipid bilayers (*15*–*17*). Alternatively, purified channel proteins or membrane vesicles can be reconstituted into liposomes (*18*) that are quite large and can be analyzed by means of conventional patch clamp. The main conceptual drawback of these methods is that ion channel proteins are extracted from their physiological environment. This procedure bears the risk that important factors, such as crucial components of the lipid membrane as well as specific modulators and accessory subunits, that are associated in vivo with the ion channel protein are lost. Additionally, copurification of proteins that nonspecifically interfere with the activity of the ion channel of interest or that form additional conductances can potentially lead to wrong interpretations of currents obtained from bilayer experiments. As a consequence, ionic current measurements in lipid bilayers are intrinsically difficult to standardize and validate. Other approaches to investigate intracellular ion channels in organelles included Ca^{2+} imaging (*19*) and flux measurements (*20*, *21*). However, these methods lack some advantages of patch clamp analysis, including the ability to directly access ion channels.

Technically, the major problem preventing the characterization of intracellular ion channels by glass pipette-based patch clamp measurements has been the maintenance of organelle integrity. Here, we describe a method that is well suited to characterize ionic currents even from lysosomes, which are the smallest cellular organelles. We use solid-matrix planar glass chips that contain a small hole to immobilize and support the lysosomes (Fig. 1). With this approach, we efficiently obtain gigaseals and electrophysiological recordings. We provide detailed instructions for the recording of endogenous ionic currents from wild-type lysosomes, as well as from lysosomes overexpressing ion channels. This Protocol assumes basic knowledge of patch clamp methods. Compared with conventional patch clamp methods, the planar patch clamp method allows reliable characterization of currents from a large number of isolated lysosomes (up to eight lysosomal recordings per preparation). Moreover, this method does not require extensive and time-consuming protein purification steps commonly required for ion channel reconstitution into lipid bilayers or liposomes. The planar patch clamp method will provide electrophysiological access not only to lysosomal ion channels, but also to a broad range of other intracellular ion channels.

Table 1. Localization, function, and channelopathies associate with intracellular ion channels. Some of the ion channels are present in intracellular organelles as well as in the plasma membrane. "Function" relates to general function of the ion channels. *, mouse model; #, human channelopathy; nd, not determined; TRP, transient receptor potential channel; ClC, chloride channel; IP_3, inositol 1,4,5-triphosphate; K_{Ca}, Ca^{2+}–dependent K^+ channel; K_{ATP}, ATP-dependent K^+ channel; K_V, voltage-dependent K^+ channel; IMAC, mitochondrial inner membrane anion channel; UCP, uncoupling protein.

Organelle	Ion channel	Ion selectivity	Function	Channelopathy	References
Lysosomes and Endosomes	TRPM1	nd	Tumor suppressor, potential role in mediating synaptic transmission in bipolar cells	Autosomal recessive congenital stationary night blindness # Metastasis and poor prognosis in melanoma#	(*30*, *31*)
	TRPM2	$Na^+ > Ca^{2+} > Mg^{2+} > Cs^+$	Oxidant stress sensor, mediates H_2O_2 dependent cell death	Guamanian amyotrophic lateral sclerosis/parkinsonism dementia complex	
	TRPM7	$Zn^{2+} > Ni^{2+} > Ba^{2+} > Mg^{2+} > Mn^{2+} > Sr^{2+} > Cd^{2+} > Ca^{2+}$	Synaptic vesicle function Anoxia-induced cell death	Guamanian amyotrophic lateral sclerosis/parkinsonism dementia complex#	
	TRPML1	$K^+ > Na^+ > Ba^{2+} > Sr^{2+} > Ca^{2+}$	Membrane sorting, late steps of endocytosis, or both	Mucolipidosis 4#	(*30*, *31*)
	TRPML2	Cation nonselective	nd	nd	
	TRPML3	Cation nonselective	nd	Varitint-Waddler mouse*	
	TRPV1	$Ca^{2+} > Mg^{2+} > Cs^+ = K^+ = Na^+$	Thermosensation and nociception	nd	(*30*, *31*)
	TRPV2	$Ca^{2+} > Mg^{2+} > Cs^+ = K^+ = Na^+$	Thermosensation and nociception	nd	
	TRPV5	Ca^{2+}	Ca^{2+} reabsorption	Osteoporosis, hypercalciuria*	
	TRPV6	$Ca^{2+} > Sr^{2+} = Ba^{2+} > Mg^{2+}$	Ca^{2+} reabsorption	Alopecia, dermatitis, decreased intestinal Ca^{2+} reabsorption*	
	TRPC3	$Ca^{2+} > Na^+$	BDNF-induced chemoattractive turning	Cerebellar ataxia (moonwalker mouse)*	(*30*, *31*)
	TRPC5	$Ca^{2+} > K^+ = Cs^+ = Na^+$	Regulation of growth cone extension	Susceptibility to pyloric stenosis#	
	TPCN 2	Ca^{2+}	NAADP-dependent Ca^{2+} release	Polymorphic TPCN2 variants are associated with blond hair color	(*22, 23, 26*)
	TPCN1/3	nd	Possible NAADP-dependent Ca^{2+} release	nd	
	ClC3	Cl^-	Acidification of endosomes and synaptic vesicles	Loss of hippocampus, blindness*	(*32*)
	ClC5	Cl^-	Acidification of endosomes	Dent's disease characterized by proteinuria and kidney stones#	
	ClC7	Cl^-	Acidification of lysosomes, resorption lacuna of osteoclasts	Osteopetrosis and lysosomal storage disease#	
	ClC4 and ClC6	Cl^-	nd	nd	

Continued on next page

Organelle	Ion channel	Ion selectivity	Function	Channelopathy	References
Melanosomes	TRPM1	See text	See text	See text	
	TRPML3	See text	See text	See text	
Synaptic vesicles	TRPM7	See text	See text	See text	
	ClC3	See text	See text	See text	
Endo/ sarcoplasmic reticulum	IP_3 receptor	Ca^{2+}	IP_3 dependent Ca^{2+} release	Cerebellar ataxia#	(*30, 33*)
	Ryanodine receptor	Ca^{2+}	Ca^{2+} induced Ca^{2+} release	Susceptibility to malignant hyperthermia#, central core disease#, arrhythmia#	(*3, 30, 34*)
	TRPV1	See text	See text	See text	
	TRPM8	$Cs^+ > K^+ > Na^+$	A cold and menthol receptor Integration of thermal and chemical stimuli	nd	(*30, 31*)
	TRPP1	K^+	nd	Polycystic kidney disease#	(*30, 31*)
	TRPP2	$Na^+ > Ca^{2+} = Sr^{2+} = Ba^{2+}$	Acid sensing in sour taste and cerebrospinal fluid	nd	
trans-Golgi	TRPV1	See text	See text	See text	
	IP_3 receptor	See text	See text	See text	
Mitochondria	K_{Ca}	K^+	Volume regulation	SNP associated with hypertension, myocardial infarction, and stroke#	(*35, 36*)
	K_{ATP}	K^+	Volume regulation, protection against apoptosis/ischemic injury	Diabetes, hyperinsulinism, dilated cardiomyopathy, adrenergic atrial fibrillation#	(*35, 37, 38*)
	$Kv_{1.3}$	K^+	Cell death	Knockout mice were protected from diet-induced obesity	(*30, 35*)
	IMACs	Anions	Volume regulation	nd	(*35*)
	UCP1-3	H^+	Thermogenesis	nd	(*35*)
	VDAC	Ca^{2+}, K^+, Na^+, ATP, ADP, P_i	Metabolite transport, apoptosis	nd	(*35*)

Materials

5-ml microfuge test tube

175-cm^2 dishes for cell culture (Sarstedt, #831803)

2-, 10-, 200- and 1000-μl pipettes

25-cm cell scrapers (BDFalcon, #353086)

Agar (Applicam, #A0949)

Bleach solution (Nanion) Sodium hypochlorite solution (NaClO), 12% Cl

$CaCl_2$-$2H_2O$

CaMSA

Cell culture flasks (75 cm^2; Greiner Bio one, #658175)

Complete protease inhibitor cocktail, EDTA-free (Roche, #04693132)

DMSO

Dulbecco's modified Eagle medium containing 25 mM glucose (DMEM supplemented with 4.5 g/l glucose and pyruvate and Glutamax; Invitrogen, #31966-021).

EGTA

Fetal bovine serum (FBS; Biochrom, #S0615)

HCl

Human embryonic kidney (HEK) 293 cells stably overexpressing ion channels under investigation; here, mTPCN2

HEPES

Hygromycin B, 50 mg/ml solution (Carl Roth, #CP12.2)

KCl

KF

KH_2PO_4

KMSA

KOH

Mannitol

Methanesulfonic acid (Fluka, #64280)

$MgCl_2$

Micropipettors

Na_2HPO_4-$2H_2O$

NaCl

Pen-strep (penicillin 10,000 units/ml; streptomycin 10,000 μg/ml; Biochrom)

Sterile syringe filters 0.2 μm (VWR, #5140061)

Sterile syringes (VWR, #612-0120)

Sucrose (Sigma, #84100)

Tris(hydroxymethyl)aminomethane (Tris, Prolabo, #103156x)

Vacuolin-1 (Sigma, #V7139)

Equipment

Cell Culture

Humidified, cell culture incubator at 37°C, 10% CO_2

Laminar flow hood

Water bath, 37°C

Lysosomal Preparation

10-ml, round-bottomed, open top, thick-walled polycarbonate tube (Beckman, #355630)

Beckman 45 Ti fixed-angle rotor

Motor-driven tightly fitting glass/Teflon Potter homogenizer (Potter S, B. Braun)

Refrigerated centrifuge for 1.5 microfuge tubes (Eppendorf centrifuge 5415R)

Rotamax 120 rotary shaker (Heidolph)

Rubber adapter sleeve for centrifuge tube 16-mm delrin adaptor tube (Beckman, #303448)

Ultracentrifuge (Sorvall discovery 90)

Electrophysiology

Computer with 21-inch TFT monitor (Dell)

Freezing-point osmometer OM802 (Vogel)

NPC-1 chips (single use, disposable) microstructured glass chip containing an aperture of ~1 μm diameter (Nanion)

Patch-clamp amplifier (EPC-10, HEKA Instruments Inc.)

PatchControl Software (Nanion Technologies)

Port-a-Patch (Nanion Technologies)

Software for data acquisition (Patchmaster, HEKA Instruments Inc.)

Software for data analysis (OriginPro7.5, OriginLab Corporation)

Recipes

Recipe 1: Cell Culture Medium

Fetal bovine serum	10%
Pen-strep	100 U/ml
Hygromycin B	100 μg/ml
DMEM	500 ml

Mix components and filter-sterilize. Store at 4°C; warm to 37°C before use.

Recipe 2: Stock Solution Vacuolin 1 mM

Dissolve 1 mg of vacuolin in 1.732 ml of DMSO; mix well and store at 4°C.

Recipe 3: 16 mM $CaCl_2$

Dissolve 0.2352 g of $CaCl_2$ in 100 ml of distilled water; mix well and store at 4°C.

Recipe 4: Complete Protease Inhibitor Cocktail

Dissolve 1 tablet in 2 ml distilled water to prepare a 25× EDTA-free solution and store at 4°C or for long-term storage prepare aliquots of 250 μl and store at –20°C.

Recipe 5: Phosphate-Buffered Saline (PBS)

NaCl	137 mM
$Na_2HPO_4x2H_2O$	8 mM
KH_2PO_4	1.76 mM
KCl	2.7 mM

Adjust pH to 7.4 with HCl, prepare 500-ml aliquots, heat sterilize, and store at room temperature up to several months.

Recipe 6: Homogenization Buffer

Sucrose	0.25 M
Tris	10 mM

Adjust pH to 7.4 with HCl, sterilize by passing through a 0.2-μm filter, prepare 1-ml aliquots, and store at –20°C for several months. Before use, add 40 μl of Complete Protease Inhibitor Cocktail (Recipe 4) (final concentration 1×) per aliquot of homogenization buffer.

Recipe 7: Washing Buffer

KCl	150 mM
Tris	10 mM

Adjust pH to 7.4 with HCl, sterilize by passing through a 0.2-μm filter, prepare 4-ml aliquots, and store at –20°C for several months. Before use, add 160 μl of Complete Protease Inhibitor Cocktail (Recipe 4) (final concentration 1×) per aliquot of Washing Buffer.

Note: Recipes 8 through 14 refer to lysosomal recording solutions. Carefully adjust the osmolarity and the pH. Intralysosomal pH (pH 4.6) regulates several lysosomal ion channels. Measure the osmolarity of recording solutions with a freezing-point osmometer and adjust if necessary with nonpermeating molecules, such as mannitol or sucrose, to 290 mOsM for all internal solutions and between 290 and 310 mOsM for all external solutions, unless otherwise stated. External osmolarity should always be higher than the internal. Solutions should be warmed to room temperature (20 ± 2°C) before use.

Recipe 8: 200 mM CaMSA Stock Solution

Dissolve 0.2303 g CaMSA in 5 ml distilled water, sterilize by passing through a 0.2-μm filter, and store at 4°C.

Recipe 9: 200 mM $CaCl_2$ Stock Solution

Dissolve 0.1470 g $CaCl_2$ in 5 ml distilled water, sterilize by passing through a 0.2-μm filter, and store at 4°C.

Recipe 10: Standard Intralysosomal Solution

Reagent final concentration

KMSA	70 mM
CaMSA	60 mM
$MgCl_2$	2 mM
HEPES	10 mM

Adjust pH to 4.6 with MSA, sterilize by passing through a 0.2-μm filter, prepare 1-ml aliquots, and store at –20°C for several months.

Recipe 11: Standard Extralysosomal Solution

Reagent final concentration

KMSA	60 mM
KF	60 mM
HEPES	10 mM

Adjust pH to 7.2 with KOH, sterilize by passing through a 0.2-μm filter, prepare 4-ml aliquots, and store at –20°C for several months.

CaMSA (Recipe 8)	2 mM

Add CaMSA immediately before starting the measurements to avoid precipitation of CaF_2.

Recipe 12: Extralysosomal High Chloride Solution (mM)

Reagent	final concentration
KCl	60 mM
KF	60 mM
HEPES	10 mM

Adjust pH to 7.2 with KOH, sterilize by passing through a 0.2-μm filter, prepare 4-ml aliquots, and store at –20°C for several months.

$CaCl_2$ (Recipe 9)	2 mM

Add $CaCl_2$ immediately before starting the measurements to avoid precipitation of CaF_2.

Recipe 13: Seal Enhancer Solution

Reagent	final concentration
KMSA	60 mM
KF	60 mM
EGTA	10 mM
HEPES	10 mM

Adjust pH to 7.2 with KOH, sterilize by passing through a 0.2-μm filter, prepare 4-ml aliquots, and store at –20°C for several months.

Recipe 14: Extralysosomal Bath Solution

Reagent	final concentration
KMSA	120 mM
EGTA	10 mM
HEPES	10 mM

Adjust pH to 7.2 with KOH, sterilize by passing through a 0.2-μm filter, prepare 1-ml aliquots, and store at –20°C for several months.

Instructions

Chloridating Electrodes

The electrodes are manufactured from Ag/AgCl-coated steel and need to be regularly chloridated in bleach solution. Generally, electrodes should be replaced every 2 months.

1. Place electrodes requiring rechloridating into a bleach solution.
2. Wait approximately 15 min until a black AgCl-layer is obvious on the silver wire.
3. Rinse in clean water and dry the electrodes.

Cell Culture

Creating a cell line stably and abundantly expressing the ion channel in lysosomes is a critical parameter for successfully obtaining lysosomal recordings. We obtain the best results with cells up to passage 15 corresponding to a culture time of 4 to 5 weeks after thawing the cell stocks. We recommend performing pilot experiments designed to establish the lysosomal preparation—for example, by starting with a stable cell line that overexpresses a green fluorescent protein (GFP)–channel fusion protein as a positive control. Once the yield and the quality of the lysosomal preparation have been evaluated with epifluorescence microscopy or Western blotting of the lysosomal preparation from the cells expressing the fusion protein, then the organelle preparation can be performed with cells expressing untagged channels. The use of untagged channels is recommended to rule out interference of the tag with channel properties. We

use HEK293 cells stably expressing TPCN2 channels, which are calcium channels localized to lysosomes (*22*, *23*).

1. Two or three days before performing the experiments, plate 4×10^6 HEK293 cells per dish in two 175-cm^2 tissue-culture dishes with 25 ml of Cell Culture Medium (Recipe 1) for each dish.
2. Grow the cells homogeneously to almost 95% confluence on the day of the experiment. Grow cells at 37°C in a humidified atmosphere of 10% CO_2 in air.
3. Two hours before beginning the lysosomal preparation, add 25 μl Vacuolin Stock (Recipe 2) to each dish.

Preparation of Lysosomes

We describe a method to isolate lysosomes from HEK293 cells stably expressing lysosomal ion channels (Figs. 1 and 2). Before starting the lysosomal preparation, the cells are exposed to vacuolin to enlarge lysosomes (*24*). All steps in this part of the Protocol must be performed on ice. Lysosomes should be used for electrophysiological recordings within 1 to 3 hours of isolation.

The quality of the lysosomal preparation can be monitored by several methods. If HEK293 cells stably expressing a GFP-tagged lysosomal ion channel are available, the lysosome preparation can easily be assessed with an epifluorescence microscope. Alternatively, evaluate the lysosome preparation by performing Western blot experiments to demonstrate that the protein of interest copurifies with lysosomal marker proteins, such as lamp1 or lamp2. A β-hexosaminidase assay can be used to determine the yield of intact lysosomes according to (*25*, *26*).

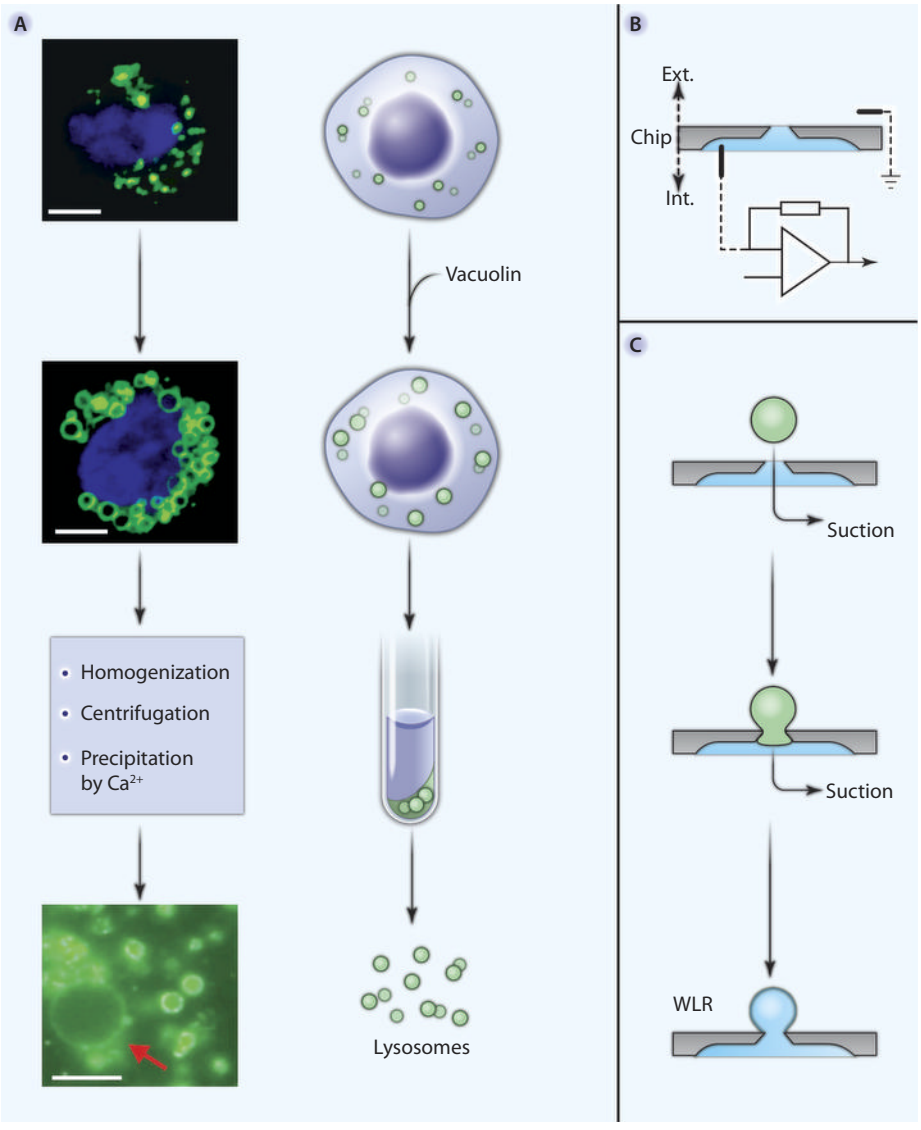

Fig. 1. Lysosomal preparation and the planar patch clamp approach used for lysosomal recordings. (**A**) HEK293 cells stably overexpressing TPCN2 before (top row) and after treatment with vacuolin (second row). After the isolation procedure (third row), highly purified lysosomes are obtained (bottom row). The arrow indicates an enlarged lysosome. Scale bar, 5 μm. (**B**) Schematic of the planar patch clamp method. Both the recording electrode of the amplifier circuitry and the reference electrode are connected to the recording solutions through agar bridges. ext., extralysosomal side of the planar glass chip containing the extralysosomal recording solution; int., intralysosomal side of the chip containing the intralysosomal recording solution (green). (**C**) For whole-cell lysosomal recordings (WLR), suction is applied to the chip in order to attach a single lysosome to the chip (top). After a high seal is obtained, a suction pulse (middle) ruptures the lysosomal membrane to obtain the whole lysosomal configuration (bottom).

1. Remove the medium from the cells and wash the cells once with 15 ml PBS (Recipe 5).
2. Remove PBS and add 250 μl pre-cooled Homogenization Buffer (Recipe 6).
3. Detach the cells with a cell scraper.
4. Transfer cell suspension to the glass-grinding vessel of the potter homogenizer.

Note: Pre-cool the glassware in an ice bath for 5 min before starting the procedure. Homogenization, as well as the following steps, must be performed at 4°C to minimize the activation of damaging phospholipases and proteases.

5. Wash the plate once with 250 μl Homogenization Buffer (Recipe 6) to detach the remaining cells.
6. Transfer the cells to the same glass-grinding vessel containing the rest of the cells.
7. Assemble the potter homogenizer and homogenize the cells using a Teflon pestle operated at 900 rotations per minute (rpm). Stroke the cell suspension placed in the glass grinding vessel 12 times.

   Note: The Teflon–glass coupling represents the best compromise between homogenization of the cells and the preservation of lysosomal integrity. Harsher techniques, including glass pestle in a glass potter, can easily damage lysosomes.
8. Transfer the homogenate to a 1.5-ml microfuge test tube and centrifuge at 14,000*g* for 15 min at 4°C.
9. Collect the supernatant and transfer it to a 10-ml polycarbonate centrifuge tube.

   Note: If desired, collect 5 μl of the supernatant for the β-hexosaminidase assay or 50 μl for Western blot analysis. This is optional, but provides a sample for establishing that the preparation contains lysosomes.
10. Add an equal volume (typically 1.6 ml) of 16 mM $CaCl_2$ (Recipe 3; final concentration 8 mM) to precipitate lysosomes.
11. Transfer the tube to a rotary shaker and shake at 150 rpm for 5 min at 4°C.

Fig. 2. Workflow of lysosomal preparation from HEK293 cells.

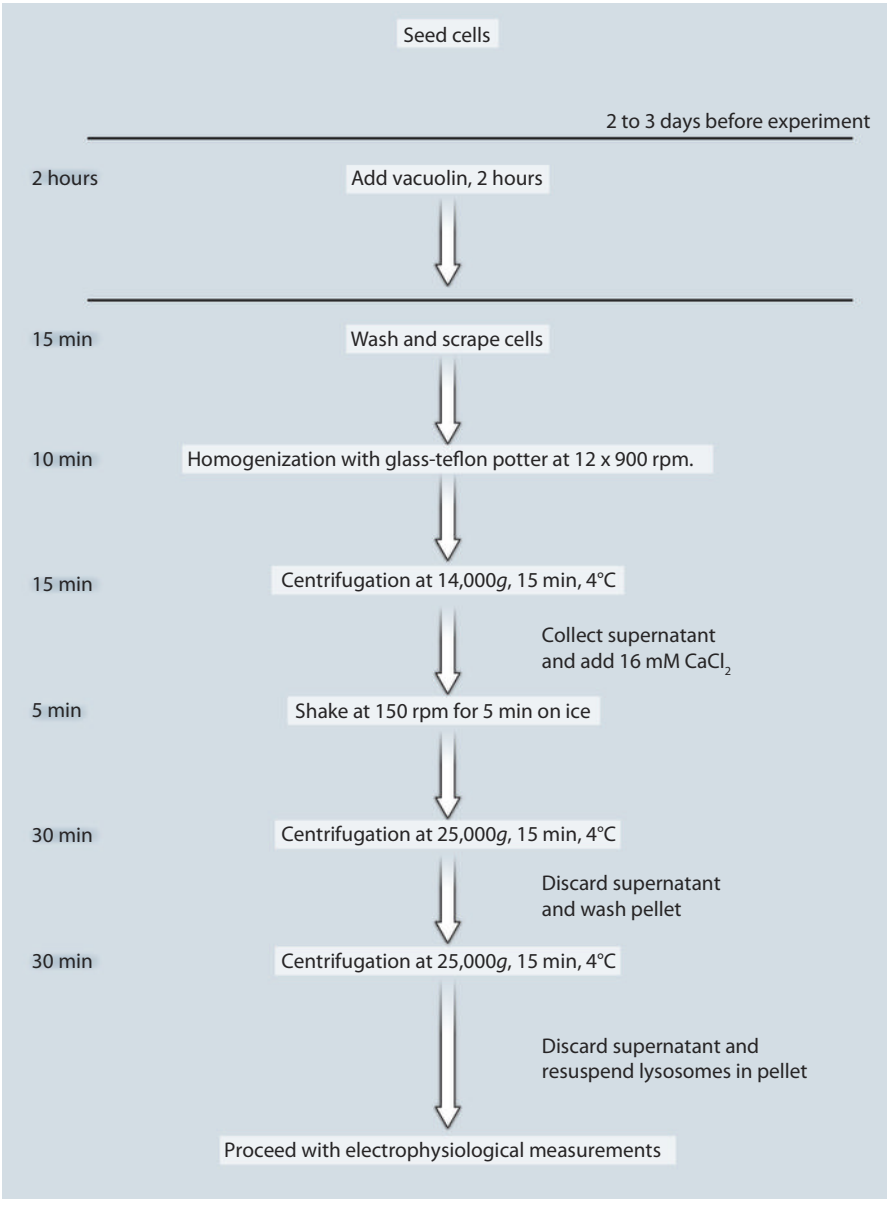

12. Centrifuge at 25,000*g* for 15 min at 4°C in an ultracentrifuge.
13. Discard the supernatant and resuspend the pellet in one volume (typically 3.2 ml) of ice cold Washing Buffer (Recipe 7).
14. Centrifuge at 25,000*g* for 15 min at 4°C in an ultracentrifuge.
15. Discard the supernatant, resuspend pellet containing lysosomes in 20 μl of Washing Buffer (Recipe 7), and transfer the suspension to a 1.5-ml microfuge tube.

    Note: Resuspend the pellet using a 200-μl pipette tip. If resuspension is poor and sample contains large aggregates, then resuspend through a smaller pipette tip more vigorously.
16. Add 20 μl of Washing Buffer (Recipe 7) to the tube that contained the pellet to resuspend, with a 200-μl pipette tip, any remaining pellet. Transfer the suspension to the same microfuge tube from the previous step.

Fig. 3. Configuration of suction and voltage parameters required for seal formation and membrane rupture in planar lysosomal patch clamp. The parameter window of the PatchControl software contains eight tabs. Exact parameters are shown in the screen shots. The "improve seal 1" tab and the "wait for whole cell" tab are deactivated and are not shown.

PatchControl and Patchmaster Software Setup

The PatchControl software controls the Port-a-Patch device. Patchmaster is the acquisition software that controls the HEKA EPC10 amplifier. The handling of Patchmaster is exactly like that for conventional patch clamp. The instructions below provide the general guidelines for setting the parameters for cell positioning, seal formation, and the cell-opening procedure in PatchControl; the exact settings are provided in Fig. 3.

1. Start PatchControl.
2. Select the "experiment window." Make sure that "batch communication" is turned on to enable communication with Patchmaster and to obtain seal parameters and apply command voltages.
3. Load a preprogrammed PatchControl parameter file—for example, "nanion_fragile.ppf."
4. Enter the "edit mode" to access parameter tabs in the parameter window. From this window, edit the parameters for the cell positioning, seal formation, and cell opening procedure (Fig. 3).

5. Select the "wait for contact" tab to monitor the formation of contact between the electrodes and the solution. Patchmaster reads the membrane resistance.
6. Select "adjust VpOffset" to activate the AutoOffset function in Patchmaster.
7. Select the "wait for cell" tab to apply a negative pressure. Set the system to progressively increase the pressure in steps of 10 mB up to a maximum of –40 mB. This will facilitate the attachment of a single lysosome onto the aperture of the glass chip and improve the seal formation during the experiment.

   Note: Setting these parameters correctly is critical, because the lysosomal membrane is very fragile and the applied pressure is considerably lower than that used for cells.
8. Select the "wait for seal" tab and set the system to increase the seal resistance by changing the pressure and membrane potential. Set the system so that you can apply progressively increasing pressure pulses (–20 to –40 mB; step size, 5 mB) every 10 s. When this step is performed with a lysosome, in parallel PatchControl will progressively hyperpolarize the membrane potential every 0.3 s in steps of 2 mV until the final value of –40 mV is reached.
9. Deactivate the "improve seal1" tab by clicking the khaki-colored tab on the bottom of the parameter window (fifth from the left) (Fig. 3).
10. Select "improve seal2" tab to allow PatchControl to switch pressure between a defined pressure and atmospheric pressure depending on the development of the seal formation over time (dR/dt, time dependent change in seal resistance) (Fig. 3). If the seal improves with a rate greater than the threshold defined, PatchControl will not change the parameters. If not, PatchControl will switch the pressure from defined to atmospheric or vice versa and repeat the routine automatically.
11. Deactivate the "wait for whole cell" tab by clicking the light blue colored tab on the bottom of the parameter window (second from the right; Fig. 3).
12. Select the "maintain whole cell" tab. For lysosomes, set this to apply a constant pressure of –20 mB to maintain the seal during electrophysiological measurements. The holding potential is –80 mV.

    Note: The values required for other intracellular organelles will have to be empirically determined.
13. Save the parameter settings as a parameter file in a user-defined folder.

    Note: Once a parameter file is optimized for a particular organelle, it is suitable for further use with the same organelle type without additional modifications.

Electrophysiological Recordings

The instructions below assume a basic understanding of patch clamp recording. Details of performing the patch clamp recordings and data analysis are not described. Only those steps that are specific to recording from lysosome preparations are described in detail. The appropriate NPC-1 chip for lysosomal recordings, based on our experience, has a chip resistance of 8 to 15 megohms. Of the devices we used, the Port-a-Patch device provided the best results. It is essential to form a high-resistance seal (gigaseal) with the membrane of the lysosome or organelle of interest. Gigaseals are formed usually with the aid of Seal Enhancer Solution (Recipe 13). Seal Enhancer Solution (Recipe 13) contains a high concentration of fluoride, whereas the Standard Intralysosomal Solution (Recipe 10) contains a high concentration of Ca^{2+}. For tight-seal lysosomal patch clamp recordings, it is crucial to have solutions containing high Ca^{2+} on one side of the glass chip and solution containing high fluoride at the other side during seal formation. Omitting either of the ions from the respective solutions after seal formation can cause loss of seal quality and patch clamp stability. Inclusion of fluoride improves patch clamp sealing and stabilizes the cell membrane, resulting in longer, more stable patch clamp recordings (*27*); the mechanism of this effect is unknown. Typically, after seal formation, seal enhancer solution is exchanged for those appropriate to the ion channel under investigation. Both internal and external chip solution can easily be changed. We describe how to change the solutions manually; however, an automated internal and external solution exchanger is available from Nanion.

1. Backfill the NPC-1 chip with 5 μl of the same internal recording solution that will be used during data collection—for example, Standard Intralysosomal Solution (Recipe 10)—and screw the chip onto the chip holder of the Port-a-Patch device.
2. Add 5 μl Extralysosomal Bath Solution (Recipe 14).
3. Put the Faraday top in place and adjust the ground electrode so it is in contact with the external solution.
4. In the "Experiment window" of PatchControl, press "Play," which will establish electrical contact once the resistance drops below the preset threshold (parameter "R" in the "wait for contact" tab).

   Note: Usually, the electrical contact is established within 2 min (the surface tension of the chip is quite high). Check the electrical contact between electrodes and solutions when contact is not established quickly.

5. Click the button "Add cells," which adjusts the voltage offset before the lysosomes are added.
6. Dispense 5 μl of isolated lysosomes into the chamber containing Extralysosomal Bath Solution (Recipe 14) immediately after you hear the suction control unit changing the pressure. PatchControl applies suction pulses from below the chip to bring a lysosome onto the aperture. Contact of a lysosome is recognized by an increase in "Rmembr" during each suction pulse.

   Note: If membrane resistance suddenly jumps to a very high value (above 40 megohms), it is likely that the chip opening is clogged by dirt particles. Use a new chip.
7. Once a lysosome has been "captured," add 30 μl of Seal Enhancer Solution (Recipe 13) to the Extralysosomal Bath Solution to help seal formation.
8. Allow PatchControl to perform the steps predefined in the parameters section (see previous section) to optimize seal formation.

   Note: After completion of the full protocol to optimize seal formation, PatchControl enters measurement mode. If seal fails to form, then changing the seal enhancer solution, adjusting the membrane potential, increasing the suction pulse, or applying a voltage ramp may be helpful (see details in later section).
9. After seal formation, exchange Seal Enhancer Solution for those appropriate to the ion channel under investigation. Exchange the external solutions manually with a pipettor by replacing the external solution with one volume of standard extralysosomal solution (Recipe 11) four to five times.

   Note: Solutions containing pharmacological agents or different ionic compositions may also be used to characterize channel properties. Directions for manually exchanging the internal solution are provided in the next section.
10. Perform the electrophysiological recordings with Patchmaster, using the same methods as for conventional patch clamp experiments, with a protocol appropriate to characterize the ion channel of interest using a pulse generator file.
11. After completion of the electrophysiological recording session, close the PatchControl software by selecting "quit." Select "save and exit" when shutting down Patchmaster to ensure that the data files are saved properly.
12. Perform data analysis in the same way as in conventional patch clamp experiments. We usually directly export the data with the standard export functions of the HEKA software and analyze the data in OriginPro 7.5.

Manual Exchange of the Internal Solution

This is optional.

1. Deactivate the suction by clicking "enable" in the "pressure control window" in PatchControl.
2. Remove the Faraday top.
3. Disconnect the NPC-1 chip from the chip holder.
4. Exchange the internal solution with a pipettor by replacing 5 μl of Intralysosomal Solution five times with the new solution.

   Note: Be careful not to lose the external solution (Fig. 4).
5. Screw the NPC-1 chip onto the chip holder.
6. Put the Faraday top in place and adjust the ground electrode.
7. Perform electrophysiologial recording, save and export data, and analyze.

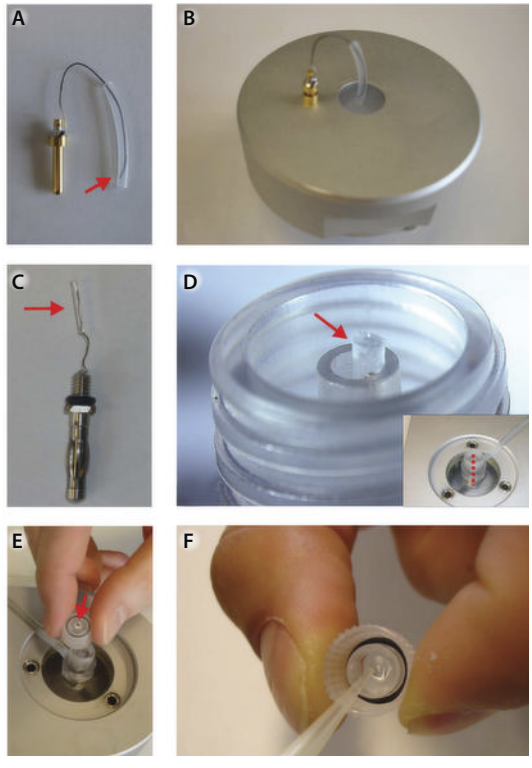

Fig. 4. Preparation and mounting of agar bridges and exchange of intracellular solution. (**A**) Extralysosomal agar bridge. The red arrow marks the position of the electrode tip. (**B**) Extralysosomal agar bridge connected to the Faraday top of the Port-a-Patch. (**C**) Internal recording electrode with an intralysosomal agar bridge. (**D**) The intralysosomal agar bridge (red arrow) is mounted to the chip holder. (Inset) Overview of the Port-a-Patch containing the chip holder. The red dotted line marks the position of the intralysosomal agar bridge. (**E** and **F**) Exchange of the intralysosomal recording solution. (E) The chip is disconnected from the holder and flipped 180° without losing the external recording solution (arrow indicates the droplet of the external recording solution). The internal solution is now changed with a pipettor (F).

Improving Seal Formation

If a seal fails to form, then there are several steps that may improve seal formation.

1. Replace the Seal Enhancer Solution (Recipe 13).
2. Step the membrane potential to 0 mV.
3. Increase suction pulse to a maximum of –80 mB.

   Note: This can improve the seal, but the lysosome might be sucked through the chip.
4. Step the membrane potential to +40 mV
5. Apply a voltage ramp from –100 mV to +100 mV from a holding potential of –80 mV.

   Note: This step is optional and can be avoided if the previous steps result in a seal.

Preparation and Placement of Agar Bridges

To avoid voltage offsets, if internal or external solutions containing low concentrations of chloride are used, then agar bridges need to be used instead of plain Ag/AgCl electrodes. As in conventional patch clamp, agar bridges are used for the reference electrode. In addition, in planar patch clamp it is also possible to use internal agar bridges (Fig. 4).

1. Dissolve 4 mg of agar in 100 ml of 3M KCl solution by boiling and transfer to 10-cm dishes.
2. After the agar has cooled, fill a small silicon tube (1 mm diameter) with agar by sticking the tube into the cooled agar (Fig. 4). This plugs the tip of the tube with agar.
3. Fill the tube with a solution of 3M KCl and push the tip of the reference electrode or the internal electrode into the agar (do not push the electrode completely through the agar) (Fig. 4).

Troubleshooting

Poor or No Lysosome Recovery

If no lysosomal pellet is obtained or if lysosomal recovery is low from the lysosomal preparation, then the density of the cells may be too low, homogenization may be too harsh, or lysosomes may be poorly resuspended. We recommend growing the cells to 90 to 95% confluence. If the confluence is less, decrease the volume of Homogenization Buffer (Recipe 6). Avoid homogenizing with a glass pestle in a glass potter, which can easily damage lysosomes. If the resuspension step was not complete, then the lysosomal preparation will contain large aggregates of lysosomes. For more complete resuspension and separation of lysosomes, use smaller pipette tips and resuspend longer or more vigorously.

Inadequate Seal Formation or Unstable Seal

If the lysosome preparation is not good quality, then it will be difficult to find a lysosome that forms a good seal even in the presence of seal enhancer.

If analysis of lysosomes by means of β-hexosaminidase assay or Western blotting suggests that lysosome preparation is good, then we recommend using a seal enhancer.

If in the presence of seal enhancer, a seal fails to form, then changing the seal enhancer solution, adjusting the membrane potential, increasing the suction pulse, or applying a voltage ramp may be helpful (see Instructions).

The seal is fragile and can be lost when exchanging solutions. It is critical to gently exchange solutions. The exchange of the internal solution is technically demanding, and during this process it is critical not to lose the drop of external solution (Fig. 3, E and F).

During the time course of a patch clamp session, the quality of the lysosomal preparation and the ability to form seals usually gradually decreases with time. In our hands, electrophysiological experiments can be performed for up to 2 to 3 hours after the lysosomes have been prepared. Thereafter, a new lysosomal preparation should be used for electrophysiological recordings.

Notes and Remarks

The experimental conditions may be optimized on the basis of data obtained. There are various aspects to optimize—including lysosome preparation, size of the aperture of the glass chips, ionic solutions during seal formation, and suction and voltage parameters for forming seals—and to breaking through to achieve the whole-lysosome configuration.

We found that lysosomal recordings were most efficiently performed in the whole-lysosome configuration. The lysosomal membrane is very fragile. After breaking through the lysosomal membrane, stable recordings can be obtained for more than 20 min. In contrast, it is much more difficult to obtain stable lysosome-attached recordings for a long period of time. We found that rapidly after obtaining the lysosome-attached mode, the lysosomal membrane spontaneously broke open without losing the seal. Thus, the configuration is converted to whole-lysosome mode.

The current conventions for electrophysiological experiments of lysosomes and other organelles is the same as for conventional patch clamp. An inward current is defined as a current that flows out of the organelle into the cytosol. It is therefore necessary to perform lysosomal recordings using the "inside out" configuration in Patchmaster. Alternatively, the *x* axes and the *y* axes of data recorded by using the "whole cell mode" in Patchmaster need to be inverted.

We briefly outline here the expected results for two examples that illustrate applications of the planar patch clamp method of whole lysosomes. First, we applied our method to native lysosomes isolated from control HEK293 cells. We resolved endogenous lysosomal currents, specifically chloride currents (Fig. 5). The reversal potential of endogenous chloride currents [70.5 ± 1.3 mV (n = 4 different lysosomes)] closely matches the calculated reversal potential for chloride 71.2 mV. We commonly obtained up to eight recordings of native chloride currents per lysosomal preparation. Second, we have detected NAADP (nicotinic acid adenine dinucleotide phosphate)–sensitive current (I_{NAADP}) from lysosomes stably expressing a GFP-tagged TPCN2, which is a member of the two-pore channel family (Fig. 5). Here, the success rate ranged between four to five recordings per preparation. Two-pore channels (TPCN1,2,3) belong to the superfamily of voltage-gated ion channels. Within this superfamily, TPCN channels are most closely related to some members of the TRP (transient receptor potential) cation channels (*28*). TPCNs are localized in endosomal and lysosomal stores and form NAADP-gated Ca^{2+}-release channels (*22*, *23*). NAADP is a second messenger that at low nanomolar concentrations releases Ca^{2+} from endolysosomal stores. NAADP-evoked Ca^{2+}-release has been demonstrated in invertebrates and numerous mammalian cell types, including pancreatic acinar and β cells, cardiac and smooth muscle cells, T lymphocytes, platelets, and neurons (*29*).

These examples illustrate the application of this Protocol to investigate lysosomal ion channels. This glass chip–based method should provide electrophysiological access not only to lysosomal TPCN channels, but also to various ion channels in other types of organelles and intracellular compartments.

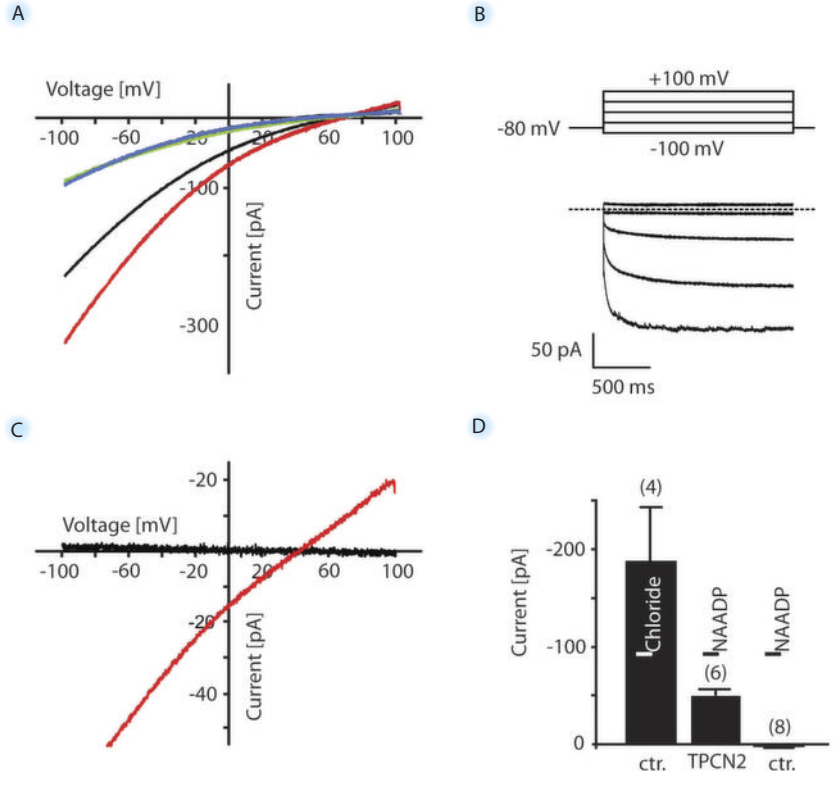

Fig. 5. Example of lysosomal current recordings. (**A**) Endogenous chloride currents recorded from wild-type lysosomes. Current-voltage (*IV*) curves were recorded in the absence [Standard Extralysosomal Solution (Recipe 11)] and presence of external Cl^- [Extralysosomal $_{highCl}$ Solution (Recipe 12)]. The internal solution was Standard Intralysosomal Solution (Recipe 10). Chloride currents were determined as the difference currents between these *IV* curves. The membrane potential was held at –80 mV, and 500 ms voltage ramps from –100 to +100 mV were applied every 5 s. Representative current recordings from four lysosomes are shown in different colors. (**B**) Family of endogenous chloride current traces recorded from wild-type lysosomes. The membrane potential was held at –80 mV, and test pulses were applied from –100 mV to +100 mV (step size, 50 mV). (**C**) Current-voltage relations for Ca^{2+} currents through TPCN2 channels from a single lysosome in the presence of 60 nM NAADP (red). Black trace, NAADP-dependent current of a wild-type lysosome. The protocol was the same as in (A). Currents were recorded with standard extralysosomal and intralysosomal solution (Recipes 10 and 11). (**D**) Population data for current amplitudes at –100 mV obtained from similar experiments as shown in (A) and (C). Inward currents are currents that flow out of the lysosomes into the cytosol. Ctr, control.

References and Notes

1. O. P. Hamill, A. Marty, E. Neher, B. Sakmann, F. J. Sigworth, Improved patch-clamp techniques for high-resolution current recording from cells and cell-free membrane patches. *Pflugers Arch.* **391**, 85–100 (1981).
2. M. J. Berridge, P. Lipp, M. D. Bootman, The versatility and universality of calcium signalling. *Nat. Rev. Mol. Cell Biol.* **1**, 11–21 (2000).
3. R. Zalk, S. E. Lehnart, A. R. Marks, Modulation of the ryanodine receptor and intracellular calcium. *Annu. Rev. Biochem.* **76**, 367–385 (2007).
4. M. Fill, J. A. Copello, Ryanodine receptor calcium release channels. *Physiol. Rev.* **82**, 893–922 (2002).
5. K. Mikoshiba, Inositol 1,4,5-trisphosphate receptor. *Trends Pharmacol. Sci.* **14**, 86–89 (1993).
6. K. Mikoshiba, IP3 receptor/Ca2+ channel: from discovery to new signaling concepts. *J. Neurochem.* **102**, 1426–1446 (2007).
7. A. Galione, O. H. Petersen, The NAADP receptor: New receptors or new regulation? *Mol. Interv.* **5**, 73–79 (2005).
8. A. H. Guse, H. C. Lee, NAADP: A universal Ca2+ trigger. *Sci. Signal.* **1**, re10 (2008).
9. H. C. Lee, R. Aarhus, A derivative of NADP mobilizes calcium stores insensitive to inositol trisphosphate and cyclic ADP-ribose. *J. Biol. Chem.* **270**, 2152–2157 (1995).
10. S. Patel, R. Docampo, In with the TRP channels: Intracellular functions for TRPM1 and TRPM2. *Sci. Signal.* **2**, pe69 (2009).
11. X. P. Dong, X. Wang, H. Xu, TRP channels of intracellular membranes. *J. Neurochem.* **113**, 313–328 (2010).
12. T. J. Jentsch, T. Maritzen, A. A. Zdebik, Chloride channel diseases resulting from impaired transepithelial transport or vesicular function. *J. Clin. Invest.* **115**, 2039–2046 (2005).
13. R. Puertollano, K. Kiselyov, TRPMLs: In sickness and in health. *Am. J. Physiol. Renal Physiol.* **296**, F1245–F1254 (2009).
14. B. Nilius, G. Owsianik, T. Voets, J. A. Peters, Transient receptor potential cation channels in disease. *Physiol. Rev.* **87**, 165–217 (2007).
15. C. Miller, *Ion Channel Reconstitution* (Springer, New York, 1986).
16. I. Favre, Y. M. Sun, E. Moczydlowski, Reconstitution of native and cloned channels into planar bilayers. *Methods Enzymol.* **294**, 287–304 (1999).
17. P. Mueller, D. O. Rudin, H. T. Tien, W. C. Wescott, Reconstitution of cell membrane structure in vitro and its transformation into an excitable system. *Nature* **194**, 979–980 (1962).
18. D. W. Tank, C. Miller, W. W. Webb, Isolated-patch recording from liposomes containing functionally reconstituted chloride channels from Torpedo electroplax. *Proc. Natl. Acad. Sci. U.S.A.* **79**, 7749–7753 (1982).
19. G. Grynkiewicz, M. Poenie, R. Y. Tsien, A new generation of Ca2+ indicators with greatly improved fluorescence properties. *J. Biol. Chem.* **260**, 3440–3450 (1985).
20. C. M. Nimigean, A radioactive uptake assay to measure ion transport across ion channel-containing liposomes. *Nat. Protoc.* **1**, 1207–1212 (2006).
21. H. Garty, B. Rudy, S. J. Karlish, A simple and sensitive procedure for measuring isotope fluxes through ion-specific channels in heterogenous populations of membrane vesicles. *J. Biol. Chem.* **258**, 13094–13099 (1983).
22. P. J. Calcraft, M. Ruas, Z. Pan, X. Cheng, A. Arredouani, X. Hao, J. Tang, K. Rietdorf, L. Teboul, K. T. Chuang, P. Lin, R. Xiao, C. Wang, Y. Zhu, Y. Lin, C. N. Wyatt, J. Parrington, J. Ma, A. M. Evans, A. Galione, M. X. Zhu, NAADP mobilizes calcium from acidic organelles through two-pore channels. *Nature* **459**, 596–600 (2009).
23. X. Zong, M. Schieder, H. Cuny, S. Fenske, C. Gruner, K. Rötzer, O. Griesbeck, H. Harz, M. Biel, C. Wahl-Schott, The two-pore channel TPCN2 mediates NAADP-dependent Ca(2+)-release from lysosomal stores. *Pflugers Arch.* **458**, 891–899 (2009).
24. X. P. Dong, X. Cheng, E. Mills, M. Delling, F. Wang, T. Kurz, H. Xu, The type IV mucolipidosis-associated protein TRPML1 is an endolysosomal iron release channel. *Nature* **455**, 992–996 (2008).
25. D. Kasper, R. Planells-Cases, J. C. Fuhrmann, O. Scheel, O. Zeitz, K. Ruether, A. Schmitt, M. Poët, R. Steinfeld, M. Schweizer, U. Kornak, T. J. Jentsch, Loss of the chloride channel ClC-7 leads to lysosomal storage disease and neurodegeneration. *EMBO J.* **24**, 1079–1091 (2005).
26. M. Schieder, K. Rötzer, A. Brüggemann, M. Biel, C. A. Wahl-Schott, Characterization of two-pore channel 2 (TPCN2)-mediated Ca2+ currents in isolated lysosomes. *J. Biol. Chem.* **285**, 21219–21222 (2010).
27. P. G. Kostyuk, O. A. Krishtal, V. I. Pidoplichko, Effect of internal fluoride and phosphate on membrane currents during intracellular dialysis of nerve cells. *Nature* **257**, 691–693 (1975).
28. F. H. Yu, W. A. Catterall, The VGL-chanome: A protein superfamily specialized for electrical signaling and ionic homeostasis. *Sci. STKE* **2004**, re15 (2004).
29. M. X. Zhu, J. Ma, J. Parrington, A. Galione, A. M. Evans, TPCs: Endolysosomal channels for Ca2+ mobilization from acidic organelles triggered by NAADP. *FEBS Lett.* **584**, 1966–1974 (2010).
30. Online Mendelian Inheritance in Man database (http://www.ncbi.nlm.nih.gov/omim).
31. D. E. Clapham, B. Nilius, G. Owsianik, Transient Receptor Potential Channels. Last modified on 2010-07-01. Accessed on 2010-10-27. *IUPHAR database (IUPHAR-DB),* http://www.iuphar-db.org/DATABASE/FamilyMenuForward?familyId=78 (2010).
32. T. J. Jentsch, M. Poët, J. C. Fuhrmann, A. A. Zdebik, Physiological functions of CLC Cl- channels gleaned from human genetic disease and mouse models. *Annu. Rev. Physiol.* **67**, 779–807 (2005).
33. J. K. Foskett, Inositol trisphosphate receptor Ca2+ release channels in neurological diseases. *Pflugers Arch.* **460**, 481–494 (2010).
34. M. J. Betzenhauser, A. R. Marks, Ryanodine receptor channelopathies. *Pflugers Arch.* **460**, 467–480 (2010).
35. B. O'Rourke, Mitochondrial ion channels. *Annu. Rev. Physiol.* **69**, 19–49 (2007).
36. R. Köhler, Single-nucleotide polymorphisms in vascular Ca2+-activated K+-channel genes and cardiovascular disease. *Pflugers Arch.* **460**, 343–351 (2010).
37. M. S. Remedi, J. C. Koster, K(ATP) channelopathies in the pancreas. *Pflugers Arch.* **460**, 307–320 (2010).
38. T. M. Olson, A. Terzic, Human K(ATP) channelopathies: diseases of metabolic homeostasis. *Pflugers Arch.* **460**, 295–306 (2010).

39. **Funding:** This work was supported by the Deutsche Forschungsgemeinschaft (DFG) and by the Bayerische Forschungsstiftung. **Author contributions:** M.S., K.R., and A.B. performed, designed, and analyzed experiments; M.B. and C.W.S. designed experiments, analyzed data, and wrote the paper.

10.1126/scisignal.3151pl3

Citation: M. Schieder, K. Rötzer, A. Brüggemann, M. Biel, C. Wahl-Schott, Planar patch clamp approach to characterize ionic currents from intact lysosomes. *Sci. Signal.* **3**, pl3 (2010).